EFFECT OF HYDRODYNAMICS ON DISSOLUTION RATE OF POORLY

SOLUBLE DRUGS IN THE FLOW THROUGH APPARATUS

EFFECT OF HYDRODYNAMICS ON DISSOLUTION RATE OF POORLY SOLUBLE

DRUGS IN THE FLOW THROUGH APPARATUS

By

Hanumantha Rao Kurapati, B. Pharm.

Being a thesis submitted for the degree of

M. Sc. by research in pharmaceutical technology

At

University of Dublin

Trinity College

Under the supervision and direction of

Dr. Deirdre M. D'Arcy, M. Pharm., Dip. Clin. Pharm., M.P.S.I.,
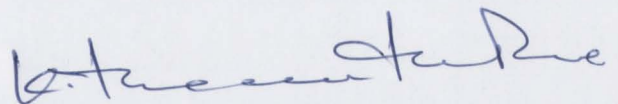
October 2009
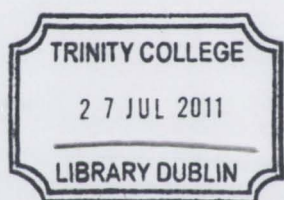
DECLARATION

This thesis is submitted by the undersigned to the University of Dublin, Trinity College, for examination for the degree of M. Sc by research. It has not been submitted for a degree at any other university. I myself carried out all the practical work except where duly acknowledged. This manuscript was written by me with the editorial advice from Dr. Deirdre M. D'Arcy. The library may lend or copy this thesis upon request and this permission covers only single copies made for study purposes, subject to normal conditions of acknowledgement.

Hanumantha Rao Kurapati

Summary

The aim of the project is to study the effect of hydrodynamics on the dissolution rate of ibuprofen drug particles (in the powder form) in the flow through apparatus. Dissolutions were carried out in the tablet cell and powder cell. In the powder cell two methods were employed for dissolution, the names of the methods used given as method 1 and 2. These two methods differ in the placement of insert. Dissolutions were carried out in different dissolution media to simulate the gastrointestinal conditions. The media used were phosphate buffer pH 6.6, 0.1 M HCl and viscous medium (0.5 % and 1.0% HPMC). Sodium lauryl sulphate (SLS) was used as wetting agent (0.018 %).

To determine the relative velocity of the particles and fluid a MATLAB code was used which was written by Dr. Tim Persoons from Mechanical and Manufacturing Engineering Department, TCD. The particle motion equation was used to develop MATLAB code. Using the relative velocity values dissolution was predicted in different media.

Using Bio classification system (BCS) principle the dissolution was predicted. The principle involved in the BCS equation is the dissolution number which can be defined as the ratio of the mean residence time to the dissolution time. Dissolution time was used in predicting the dissolution.

The experimental dissolutions were compared with the predicted dissolution using particle motion equation and the BCS equation. The experimental dissolution without sodium lauryl sulphate (SLS) was comparable with the BCS predicted dissolution. The experimental dissolution was not comparable with the predicted dissolution using particle motion equation. The experimental dissolution was slower than the predicted dissolution using particle motion equation. This might be due to clumping of particles which reduces the total surface area exposed resulting in a slower dissolution rate.Dissolution using sodium lauryl sulphate (SLS) and 5 mg of drug were comparable with the predicted dissolution using relative velocity and faster than the BCS predicted dissolution which might be due to the use of sodium lauryl sulphate (SLS) which makes drug particles free from clumping.

Dissolutions in viscous medium were carried out to simulate the fasting and fed state of Gastro intestine. The viscous medium didn't run through the powder cell as the powder cell has filters to filter the undissolved particles which blocked the flow of viscous medium. So dissolutions were carried out without bottom filters in 0.5 % HPMC. In 1 % HPMC dissolution the bottom and top filters were not used as the fluid is highly viscous.The conclusion of the project is, the dissolution rate didn't increase with the increase in the flow rate. Use of sodium lauryl sulphate (SLS) makes dissolution easier.

TABLE OF CONTENTS

ACKNOWLEDGEMENTS

PRESENTATIONS AND PUBLICATIONS ASSOCIATED WITH THIS THESIS

POSTER PRESENTATIONS

1. Effect of hydrodynamics on particulate dissolution in the flow through apparatus. H Kurapati et.al. 30th All Ireland School of pharmacy research seminar 2009, Trinity College, Dublin.

ABBREVATIONS AND SYMBOLS

B.P	British pharmacopoeia
d	Diameter
d_p	Particle diameter
C_s	Saturated solubility
C_t	Concentration of drug in the bulk solution at time t
D	Diffusion coefficient
D_{eff}	Effective diffusion coefficient
F_d	Drag force
GIT	Gastrointestinal tract
h_{app}	Hydrodynamic diffusion layer thickness
HCl	Hydrochloric acid
I	Diameter of the paddle
J	Diffusion flux
K	Cube root dissolution rate constant
K_1	Constant in Noyes-Whitney equation
K_d	Dissolution rate constant
KH_2PO_4	Potassium dihydrogen phosphate
L	Length of pipe
$M_o^{1/3}$	Cube root of initial amount of drug

$M_t^{1/3}$	Cube root of drug at time, t
ml/min	Flow rate
NaOH	Sodium hydroxide
pH	Minus log of hydrogen ion concentration
Ph. Eur	European Pharmacopoeia
ρ	Density
r	Radius
R	Rotations per minute
Re	Reynolds number
R2	Correlation coefficient
Sh	Sherwood number
SLS	Sodium lauryl sulphate
S.D	Standard deviation
S	Surface area
$\tilde{U}_p$	Instantaneous particle velocity
$\tilde{U}_f$	Instantaneous fluid velocity
U_f	Fluid velocity
$U_{f, av}$	Average fluid velocity
U_p	Particle velocity
$U_{p, av}$	Average particle velocity

USP	United States Pharmacopoeia
Vo	Instantaneous relative velocity
V	Volume of dissolution fluid
W_o	Initial weight of drug
W_t	weight of drug at time, t
X	Distance
Φ	Mass transfer coefficient
μ	Kinematic viscosity
$μ_d$	Fluid dynamic viscosity
ε	Energy
γ	Rate of surface renewal
$ρ_p$	Particle density
$ρ_f$	Fluid density
psia	Pressure

INTRODUCTION

Origin and scope of the thesis

The dissolution of the drug is an important physical process which acts as a limiting step in the absorption of poorly soluble drugs. Dissolution is an important testing tool in the quality control of products. Dissolution testing is also used to discover best formulation for a novel drug. To conduct dissolution different types of USP apparatuses are available.

Up to now the behaviour of dissolution and the phenomenon of dissolution were examined extensively using USP 1 and 2. In the flow through apparatus much work was done relating the tablet position at different flow rates in the standard cell (diameter 22.6 mm). Zhang et al (1994), Cammarn and Sakr (2000) and Wu and Ghaly (2006) studied the dissolution in the flow through apparatus using tablets. Emara et al (2009) studied the effect of different conditions like flow rate, temperature, cell size, dissolution medium and tablet position on the dissolution rate of tablets using flow through apparatus.

Bhattachar et al, (2002) studied the behaviour of powdered drug using flow through apparatus and concluded that the loading of drug plays an important role in the dissolution profile. However until now no literature is available regarding the effect of hydrodynamics on the dissolution rate of poorly soluble drugs in the particulate form. No studies have been found to date, to the best of our knowledge, relating the relative velocity with the particulate dissolution in the flow through apparatus.

There were many studies which relate the in vivo conditions using basket apparatus and paddle apparatus but not using flow through apparatus

The main objectives of the current project were

1. To study the effect of hydrodynamics using flow through apparatus on the particulate dissolution.

2. To relate the relative velocity with the particulate dissolution using flow through apparatus

3. To simulate the particulate dissolution with the gastrointestinal conditions using the flow through apparatus (to study the dissolution behavior of powder in the flow through apparatus)

1.1 History of dissolution testing

Dokoumetzidis and Macheras have reviewed a century of dissolution research from a historical point of view (Dokoumetzidis and Macheras, 2006). Dissolution research was started about 100 years ago in the field of physical chemistry. The first dissolution experiments were conducted by Noyes-Whitney in 1897 who published an article "the rate of solution of solid substances in their own substances" (Noyes and Whitney, 1897). Noyes and Whitney stated that the dissolution rate is proportional to the difference of saturated solubility and instantaneous concentration at time t and formulated as

$$dc/dt = K_1 \text{ (cs-ct)} \qquad \text{Eqn 1.1}$$

Where K_1 – is a constant

Noyes and Whitney attributed the mechanism of dissolution to a thin diffusion layer. The thin diffusion layer is formed around the surface of particles and through which molecules diffuse into an aqueous phase.

In 1900 an article was published by Erich Brunner and Tolloczko who extended the conditions of equation 1.1. Brunner and Tolloczko showed that the dissolution rate depends on the surface area exposed the rate of stirring, temperature, and structure of surface area and arrangement of apparatus (Brunner and Tolloczko, 1900).

$$dm/dt = K_d S \text{ (cs-ct)} \qquad \text{Eqn 1.2}$$

Where $k_d = K_1/S$, S – surface area.

The next contribution was made by Nernst and Burner in 1904. Nernst and Burner published an article in which modified the constant K_d in equation 1.2 based on the diffusion layer concept and Fick's second law as

$$dc/dt = DS/Vh(cs-ct) \qquad \text{Eqn 1.3}$$

Where, D – diffusion coefficient, h – thickness of the diffusion layer, V- volume of dissolution medium.

Hixson and Crowell in 1931 proposed a modified form of equation 1.2 with the surface area, S defined with respect to weight, W (Hixson and Crowell, 1931). When equation 1.2 is integrated assuming surface with respect to weight, it yields an equation which relates time with cube-root of weight.

$$Wo1/3\text{-}Wt1/3 = Kt \qquad \text{Eqn 1.4}$$

Where   Wo - initial weight of drug

Wt - weight of drug at time t

K – Cube root dissolution rate constant

 The cube root law is derived based on the following assumptions:

1. Dissolution takes place on the surface of a solid

2. Effect of agitation is uniform

3. There is no stagnation of the liquid

4. Solid particles stay intact

5. The dissolving particles are Spherical

The equations 1.1, 1.2, 1.3 and 1.4 can be categorized as various expressions of the diffusion layer model of the dissolution process in which the rate limiting step is a stagnant film around the surface of solid through which molecules diffuse.

By the 1950's two more models explaining the rate limiting step were available and reviewed by Higuchi (1961). The interfacial barrier model, proposed by Wilderman (1909) and the Danckwert's model (1951). The Interfacial barrier model considered interfacial transport instead of a diffusion layer (Wilderman, 1909) and the Danckwert's model considered an existence of constantly renewing macroscopic pockets of solvent transferring solute molecule (Danckwerts, 1951).

Until the 1950's the concept of dissolution was not used for in vivo studies. Before implementing the dissolution test the in vivo availability of drug was determined using the disintegration test. In 1950 the United States Pharmacopoeia introduced a disintegration test for tablet in the 14th edition. A sophisticated method was proposed by Fillborn in 1948 which introduced an artificial stomach and simulated in vivo conditions including pH and peristalsis (Filleborn, 1948).

Edwards in 1951 postulated the dissolution of aspirin tablets in the stomach and intestine as the rate limiting process controlling the absorption of aspirin in the blood stream (Edwards, 1951). In 1957 Nelson related the blood levels of theophylline with the in vitro dissolution rates (Nelson, 1957).

The term bioavailability was coined in the 1960's. The formulation of a drug could lead to differences in onset of action, the intensity of action and the drug response time. The term bioavailability is used to describe the rate and fraction of drug reaching the systemic circulation.

Dissolutions of different formulations of Digoxin and Phenytoin were studied in the 1970's and concluded that the bioavailability of a drug depends on the formulation. Hence a dissolution requirement for tablets and capsule monograph in Pharmacopoeia

4

monographs was introduced to avoid toxic effects and at the same time dissolution was recognized as a tool in quality control.

In 1970 the USP and National formulary adopted "basket-stirred-flask test" as an official dissolution testing apparatus. In 1978 the USP adopted "paddle method"- USP 2 as an official apparatus. In 1990 the USP adopted "reciprocating cylinder method" as an official apparatus for extended release formulations and in 1995 the USP adopted "flow through apparatus" (USP 4) officially for extended release formulations.

Dissolution was developed as a prognostic tool for oral drug absorption in 1990's. A microscopic model proposed three fundamental parameters which control the oral absorption. The three parameters are dissolution, absorption and dissolution number (Oh et al, 1993). This bio-classification system of drugs (BCS) was based on work of Amidon (Amidon et al, 1995). BCS classified drugs based on drug solubility and intestinal permeability. According to the BCS, four classes of drug were defined as follows

Class 1   drugs having high solubility and high permeability
Class 2   drugs having low solubility and high permeability
Class 3   drugs having high solubility and low permeability
Class 4   drugs having low solubility and low permeability

The evolution of bio-relevant medium for correlating dissolution and in vivo absorption was described by Dressman (Dressman et al, 1998). Even though bio-relevant media were studied well and developed, the simulation of biorelevant hydrodynamic conditions is a potential barrier for correlating dissolution with in vivo absorption.

Fasted state simulated intestinal fluids and fed state simulated intestinal fluids were introduced by Dressman and Reppas (2000) which simulate human gastrointestinal tract (GIT) and provide similar physiochemical properties. Dissolution in bio-relevant medium can be used to predict the in vivo performance (Dressman et al, 2005).

Currently dissolution testing is using for drug development, quality control of manufacturing process, and to identify bioavailability problems and bioequivalent formulations (Gohel and Panchal, 2002). In drug development dissolution testing is used to select the best formulation for a drug. In quality control the oral dosage form need dissolution testing as a measure of quality control and must meet pharmacopoeia/regulatory specifications.

1.2 Hydrodynamics and dissolution

According to Noyes-Whitney equation the rate of drug dissolved is directly proportional to the diffusivity of the drug, the surface area that is exposed to the volume of the dissolution media and the driving force (Cs-Ct) which is the concentration gradient (equation 1.3)

$$Dc/dt = SD(Cs-Ct)/Vh$$

Noyes-Whitney discussed the diffusion layer thickness in the equation. The rate of drug dissolved is inversely proportional to the diffusion layer thickness. The diffusion layer thickness is related to the hydrodynamic boundary layer thickness, with the hydrodynamic boundary layer being greater than the diffusion layer thickness (Levich, 1962). The ratio of diffusivity to the diffusion layer thickness is the dissolution rate constant.

1.2.1 Fluid flow: Fluid flow can be classified into two types.

Laminar flow: Laminar flow is also called as viscous flow or stream line flow. In laminar flow the particles move in an ordered manner retaining the same relative positions so laminar flow in circular pipe seems to have annular layers as shown in fig 1.1. The velocity of the layer increases from zero to maximum from the wall to the centre of the pipe (Bently, 2005).

6
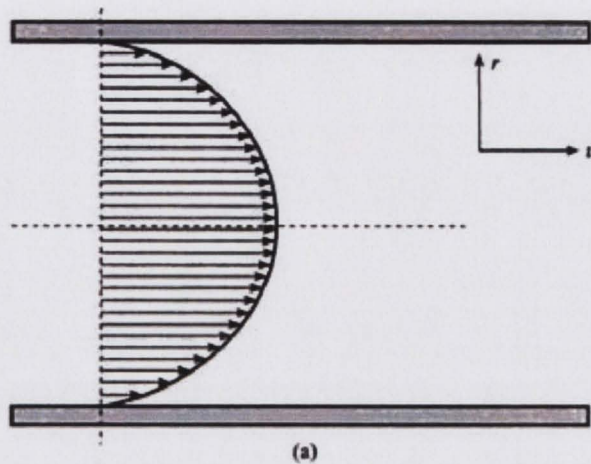
Fig 1.1 layer velocity v vs. distance r of layer from centre (Bently, 2005).

Turbulent flow: In turbulent flow particles move in highly disordered manner and the relative position of the particles changes randomly as shown in fig 1.2. The viscous friction force is less in turbulent flow compared to laminar flow (Bently, 2005).
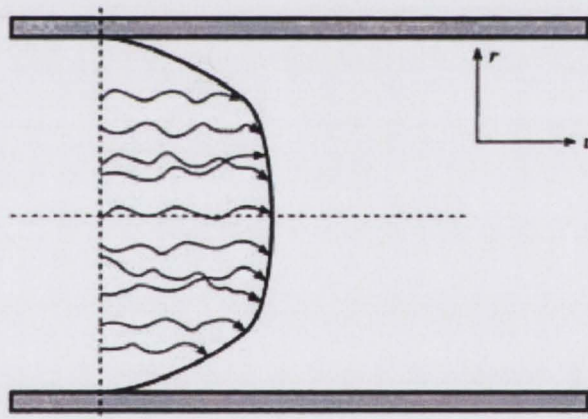
Fig 1.2 A typical turbulent flow profile. Taking radius at one point r, measuring the average v of the velocity component at that point (Bently, 2005)

1.2.2 Reynolds Number, Re

Osborne Reynolds proposed the Reynolds number in the year 1883. It can be defined as the ratio of inertial forces to the viscous forces. It is used to quantify the type of flow and it is a dimensionless number.

$$Re = \rho_f u_f L / \mu_d \qquad\qquad \text{Eqn 1.5}$$

Where $\quad \rho_f \quad$ – density of fluid

$\qquad u_f$ – velocity of fluid

$\qquad L$ – Length of pipe

$\qquad \mu_d$ - dynamic viscosity

The turbulent instability in a turbulent flow are called eddies. The formation of eddies is due to obstruction to the flow of fluid or formed along with the flow. It is proved that the mass transfer coefficient increases in the dissolution process due to eddies (Dressmann et al, 2005). The velocity of the eddies depend on the size of the eddy. If the eddy is bigger, the mean velocity of the eddy will be more and vice versa with the smaller eddy. This mean velocity of the eddy is called "scale of motion" (SOM) (Sherwood and Woertz, 1939). In a turbulent flow different sized eddies will form and these eddies transfer kinetic energy. The bigger the eddy the longer the SOM. It will convert into a smaller eddy by transferring eddies until very small eddies are formed and the transferring of kinetic energy is called an "Energy cascade". In viscous media the formation of eddies is low as the flow of fluid is less.

1.2.3 Hydrodynamics depends on paddle speed

Plummer and Wigley derived an equation which relates energy and hydrodynamics (Plummer and Wigley, 1976). This can be used to calculate the energy of fluid per unit mass of fluid and can be used only for a closed system with rotating paddle on shaft.

$$\varepsilon = Pl^5 R^3 / V \qquad\qquad \text{Eqn 1.6}$$

Where ε = energy has a dimension l^2/t^3

R = rotations per minute, $\qquad\qquad$ I = diameter of the paddle

V = volume of the fluid $\qquad\qquad$ P = constant depends on laminar or turbulent flow

8

The equation itself suggests that the energy of the fluid depends on the paddle rotation and the diameter of the paddle. If energy is calculated by using the equation, the energy of fluid raises exponentially along with the increase of paddle speed. If there is increase of the speed the energy increases due to which there is a change of fluid flow from laminar to turbulent with a considerable increase of paddle speed.

1.3 Flow-through apparatus

The flow-through apparatus (USP 4) was adopted officially by the USP in 1995 and has been incorporated in several international pharmacopoeias (Looney, 1997).

In 1968 Pernarwoski et al published a "continuous flow-through apparatus" which has 1000 ml flask with stirrer/basket to provide hydrodynamic conditions and has a liquid flow up to 70 ml/min (Pernarowksi et al, 1968).

The flow through apparatus consists of a testing chamber in which the dosage form to be tested is placed. The testing chamber is maintained at 37°C and the drug is released from the dosage form under continuous flow conditions. The dissolution medium is pumped through a heat exchanger for temperature control in to the testing chamber. The pumping of the dissolution medium is by a piston pump which can a flow rate of up to 50 ml/min. In the testing chamber filters are arranged which filter the undissolved drug particles.

Fig 1.3 Flow through apparatus used for dissolution testing (Sotax online information sources)

The flow through apparatus is used to study the dissolution rate of extended release products and to study tablets, capsules, suppositories, soft gelatin capsules, implants, powders and granules.

The advantages of the flow through apparatus are as follows:

1. It solves the problem of non sink condition which is the problematic in USP 1 and 2.

2. It is easy to change pH conditions to stimulate physiological conditions.

3. It can be used for wide variety of dosage forms. Special cells were designed for each dosage form.

4. It can be operated as an open or closed system.

The testing chamber used for the dissolution test is called the "cell" in which the dosage form is placed. In the flow through apparatus 6-7 cells are arranged. The dissolution medium is passed through an electronically regulated water bath before entering into the cell.

Different types of cells are available to conduct dissolution tests. 12 mm and 22.6 mm diameter cell are available. To study the dissolution rate of powders, a powder cell can be used as the powder cell is equipped with an insert and two screens. The powder is placed between two screens and studied under selected flow conditions.

Flow conditions: In the flow through apparatus two types of flow can be operated. To produce laminar flow the cell must be filled with 1 mm beads and to produce turbulent flow the dosage form should placed in the cell without any beads (in the past this was thought to provide turbulent flow but a recent analysis suggests that it is not turbulent (Kakhi, 2009)). The laminar flow condition can be operated to study the dissolution of tablets, hard gelatin capsules, powders and granules. The dissolution medium is passed through the cell and through a filter fitted at the filter heads and is collected for analysis. USP recommends a flow rate of 4 ml min^{-1} – 16 ml min^{-1} and in pharmaceutical industry the standard flow rate is used, 16 ml min^{-1} (Looney, 1997). To obtain a consistent flow rate in the flow through apparatus SOTAX has developed piston pump. Piston pump has

high performance and consistent flow rate. The movement of the piston pump delivers a defined flow profile (Looney, 1997).

1.3.1 Flow profile in the flow through apparatus

Fig 1.4 shows the flow profile in the flow through apparatus. The flow profile is same at any flow rate. The fluid flow has a pulsing flow of 120 pulses min^{-1} through a cell where a dosage form is situated. At the beginning of the pulse the flow rate is zero and increases with time and reaches a maximum velocity at certain time point which corresponds to the point at which the piston has reached half way through the upstroke. From then the velocity of the pulse will go down with time and finally reaches to zero velocity and remains at zero velocity during the piston down stroke.
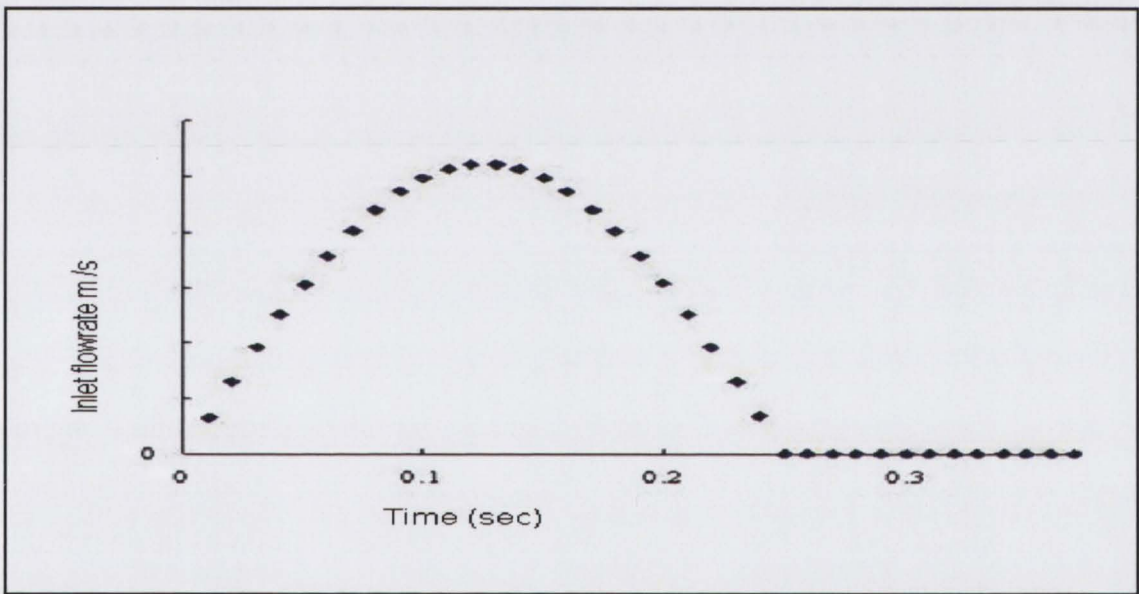
Fig 1.4 Flow profile in the flow through apparatus

In house 2-D computational fluid dynamics (CFD) simulations of flow of water at 37°C through the 12 mm cell at 16 ml min^{-1}, using the method described in the work of D'Arcy (D'Arcy et al, 2008) showed the existence of varied strain rates depending on the region

11

of the cell in the flow through apparatus. Fig 1.5 shows the average facet average strain rates at different regions.
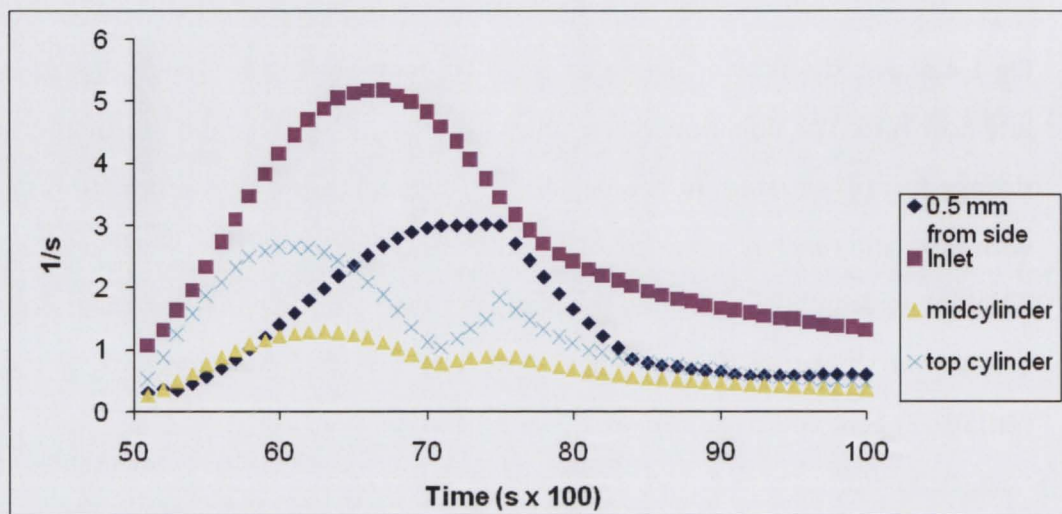
Fig 1.5 Average facet strain rates at different regions in the powder cell at 16 ml min^{-1} (D'Arcy et al, 2008)

In fig 1.5 the first line from top of the fig gives the facet strain rate at 0.5 mm from side, the second line from top shows the strain rate at the inlet, the third line from top shows the strain rate at the mid cylinder area and the bottom line shows the strain rate at area at the top the cylinder. The strain rate is very low at mid cylindrical region where is the possibility of having high velocity whereas it is high at 0.5 mm from side of the cell wall where there is the possibility of having low velocity of dissolution medium.

The flow through cell can be differentiated into various parts as various geometrically distinct areas are present. At the bottom end of the cell there is a narrow opening with a diameter of 0.8 mm which leads into a conical shaped expansion and extends into a cylindrical dissolution test zone and then a filter section before the outlet. Different fluid dynamics are observed in the cell. If the conical part of the cell is filled with beads the flow of the fluid is laminar, as it is unidirectional and consistent. In the current work the packed

12

column configuration was used. In the flow through cell two kinds of beads are present, the synthetic ruby red bead with a diameter of 5mm and small soda lime glass beads with a diameter of 1 mm. The use of the red bead is to prevent flow of dosage form from the inlet.

1.3.1.1 Flow Inlet

A piston pump sucks fluid from the reservoir and discharges fluid into the cell and the amount of fluid discharged in to the cell depends on the setting of the piston pump. It is fitted to produce different flow rates from 1 ml min^{-1} to 50 ml min^{-1}. The flow of the fluid into the cell can be characterised as pulsating flow. At the beginning the apparatus cell was designed to work with peristaltic pumps and then the cell was designed to include a centrifugal pump in place of peristaltic pump, as there is much variability in place of the peristaltic pumps, but centrifugal pump was failed due to the poor average flow rate. Consequently dual piston reciprocating pumps were fitted to get constant flow and finally positive displacement pumps became the standard ones (Kakhi, 2009).

1.3.1.2 Flow profile in the flow through cell at different regions

Flow profile at sudden contraction

Sudden contraction is the part which can be seen at the beginning of the cell (fig 1.6) and the flow in the sudden contraction area is as follows. The fluid flows in large volumes before entering into the area of contraction, then the fluid flows through area of contraction and subsequently through the conical expansion and then into the cylindrical test zone. If the flow is observed the flow of the fluid is directed towards the pipes axis until the 0.8 mm bore is reached. The critical Reynolds number is where the fluid flow transforms into turbulent from laminar flow. It was found that the Reynolds number in the 9.87 mm chamber is 515. The transitional Reynolds number is 2000< Re_{crit} >4000, so the flow in the 9.87 mm area is laminar (Kakhi, 2009).
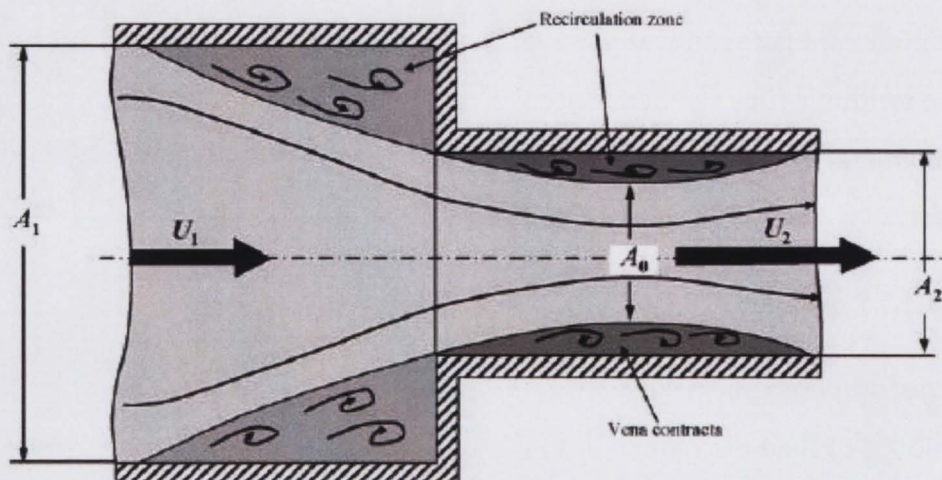
Fig 1.6 Schematic of flow in the vicinity of a sudden contraction (Kakhi, 2009).

Flow profile in the packed column bed

The flow of fluid is uniform across the diameter of the bed. The turbulent flow in the packed bed depends on Reynolds number. When the Re_b is less than 0.4 the flow is uniform, the flow is steady laminar when Re_b is between 0.4-4 and 59, the flow is unsteady laminar flow when Re_b is between 59 and 118 and the flow is turbulent when Re_b is greater than 118 (Kakhi, 2009).

The flow profile at the packed column bed depends of the flow rate employed. The expected Reynolds number in the packed column bead in the powder cell is 10, 20, 32, 41, and 64 at flow rates 4, 8, 12.6, 16 and 25 ml min^{-1} respectively (Kakhi, 2009).

1.4 Mathematical models for dissolution relating mass transfer rate with relative velocity

By using fluid dynamics the theory of mass transfer from a suspended sphere in an agitated fluid has been extensively studied by Ranz and Marshll (Ranz and Marshall, 1952). According to fluid dynamics theory the mass transfer coefficient is described as,

$$K_{mass} = D_{eff}Sh/L = D_{eff}Sh/d_p \qquad Eqn\ 1.7$$

14

Where K_{mass} – mass transfer coefficient, Sh – Sherwood number, d_p- paricle diameter, L-representative length of particle and D_{eff} – effective diffusion coefficient.

Ranz and Marshall relates Sherwood number and relative velocity as follows

$$Sh = 2 + 0.6Re_p^{1/2}Sc^{1/3} \qquad \text{Eqn 1.8}$$

Sherwood number can be defined as the ratio of convective diffusion to diffusive mass transport, Reynolds number can be defined as the ratio of inertial forces to viscous forces and the Schmidt number can be defined as the ratio of momentum diffusivity to mass diffusivity.

Ranz and Marshall define the equation 1.8 in terms of mass transfer as follows

$$\Phi d/D = 2 + 0.6 \, (dv^o_1/\mu)^{1/2} \, (\mu/D)^{1/3} \qquad \text{Eqn 1.9}$$

Where Φ- mass transfer rate (cm/s), d-diameter of particle, v^o_1 – relative velocity, D-diffusion coefficient, μ- kinematic viscosity of the fluid.

Using the ϕ- mass transfer rate as discussed in equation 1.9 the relative velocity for a dissolving particle in the flow through apparatus was determined using the particle motion equation (using MATLAB) code and the dissolution in the flow through apparatus was predicted. The value of mass transfer rate is used as the value of dissolution rate constant.

Noyes-whitney equation (1.3) is described as

$$dm/dt = Sk_d \, (c_s-c_t)$$

Where k_d – dissolution rate constant. If the units of each parameter is written except k_d it can shown that k_d is equal to mass transfer coefficient (cm/s).

The mass transfer coefficient ϕ, was determined using the relative velocity values from MATLAB, and the mass transfer coefficient inserted in equation 1.3. Using equation 1.3 the amount of drug dissolved over a period of time was determined. This was followed by

15

determination of the radius of the undissolved drug particle, to determine the relative velocity of this particle to be used to predict the dissolution rate over the next time period and so on.

1.5 Mathematical models employed in determining particle velocity

The particle motion equation was given by Basset A.B. for unsteady motion of a suspended sphere (Basset, 1888) which relates the instantaneous relative velocity to instantaneous particle velocity and instantaneous fluid velocity show in fig 1.7. The instant velocity of the particle is instantaneous particles velocity and the instant velocity of the fluid is instantaneous fluid velocity.
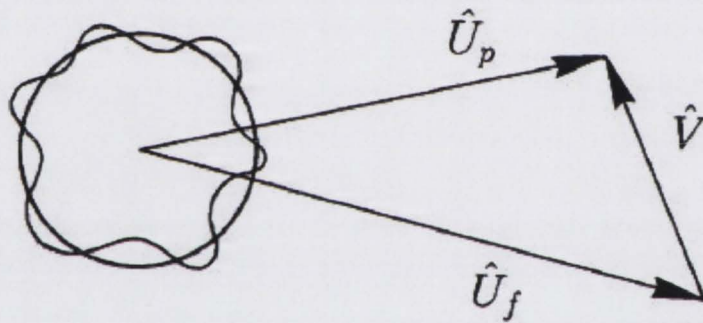
Fig 1.7 The relative motion of a suspended particle (Melling, 1997)

$\pi d_p^3/6.\rho_p\ (d\tilde{U}_p/dt)\quad =\ -\ 3\pi\mu_d d_p V\ ^\circ +\ \pi d_p^3/6\rho_f\ (d\tilde{U}_f/dt)\ -\ 1/2\ (\pi d_p^3/6)\rho_f(dv^\circ/dt)\ -$

$3/2 d_p^2(\pi\mu_d\rho_f)^{1/2} \int_{to}^t dv^\circ/d\xi.d\xi/(t-\xi)^{1/2}$ Eqn 1.10

Where, d_p- particle diameter , ρ_p- particle density, ρ_f- fluid density, μ_d- fluid dynamic viscosity, t- time, V°- instantaneous relative velocity, $\tilde{U}_p$- instantaneous particle velocity, $\tilde{U}_f$- instantaneous fluid velocity

The equation is the particle motion equation. In the equation the first two terms give the acceleration force and viscous resistance. The third term gives the additional force formed

due to the pressure gradient from the acceleration of the fluid. The fourth term gives the resistance of a viscous fluid. The first, second and fourth terms combined correspond to the acceleration force. The final term is "Basset history Integral" gives resistance raised due to the unsteadiness of flow field (Basset, 1888). To solve the particle motion equation a MATLAB code was used (Original code obtained from Dr. Tim Persoons, School of Mechanical Engineering, TCD).

The constants used in the equation were diameter of particle, particle density, fluid dynamic viscosity and fluid velocity (shown in appendix I).

The first line from top (blue lines) in the fig 1.8 represents the fluid velocity in the flow through apparatus and second line from top (black lines) represents the particle velocity. The particle velocity and the relative velocity values are displayed at the top of the figure. The simulations starts from rest (fluid and velocity = 0). Steady states establishes after a few pump periods. When the fluid stops moving the particle drifts downwards due to the density difference between the particle and the fluid.
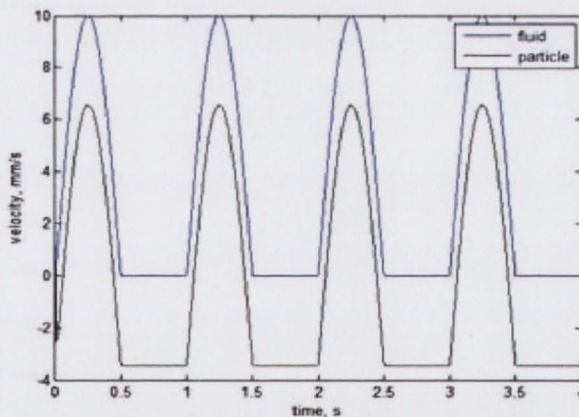
Fig 1.8 Simulated velocities of the fluid and the particle from which the relative velocity was calculated

As shown in fig 1.9 the different forces acting on the particle will be displayed. The first line from top (blue) represents the drag force, the second line from top (black) shows

17

Basset, the third line which overlaps with second line (red) represents fluid acceleration and the bottom line (green) represents the buoyancy.
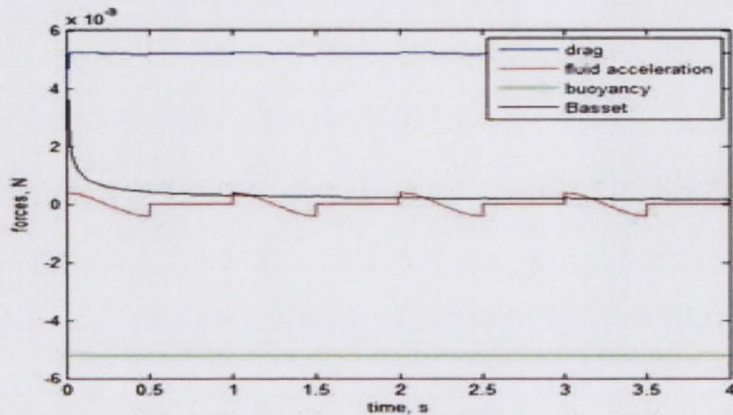
Fig 1.9 shows the different forces acting on the particle.

1.6 Drag coefficient

Drag coefficient is a quantity which is used to measure the drag force of a particle in the liquid or in the air. The drag coefficient was a term used in the particle motion equation to calculate the particle velocity and relative velocity in the fluid.

The drag coefficient (C_d) is the dimensionless form of drag force. The drag coefficient is defined as

$$F_d = C_d \, A \, \rho_f U^2/2, \hspace{3cm} \text{Eqn 1.11}$$

Where F_d =drag force (N), A= frontal surface area (=$\pi d^2/4$ (m^2), d= particle diameter (m), ρ_f=fluid density (kg/m^3), U=relative velocity (particle –fluid) (m/s).

Alternatively, a linear relation of drag force with relative velocity is typically used to describe the drag force:

$$F_d = 6\pi\mu_d d/2 \, U \hspace{3cm} \text{Eqn 1.12}$$

Where, F_d – drag force (N), μ_d - fluid dynamic viscosity (kg/m.s), d – particle diameter (m), U is the relative velocity (particle-fluid) (m/s).

18

the equation 1.12 is defined using a basic model of stokes drag, valid for low Reynolds number (Re<1) (Melling, 1997)

1.7 Particle Density

The density of a substance can be defined as weight per unit volume. The density of particle depends on the porosity, capillary spaces and microscopic cracks. Hence three types of densities can be defined.

1. True density of particles: True density of particles is the density of the particles excluding the intra particle pores and voids which are larger than the molecule or atomic dimensions. True density of porous particles can be determined using helium densitometer (Franklin, 1949)

2. Granule density: Granule density is the displacement of mercury which penetrates into pores at 10 μm of pressure. By determining the mercury consumed to fill the gaps in between the particles the granule density of the particles can be determined only when the particle weight is known with the intraparticle spaces. Strickland determined the granule density of tablet granulations using a specially designed pycnometer (Strickland et al, 1956).

3. Bulk density: The bulk density of a particle is determined by the bulk volume and the weight of dry powder in a graduated cylinder (Butler and Ransey, 1952).

1.8 Particle size distrubution

The particle size distribution of particles is a list of values or a mathematical function that describes the relative amounts of particles present in the samples separated according to the particle size (Jillavenkates et al, 2001).

To determine the particle size distribution many techniques are available. To determine the particle size distribution of Ibuprofen (the drug used in the current work) a laser

19

diffraction technique was used. The principle involved in the laser diffraction is the analysis of the angle of diffraction. When a laser beam pass through sample the diffraction of laser beam takes place. The angle of diffraction depends on the size of the particle. The particle size distribution was determined as it is required for particle motion equation and to predict the dissolution rate.

Laser diffraction was used as laser diffraction (Malvern Master sizer 2000 particle sizer) is highly advanced and has sophisticated data processor.

1.9 In vivo hydrodynamics

The solubility of a drug plays major role in the bioavailability of the drug. The dissolution of poorly soluble drugs depends on many factors like the properties of drug substance, pH of body fluids, composition of fluids and finally on the hydrodynamics of the Gastrointestinal (GI) fluids. The hydrodynamics of GI fluids can affect the diffusion layer thickness and consequently the bioavailability of the drug. Two factors are needed to study the effect of hydrodynamics in GI tract. The first factor is the finding the flow rate at which the GI fluid motility occurs and the second one is the isolation of the effect of hydrodynamics on dissolution from other factors which play a main role in the dissolution process.

GI motility

Various hydrodynamic conditions are observed in the GI tract and these are in both fed state and fasted state. The motility of the GI tract is due to nervous impulses. In the fasted condition the contraction pattern is due to the migrating myoelectric complex (IMMC) which consists of three phases lasting for 90-120 min. It starts from the proximal GI tract. The phase-1 prolongs for 45-60 minutes, in the phase 3 a phase exists called "quiescent phase" in which rapid movement of fluids occurs but only for 0-5 min. Due to the very short time the effect on dissolution is less. The phase 2 of IMMC is somewhat helpful and provides dissolution in which the same kind of motility is observed as in the quiescent phase but lasts for a longer time (30-45 min). In the case of the fed state the motility is

20

regular and chyme release serves as a dissolution medium and a rhythmic segmentation can be seen due to which the rate and frequency of the motility is different in the fed state than the fasted condition (Dressman et al, 2005).

EXPERIMENTAL

2.1 Materials and equipment used

Materials	supplier/manufacturer
Ibuprofen	Pharmatrans Sanaq AG
Potassium phosphate monobasic	Sigma
KH_2PO_4	
Sodium hydroxide	Rieldel-de Hean
Hydrochloric Acid	Sigma-Aldrich
HCl	
Sodium lauryl sulfate	Merck
Hydroxy propyl methyl cellulose	Colorcon
K4M	
Water	Elix 3/5/10/15 system

Instruments and accessories	Manufacturer
Thermostat pumping motor	Heto
UV spectrophotometer	Shimadzu
Digital IONALYSER pH meter	Orion research
Mettle analytical balance	Mettler
Malvern 2000 laser diffraction	Malvern
Particle size analyser	

Flow through apparatus, USP 4 (CE 7)	Sotax
Accupyc1330 Helium Pycnometer	Micromeritics instrument corporation
Ubblehode suspended level Viscometer	Poulten selfe & lee ltd
GF/F filter in powder cell 25 mm diameter circles which can Retain particles down to 2.7 μm	Whatman
GF/D filter in powder cell 25 mm diameter circle which can Retain particles down to 0.7 μm	Whatman
Diameter 47mm, pore size 0.45 μm, Membrane filter used for degassing	Pall Corporation
Diameter 13mm, pore size 0.2 μm, Membrane filter used for filtering Solutions	Pall Corporation
Helium gas	Air products

Computer software used	SUPPLIER
Mat lab software	IS services, TCD
Microsoft Excel	Microsoft windows 2007

2.2 Methods

2.2.1 Preparation of slurry

Slurry was prepared by taking 10 mg of drug in a 100 ml beaker to which 5 ml of dissolution fluid was added in small amounts slowly.

2.2.2 Dissolution medium used for dissolution studies

The dissolution medium used:

- Phosphate buffer pH 6.6

- Phosphate buffer pH 6.6 with 0.018 % SLS

- 0.1 M HCl with 0.018 % SLS

- Phosphate buffer pH5.8 with 0.5% HPMC & 1% HPMC

2.2.2.1 Preparation of phosphate buffer pH 6.6

0.2 M NaOH was prepared by dissolving 8 g of NaOH in a small amount of water and the solution was made up to 1 litre.

0.2 M KH_2PO_4 was prepared by adding 27.2 g of KH_2PO_4 to a small amount of water and then the solution was made up to 1 litre

Phosphate buffer pH 6.6: Phosphate buffer was prepared by adding 50 ml of 0.2 M KH_2PO_4 to deionised water and then 16.4 ml of 0.2 M NaOH was added and made up to 200 ml [United States Pharmacopoeia, 2005].

2.2.2.2 Preparation of 0.1 M HCl

8.2 ml of concentrated HCl was added to 1 litre volumetric flask and made up to 1 litre with water.

2.2.2.3 Preparation of phosphate buffer in 0.018 % SLS

0.036 g of SLS was accurately weighed and was added to a 200 ml volumetric flask along with the 0.2 M NaOH and 0.2 M KH_2PO_4 as described in the phosphate buffer preparation.

2.2.2.4 Preparation of 0.1 M HCl in 0.018 % SLS

An accurately weighed amount of 0.18 g SLS was taken in a beaker along with 8.2 ml concentrated HCl and then the resulting solution was added to 1 litre volumetric flask and made up to 1 litre.

2.2.2.5 Preparation of viscous medium pH 5.8

Viscous media was prepared by using HPMC K4M premium EP. One third of water of total water needed was heated up to 80 °C and then HPMC was dissolved in small amounts with constant stirring, the resultant dispersion was allowed to cool. The rest of water in which required amount of KH_2PO_4 and NaOH were dissolved was added to the HPMC dispersion.

2.2.2.6 Preparation of viscous medium in 0.018 % SLS

Viscous medium in 0.018 % SLS was prepared by adding 0.18 g of SLS to water and then required amount of KH_2PO_4 and NaOH were added. The prepared solution was then added to the prepared HPMC dispersion.

2.2.3 Degassing

The dissolution medium prepared (phosphate buffer pH 6.6 with SLS and without SLS, 0.1 M HCl with SLS) was degassed by using degasser to prevent interference with any gaseous matter in the solution. To degassing the dissolution medium the filters used were membrane filters of pore size 0.45 micrometer. Viscous medium was not degassed as the filters used in degassing were 0.45 micrometer through which the viscous medium did not flow.

25

2.2.4 Dissolution methods

The model drug used in the current work was Ibuprofen drug. Dissolution was carried out at different flow rates. The problem faced in using the flow through apparatus was maintaining consistency of flow rate. So immediately after setting the flow rate it is necessary to check the volume of fluid. This was done by collecting fluid in flask per minute (flow rate).

Dissolution of Ibuprofen was carried out in the tablet cell of 22.6 mm diameter size and in the powder cell of 12 mm diameter size in the flow through apparatus (fig 1.3). The Ibuprofen used was a technical sample from Pharmatrans Sanaq Ag (IBUPROFEN DC 100). Dissolution was carried out in different cells (tablet cell and powder cell) to observe the effect of hydrodynamics with the flow rate in the cell.

2.2.4.1 Dissolution in the tablet cell

In this dissolution the cells were firstly filled with a synthetic red ruby bead of diameter 5 mm to prevent leaking from the cell, and then the conical part of the cell was filled with small beads of diameter 1 mm which can provide a laminar flow in the cell (Kakhi, 2009). After filling of beads in the cell the slurry was placed, then the cap of the cell was closed and arranged in the dissolution apparatus. The apparatus was set at 37°C and the buffer solution as well kept in water bath and maintained at 37° C temperature.

The dissolution was carried out at different flow rates, five flow rates were used, and they were 4, 7, 10, 16 and 20 ml/min. From the beginning of the experiment samples were collected at regular intervals for 1-2 hrs.

2.2.4.2 Dissolution in the powder cell

In the powder cell dissolution was carried out using two methods, the methods vary in the arrangement of insert (shown in fig 2.1 and 2.2) and the methods used were named as method 1 and method 2. In the powder cell the drug was placed in the form of powder

26

instead of slurry. Dissolutions were carried out in method 1 and 2 with phosphate buffer pH6.6 (with SLS and without SLS). In 0.1 M HCl and viscous medium the dissolutions were carried out using method 1. In the powder cell the flow rates employed were 10,13,16,20 and 25 ml/min.

2.2.4.3 Cells used for dissolution

In this dissolution the cells were firstly filled with synthetic red ruby bead of diameter 5 mm to prevent leaking from the cell and then the conical part of the cell was filled with small soda lime glass beads of size 1mm which can provide a laminar flow in the cell (Kakhi, 2009).

2.2.4.4 Construction of powder cell in method 1

The powder cell has three parts, the bottom conical part, middle drug holder and the cap. The middle cylindrical part was fitted with filter sieve and then with a filter which has a retention capacity for particles up to 2.7 micrometers (25 mm diameter, GF/D membrane filter) and then second filter sieve.

Then drug (5 or 10 mg) was placed on the filter and then sieve insert was placed over the the drug on the sieve. At the top of the cell the second filter sieve was placed, followed by a GF/D membrane filter and then GF/F membrane filter as shown in fig 2.1. The apparatus was maintained at 37°C and the buffer solution also maintained at 37°C temperature. Three replicates of each dissolution were carried out. Fig 2.1 shows the construction the powder cell using method 1

outlet   filter (GF/F)   Insert

Filter (GF/D)

Ibuprofen   1 mm glass beads   Filter

sieve

Filter (GF/D)   Inlet

5 mm Red ruby bead
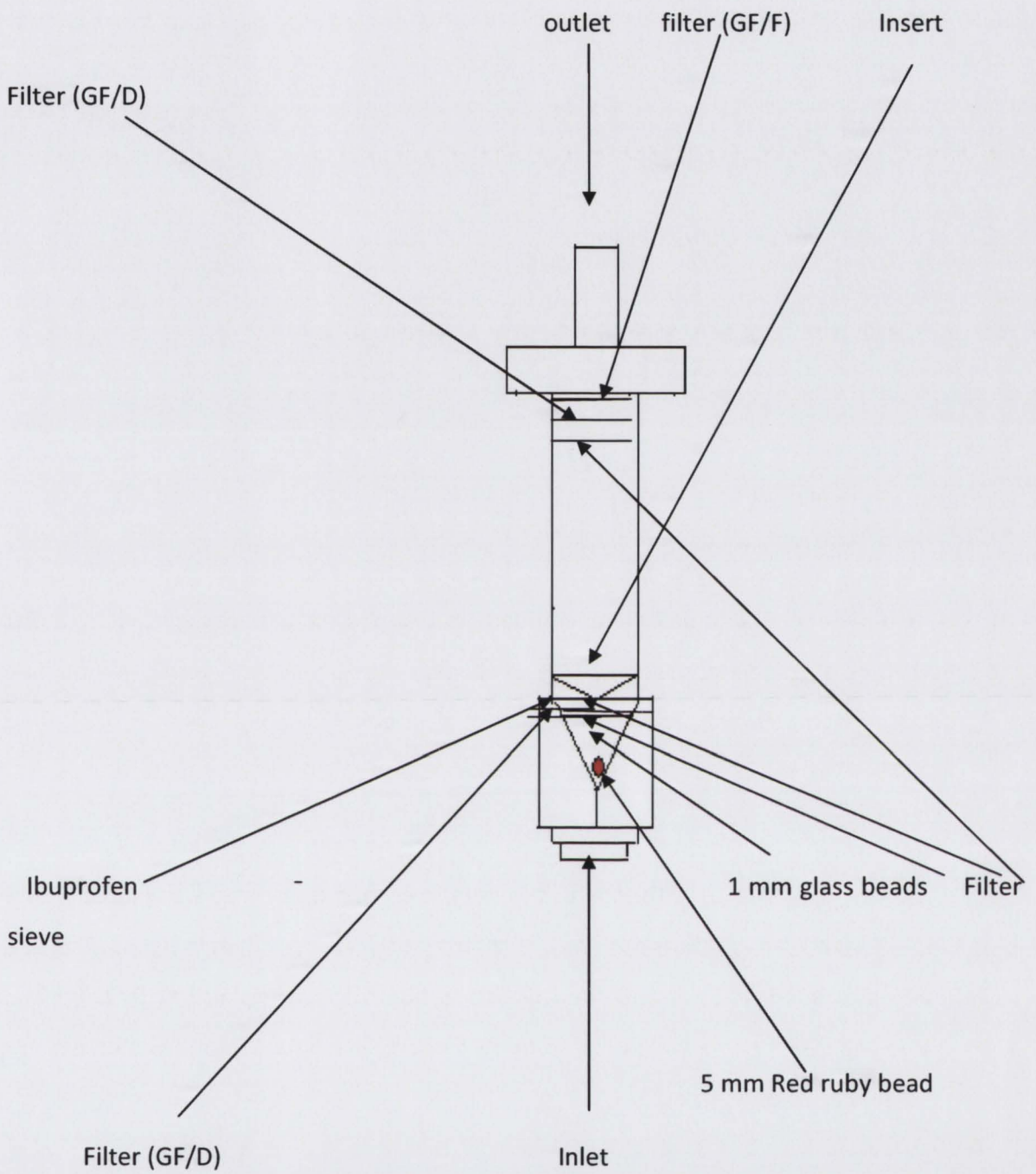
Fig 2.1 Construction of powder cell in method 1

2.2.4.5 Construction of powder cell in method 2

Outlet   Filter sieve   Insert

Filter (GF/D)   Filter (GF/F)

Ibuprofen   1mm glass beads

Filter (GF/D)   5mm red ruby bead
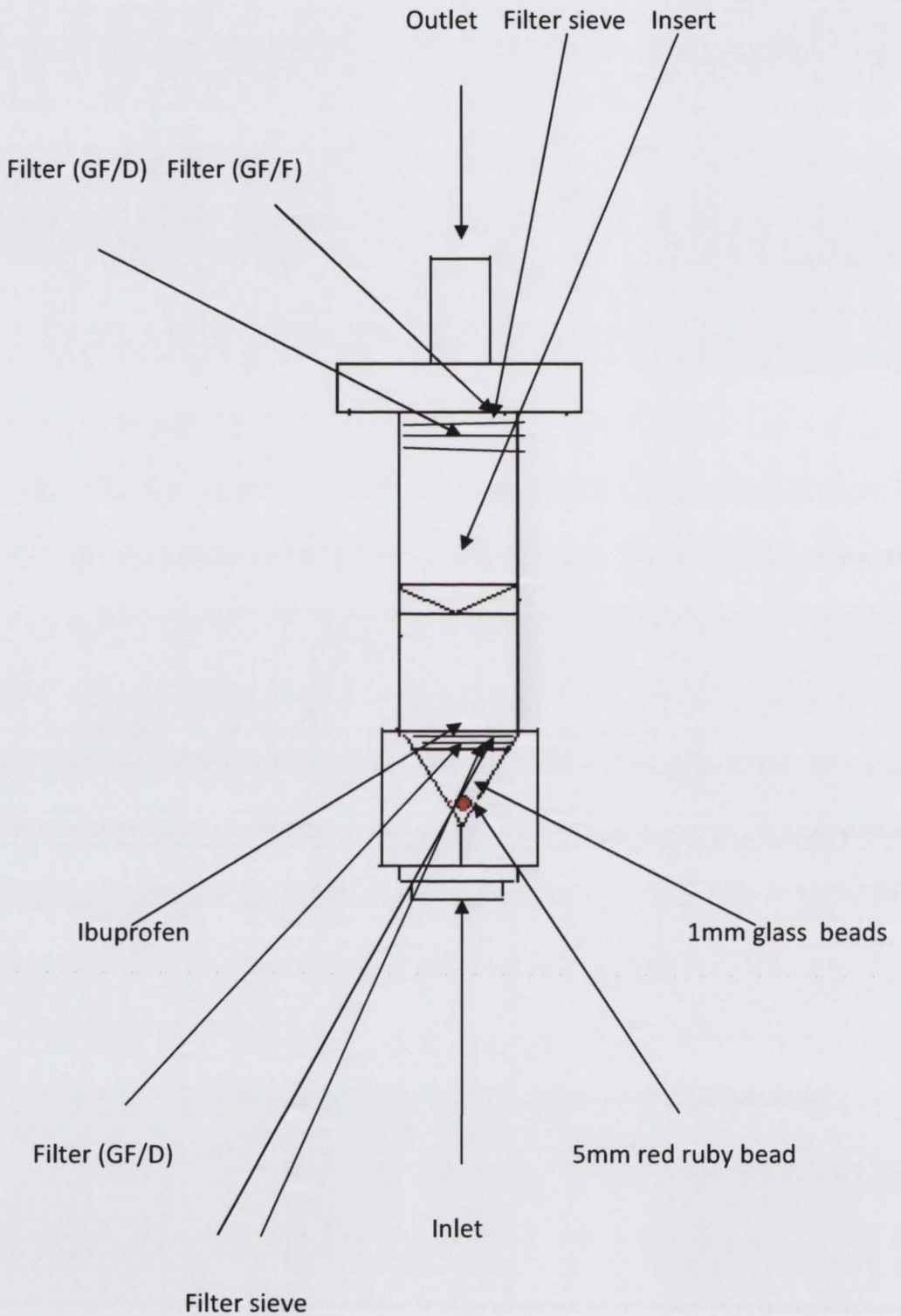
Inlet

Filter sieve

Fig 2.2 Construction of powder cell in method 2

The construction of cell in method 2 is same as in method 1 but differs only in the placement of insert. In method 2 insert was placed over the half way up the cell and the filters used were same as in method 1. Fig 2.2 shows the construction of the powder cell using method 2.

2.2.4.6 Dissolution in viscous medium

Dissolutions were done in the powder cell using viscous medium. As the dissolution medium was highly viscous the medium didn't flow freely through the powder cell, so dissolutions were carried out without the filters at the top of the cell (GF/D and GF/F) in 0.5 % HPMC dissolution medium. The same problem was encountered with 1 % HPMC dissolution medium with the filter at the bottom and without the filters at the top, so dissolutions were done without filter at the bottom of the cell and at the top of the cell. Dissolution was carried out only at flow rate 8 ml/min with the viscous medium. Higher flow rates were attempted, however, at higher flow rate the dissolution medium collected in the water bath collecting tube which is underneath the apparatus due to obstruction caused by the viscous medium at the head of the cell and the force due to higher flow rate made the dissolution medium collect in the water bath collecting tube.

Dissolutions tests were done in the flow through apparatus using closed system for the viscous medium and dissolutions were done in open system for phosphate buffer and 0.1 M HCl medium. At regular intervals samples were collected and analysed. As no filters were used in the powder cell during dissolution the collected samples were filtered and then analysed. To filter the samples in the dissolution with 0.5% HPMC the filter employed was 25 mm diameter with 0.7 μm pore size (GF/D- Whatman filter) but in dissolution with 1 % HPMC the filter used was 25 mm diameter with 2.7 μm pore size (GF/F –Whatman filter).

2.2.5 Analytical method

The samples were analysed by using UV visible spectroscopy at 221 nm (used for dissolutions in phosphate buffer and viscous medium). The samples in 0.1 M HCl were analysed using UV visible spectroscopy at 220 nm. From the results the concentration of drug, cumulative amount of drug dissolved, cube root of drug dissolved and cube root dissolution rate constant were determined.

2.2.6 Solubility measurement

To measure the solubility of Ibuprofen the method employed was super saturation solution method in which three 10 ml glass ampoules were used. In each glass ampoule 108 mg of drug was taken and 9 ml of dissolution medium was added (the saturation solubility of Ibuprofen in literature is 2 mg/ml at pH 6.4) (Healy, 1995). Glass ampoules were kept in an agitating water bath at 37°C for 24, 48, 72 and 96 hours. After 24, 48, 72 and 96 hours samples were collected from each glass ampoule, filtered, diluted and the concentration of the drug dissolved were analysed. The pH of the saturated solution was measured (as pH of a solution can affect the solubility) after analysing samples.

2.2.7 Density measurement

Dissolution medium: To measure the density of a dissolution medium a procedure was adopted in which the volume of a density bottle was determined as the first step. It was done by measuring the weight of the empty bottle, W1 and by measuring the weight of the bottle with water which is W2.Therefore the weight of water filled in the bottle is W2-W1.From the literature the density of water was found to be 997.222 kg/m^3 at 37°C (Lide, 1995-1996). The volume of bottle was determined using weight of water and the density of the water (997.222 m^3). The final step is the measurement of density of dissolution medium which was done by weighing empty bottle, W1 and then bottle was filled with the dissolution medium up to the mark and then the weight of bottle with dissolution medium was measured, W3, from which the weight of fluid was measured,W3-W1. The volume of bottle is same as the volume occupied by water from which the density of

31

dissolution medium was measured. Using the weight of dissolution medium and volume of bottle the density of dissolution medium was measured. The same procedure was repeated for three replicate samples.

True density of Ibuprofen: True density was determined by using helium pycnometer in which the weight of empty cap was measured and then with the ibuprofen particles by which the weight of particles was calculated. The sample was kept in helium pycnometer for 2 hours to measure the volume of the particles. From the results of helium pycnometer the true density of ibuprofen particles were determined.

Particle density: By using porosimetry the particle density of Ibuprofen was measured. It was done by MCA services, Meldreth Cambs, UK. The sample was analysed by using a method SC 11+ BD which informs the pore size distribution. The mercury used for the analysis has surface tension of 480.00 dynes/cm and density of 13.53 gm/ml. Mercury was passed at pressure 0.0 to 30000.00 psia. The parameters total intrusion volume of mercury, total pore area, median pore diameter, and average pore diameter, bulk density, apparent bulk density and porosity were determined.

2.2.8 Particle size distribution

Particle size distribution was performed using laser diffraction technique and carried out using a Malvern Mastersizer 2000 particlesizer (Malvern instruments Ltd.,Worcestershire,UK) with scirocco 2000 accessory. The dispersive air pressure used was 2 bar. Samples were generally run at vibration feed rate of 50 %. The particle size reported is the median particle size of the volume distribution.

2.2.9 Construction of calibration curve

The calibration curve was constructed by plotting a graph of known concentration on x-axis and the absorbance of the corresponding concentration on y-axis. Known concentrations were prepared by preparing stock solutions.

Stock solution in phosphate buffer was prepared by dissolving 50 mg of Ibuprofen in 500 ml of phosphate buffer pH 6.6

Stock solution in 0.1 M HCl was prepared by dissolving 10 mg of Ibuprofen in 1000 ml of 0.1 M HCl

To check the interference of SLS with phosphate buffer, 0.1 M HCl and viscous medium, dissolution with SLS was taken in one cuvette (as a sample) and dissolution medium without SLS in one cuvette (as a standard) and the absorbance showed no interference. Additionally dissolution medium was kept for 3-4 days with SLS and no precipitation or colour change was observed. Therefore no calibration curve was constructed for dissolution medium with SLS. Same methods were done for HPMC to check for interference and no interference was seen.

Preparation of known concentration

1. From the stock solution of Ibuprofen in phosphate buffer concentrations of 0.0001, 0.0003, 0.0005, 0.001, 0.003, 0.005, 0.01, 0.02, 0.03, 0.04, and 0.05 mg/ml were prepared

2. From the stock solution of Ibuprofen in 0.1 M HCl concentration of 0.00015, 0.00025, 0.0005, 0.0015, 0.0025, 0.005 and 0.001 mg/ml were prepared.

Absorbance was measured from the solutions of known concentration and a graph of absorbance versus concentration was plotted shown in appendix II

2.2.10 Cube root dissolution rate constant

In order to apply the cube root law the changes of remaining weight was studied with the function of time (Hixon and Crowell, 1931). According to the cube root law the dissolution rate can be calculated as there is a decrease in surface area with respect to time.

When sink conditions apply, the cube root can be written as (equation 1.4),

$$W^{1/3}{}_t = W_o{}^{1/3} - Kt$$

Where W_t denote that weight of solid remains at time t = 0, and K represents the dissolution rate constant. A plot of $W_o^{1/3} - W_t^{1/3}$ vs. time yield a straight line with slope K (Anderberg and Nystorm, 1990).

2.2.11 Prediction of dissolution using particle motion equation

Theoretically the dissolution of Ibuprofen in the phosphate buffer at pH 6.6 with and without 0.018 % SLS, 0.1 M HCl with 0.018 % SLS, Viscous medium (0.5 % HPMC and 1 % HPMC) was predicted.

To find the relative velocity and particle velocity a code was used in MATLAB. Solving the following particle motion equation (equation 1.10)

The determined relative velocity was implemented in the equation (eqn 1.9)

The dissolution rate was predicted by considering the initial particle diameter of 0.0002 m from which the relative velocity of the fluid was determined in the MATLAB. By using the equation (1.9) the value of the φ was determined.

The cumulative amount of drug was calculated from the amount of drug dissolved and from which the amount of drug undissolved was determined and finally the radius of the undissolved particle was calculated.

2.2.12 Predicting dissolution according to the BCS

The bio-pharmaceutics drug classification system was introduced to correlate in vitro drug dissolution with the in vivo bioavailability based on drug dissolution and gastrointestinal permeability.

Dose number, Dissolution number and absorption number were three dimensionless parameters which control the drug dissolution and absorption.

By using the BCS principle a dissolution rate was predicted. Dissolution number can be calculated by using the equation

$$Dn = (DCs/r_o)(4\pi r_o^2 / 4/3\pi r_o^3) t_{res}$$ Eqn 2.1

Where t_{res} is mean residence time, D – diffusion coefficient, Cs – saturated solubility

The r_o taken as the initial radius which is 0.01 cm (the average particle size distribution determined shown in appendix V), a product of DCs was determined. The amount of the drug dissolved was calculated by using the equation from BCS know as dissolution number, (Amidon et al, 1995)

$$Dn = t_{res}3DCs/\rho r_o^2$$ Eqn 2.2

When the equation was simplified with density the equation can be rewritten as

$$dm/dt = DCs4\pi r_o$$ Eqn 2.3

by using the above equation amount of drug dissolved was determined.

RESULTS

3. RESULTS

3.1. Solubility studies

Solubility is the property of solid, liquid and gas to dissolve in the solvent resulting in a homogeneous solution.

A saturated solution can be defined as a solution in which the solute is in equilibrium with the solid phase. The solubility of a compound depends on solvent used and as well as on temperature and pressure. The driving force for dissolution depends on the thickness of the diffusion layer and the concentration of the drug which is dissolved. Hence the solubility is the key factor in the Noyes- Whitney equation.

The solubility of ibuprofen: The saturated solubility of ibuprofen in phosphate buffer pH 6.6 is 2.36 mg /ml after 24 hours, 2.88 mg/ml after 48 hours and 2.63 mg/ml after 72 hours. The saturated solubility of ibuprofen in the presence of sodium lauryl sulphate is 2.66 mg/ml after 24 hours, 2.81 mg/ml after 48 hours and 2.61 gm/ml after 72 hours

3.1.1 Conclusion

Table 3.1 shows the saturated solubility values of ibuprofen in different dissolution medium. The Highest determined values were used as when the value measured at a later time point was lower, the change in the solubility was considered negligible as the standard deviation was not significantly differ between these points.

Saturated solubility in the phosphate buffer at pH 6.6 with SLS (0.018 %) and without SLS were studied. The saturated solubility of Ibuprofen in phosphate buffer at pH 6.6 with SLS (0.018 %) is 2.81 mg/ml and in phosphate buffer at pH 6.6 without SLS is 2.88 mg/ml.

Hours	Phosphate buffer C_s- (mg/ml) pH 6.6		0.1 M HCl C_s- (mg/ml)		Viscous medium 0.5 % w/v HPMC C_s- (mg/ml) pH 5.8		Viscous medium 1 % w/v HPMC. C_s- (mg/ml) pH 5.8	
	With SLS	Without SLS	With SLS	Without SLS	With SLS	Without SLS	With SLS	Without SLS
After 24 hours	2.66	2.36			0.33	0.43	0.28	0.27
(Std dev)	(0.12)	(0.62)	-	-	(0.08)	(0.08)	(0.04)	(0.06)
After 48 hours	2.81	2.88			0.53	0.4	0.29	0.37
(Std dev)	(0.18)	(0.03)	-	-	(0.15)	(0.008)	(0.01)	(0.43)
After 72 hours	2.61	2.63	0.06	0.083	0.47	0.46	0.35	0.35
(std dev)	(0.05)	(0.12)	(0.005)	(0.004)	(0.01)	(0.02)	(0.04)	(0.02)
After 96 hours	-	-	0.072	0.075	0.53	0.44	0.37	0.33
(std dev)			(0.005)	(0.005)	(0.04)	(0.03)	(0.01)	(0.02)

Table 3.1 Saturated solubility studies for Ibuprofen in different buffer solutions

3.2. Dissolution studies in the tablet cell

3.2.1 Dissolution of Ibuprofen in the tablet cell: The dissolution studies in the tablet cell were carried out at different flow rates to investigate the effect of hydrodynamics on the dissolution rate.
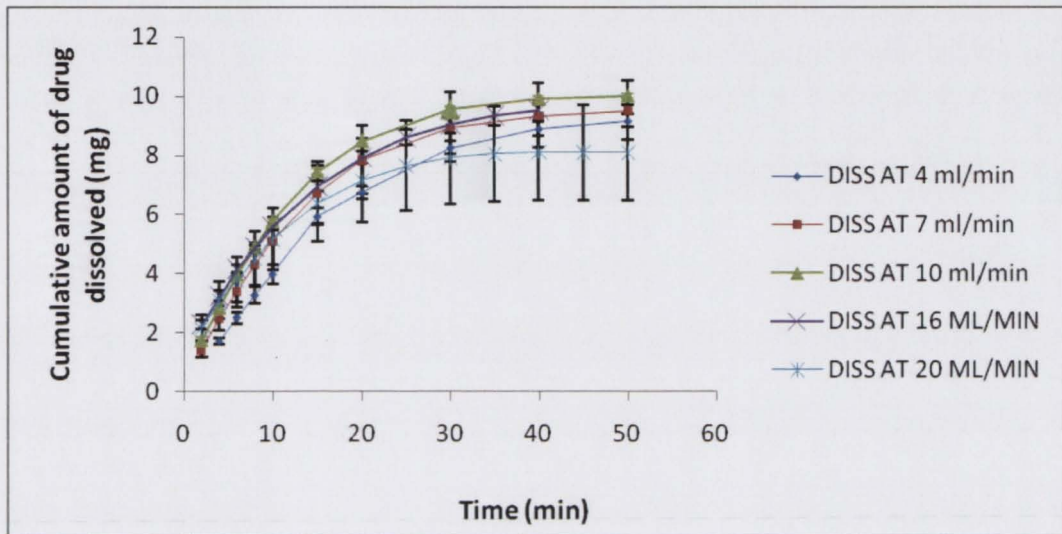

Fig 3.1 Cumulative amount of drug dissolved vs. time

The cumulative amount of drug was obtained from the amount of drug dissolved in each dissolution time period. The dissolution profile was similar at all flow rates employed as shown in the fig 3.1. The similar dissolution profile at different flow rates is due to having a constant particle relative velocity at different flow rates employed.

3.2.1 Cube root dissolution rate constant

As described in section (2.2.10) the cube root dissolution rate constant was determined. The cube root of amount drug dissolved was plotted against time which showed a similar drug release pattern at different flow rates employed (fig 3.2). Dissolution at 4 ml/min shows a slower drug dissolution which is due to the flow rate employed (4 ml/min). At lower flow rate the velocity of the dissolution medium in parts of the cell may be lower than the calculated velocity at flow rate employed due to the effect of the cell wall on fluid flow (discussed in section 1.3.1).

38

The cube root dissolution rate constant obtained was plotted against the flow rate as shown in the fig 3.3 to see the effect of flow rate on the dissolution rate constant.

From the fig 3.3 it can seen that the cube root dissolution rate constant is constant at all flow rates employed. The consistency in the cube root dissolution rate constant is due to having a constant relative velocity in the flow through apparatus shown in fig 3.4. The relative velocity at different flow rates in the tablet cell was determined to be as 0.538 mm/s.
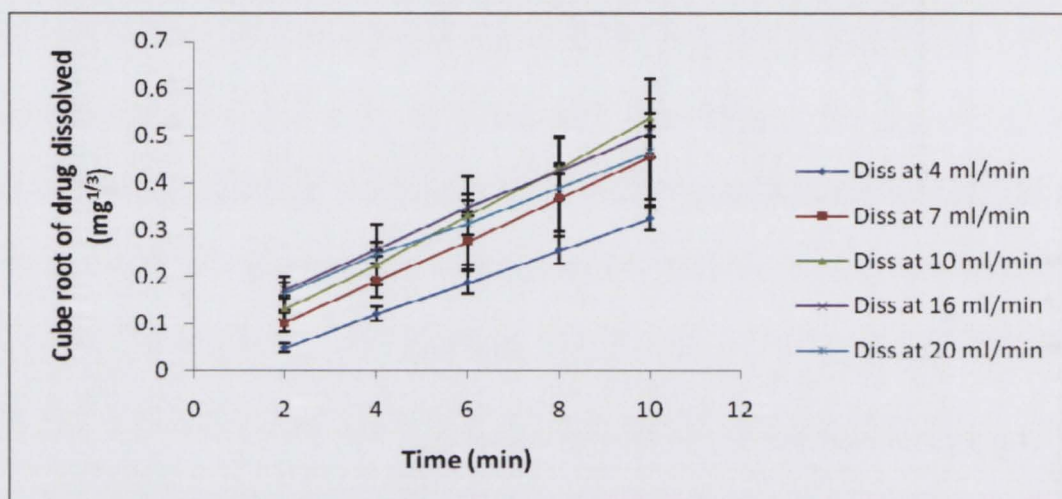

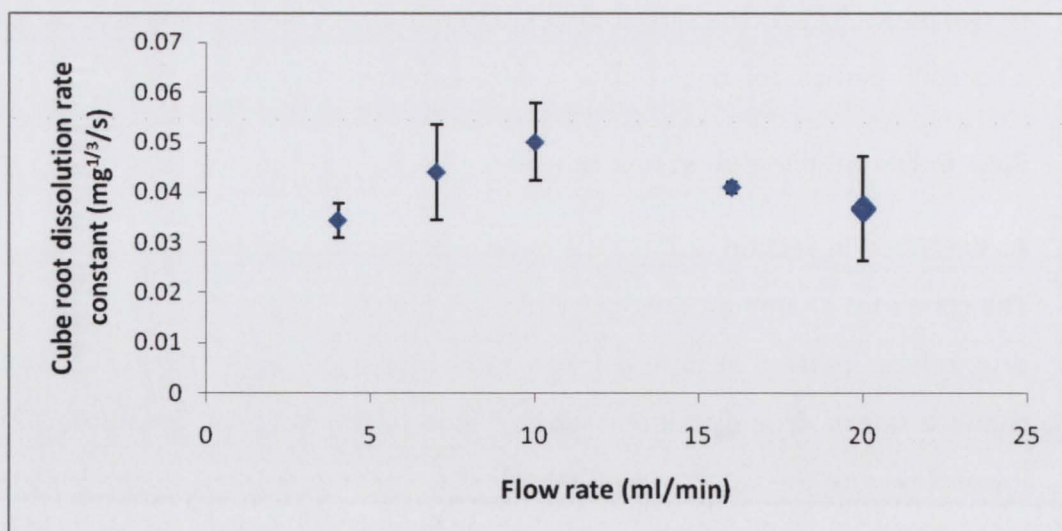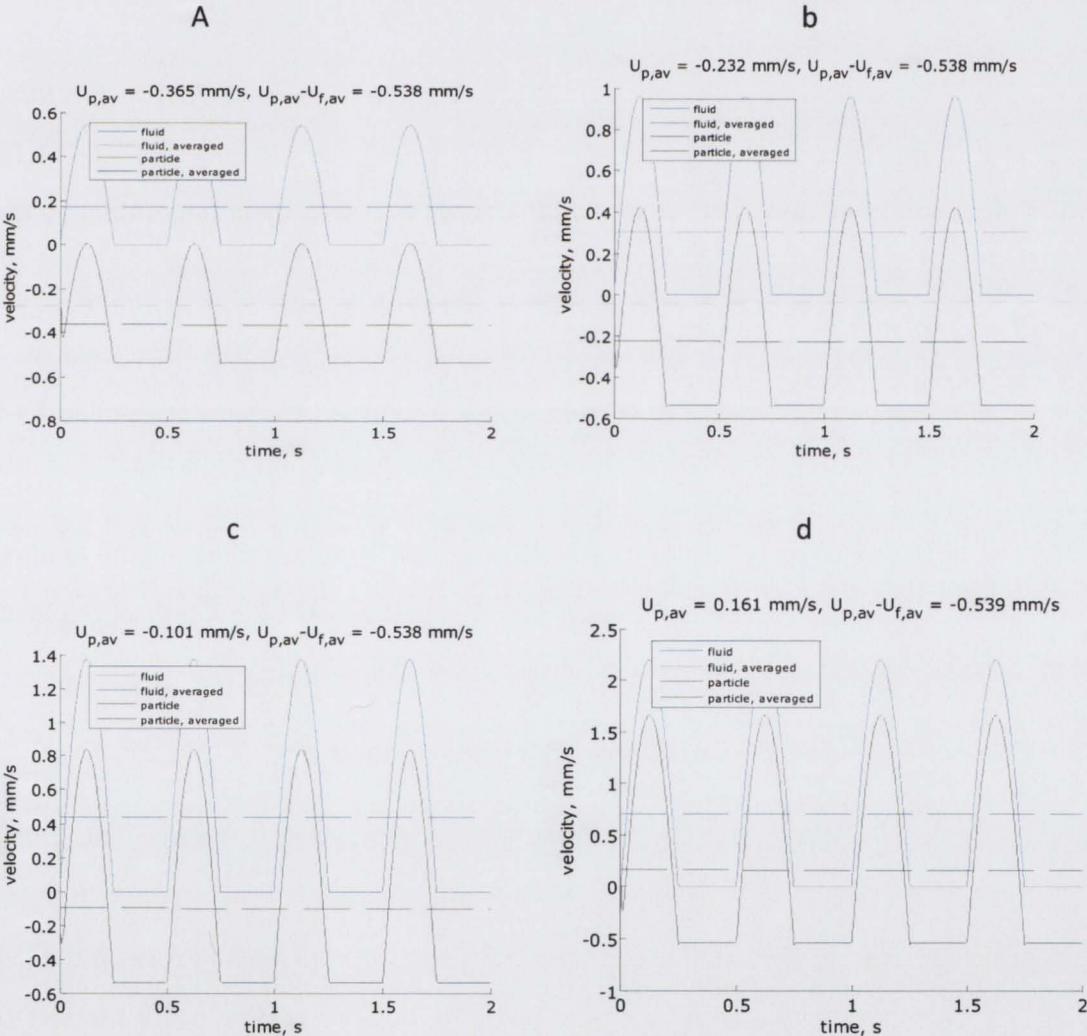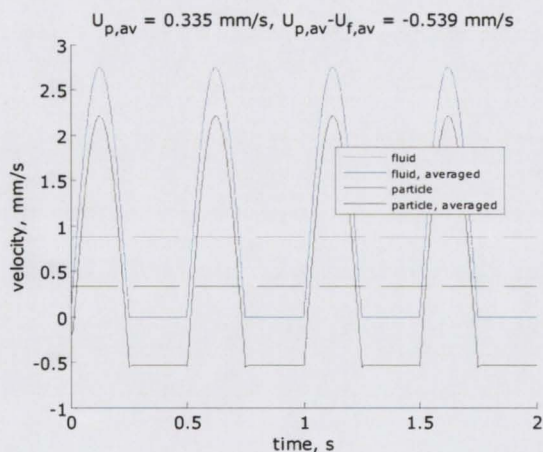*Fig 3.2 Cube root of drug dissolved with respect to time*

Fig 3.3 Cube Root Dissolution Rate Constant vs. Flow rate

39

From the fig 3.3 it can be seen that the cube root dissolution rate constant is nearly the same at different flow rates employed and didn't increase with the increase in the flow rate. The reason for having constant cube root dissolution rate constant is due to having a constant relative velocity in the tablet cell. The relative velocity in the tablet cell determined was 0.538 mm/s and constant at all flow rates employed. Fig 3.4 shows the relative velocity graphs obtained in the MATLAB at different flow rates. When the flow rate is increased the velocity of dissolution medium increased and the velocity of particles increased along with the dissolution medium.

A

$U_{p,av}$ = -0.365 mm/s, $U_{p,av}$-$U_{f,av}$ = -0.538 mm/s

b

$U_{p,av}$ = -0.232 mm/s, $U_{p,av}$-$U_{f,av}$ = -0.538 mm/s

c

$U_{p,av}$ = -0.101 mm/s, $U_{p,av}$-$U_{f,av}$ = -0.538 mm/s

d

$U_{p,av}$ = 0.161 mm/s, $U_{p,av}$-$U_{f,av}$ = -0.539 mm/s

40

$U_{p,av} = 0.335$ mm/s, $U_{p,av}-U_{f,av} = -0.539$ mm/s

e

Fig 3.4 The average particle velocity and the average relative velocity in the tablet cell at different flow rates. (a- at flow rate 4 ml min-1, b- at flow rate 7 ml min^{-1}, c- at 10 ml min^{-1}, d- at 16 ml min^{-1} and e- at 20 ml min^{-1}). The relative velocity in the graphs is represented as $U_{p,av} - U_{f,av}$. and are a constant value.

The negative value of the relative velocity represents that the flow (relative velocity) which is in opposite direction to the gravitational force (particles are pulled by both the gravitational force and the force due to the flow of dissolution medium).

Dissolutions were carried out using the powder cell as in the tablet cell the loading of drug is in the form of slurry which may affect the dissolution rate (as drug is placed in the dissolution medium (as slurry) before conducting dissolution).

3.3 Dissolution studies in the powder cell using method 1

In the powder cell two methods were employed. In method 1 the insert was placed over the drug (particles have space to move with the dissolution medium but less space compared to method 2) and in the method 2 insert was placed half way up the cell. Fig 3.5 shows the dissolution profiles obtained at different flow rates in the powder cell using method 1. The dissolution profiles were the same at all flow rates used, similar dissolution profiles were due to having constant relative velocity at all flow rates employed in the powder cell. At flow rate 10 ml/min the dissolution profile is slightly lower; this may be,

41

due to the wall effect in which the flow rate is slower at the walls than the flow rate employed.
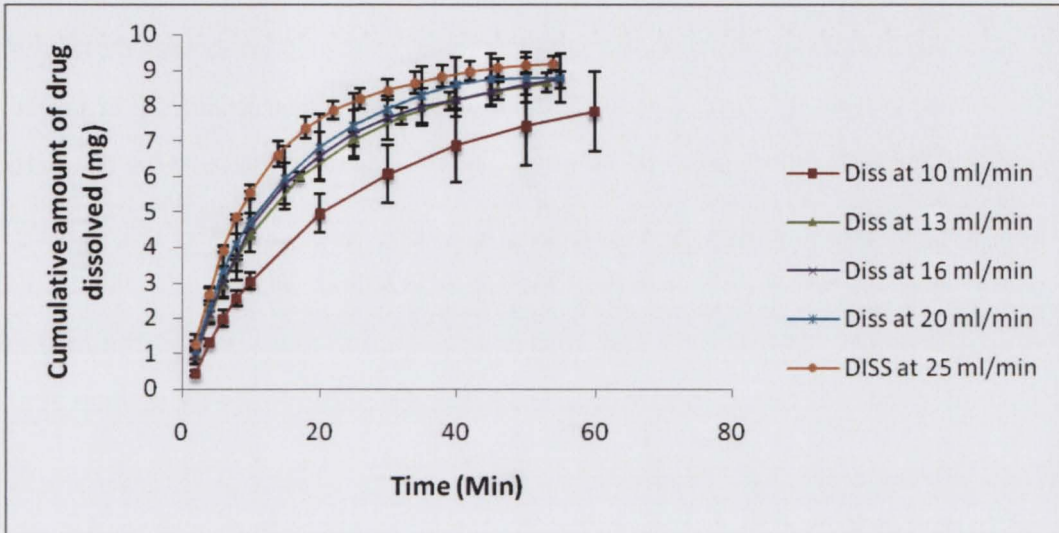

Fig 3.5 Cumulative amount of drug dissolved at different flow rates using method 1 in the powder cell

3.3.1 Cube root dissolution rate constant

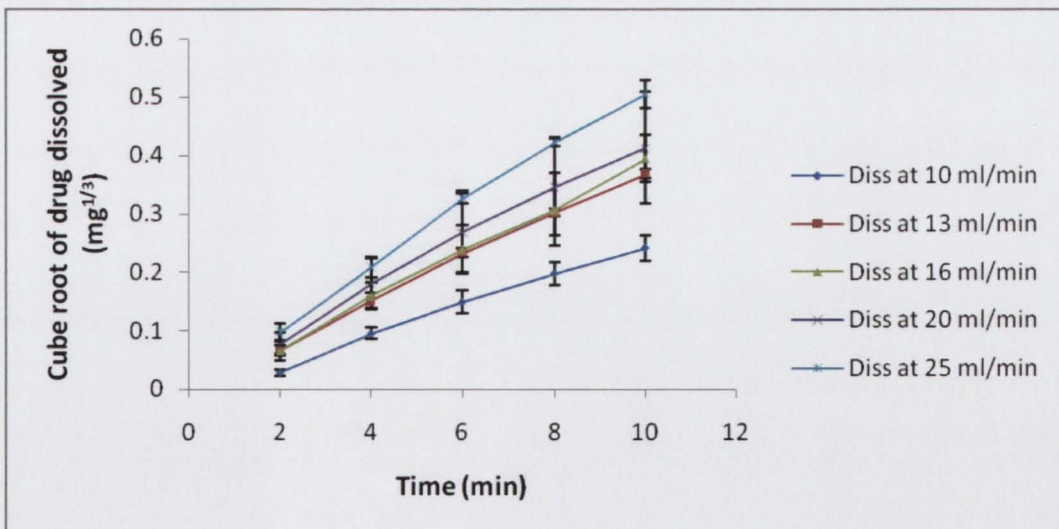As described in the section 2.2.10 the cube root dissolution rate constant was determined

Fig 3.6 Cube root of amount of drug dissolved with respect to time at different flow rates

From the fig 3.6 it can be seen that the cube root of drug dissolved at different flow rates have similar drug release pattern and the cube root of drug dissolved doesn't depend on the flow rate employed. The cube root of drug dissolved at flow rate 10 ml is slower and at 25 ml/min the cube root of drug dissolved is faster. The slower dissolution rate at 10 ml/min may be due to the wall effect which is seen predominantly at lower flow rate in which the flow of dissolution medium near the wall is lower than the actual flow rate employed (as discussed in section 1.3.1). Higher dissolution rate at 25 ml/min is due to the higher flow rate which makes the flow turbulent (discussed in section 1.3.1.2). The turbulent flow can form the eddies in the dissolution medium and the formed eddies can increase the mass transfer rate and finally the dissolution rate (Dressman et al, 2005).
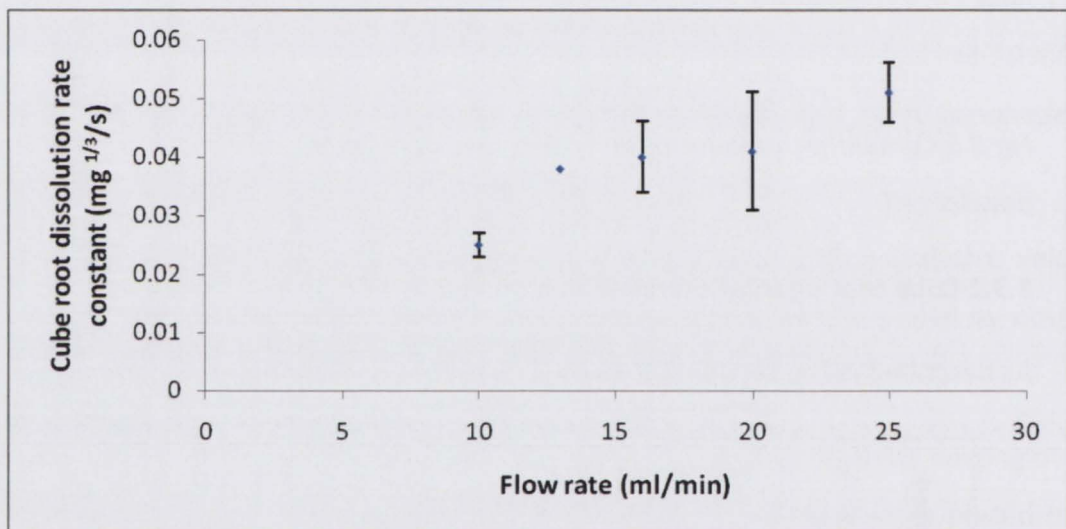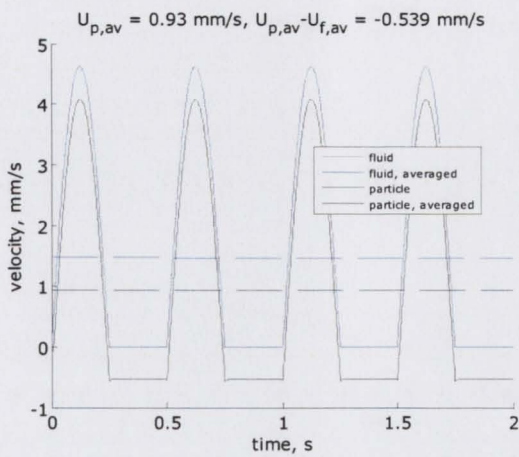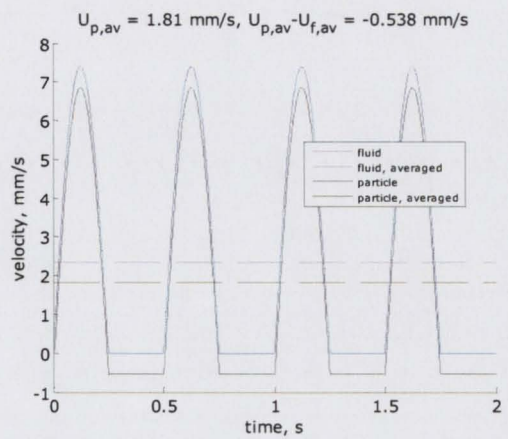

Fig 3.7 Cube root dissolution rate constant against flow rate
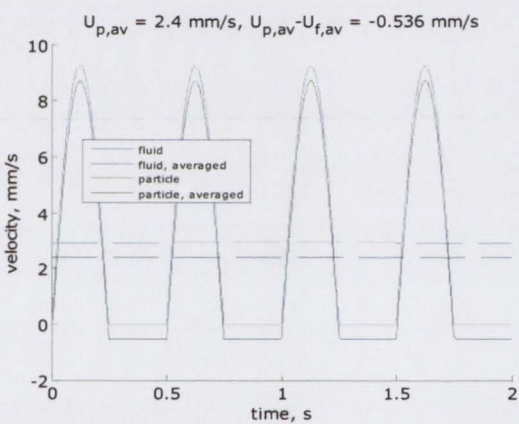
From the fig 3.7 it can be concluded that overall cube root dissolution rate constant didn't change with the flow rate but at flow rates 10 and 25 ml/min the cube root dissolution rate constant was slightly different.
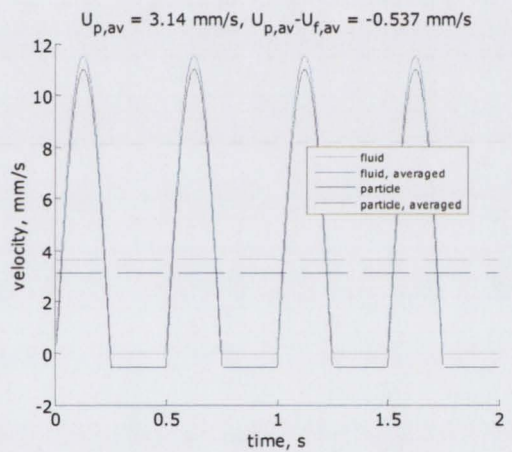
Fig 3.8 The average particle velocity and average relative velocity values for dissolutions in the powder cell using method 1 (a-at flow rate 10 ml min^{-1}, b- at flow rate 13 ml min^{-1}, c- at flow rate 16 ml min^{-1}, d- at flow rate 20 ml min^{-1} and e- at flow rate 25 ml min^{-1}). The relative velocity in the graphs is represented as $U_{p,av} - U_{f,av}$ and a constant value.

3.3.2 Predicted dissolution using particle motion equation

A s discussed in the section 2.2.11 dissolution was predicted in phosphate buffer pH 6.6.
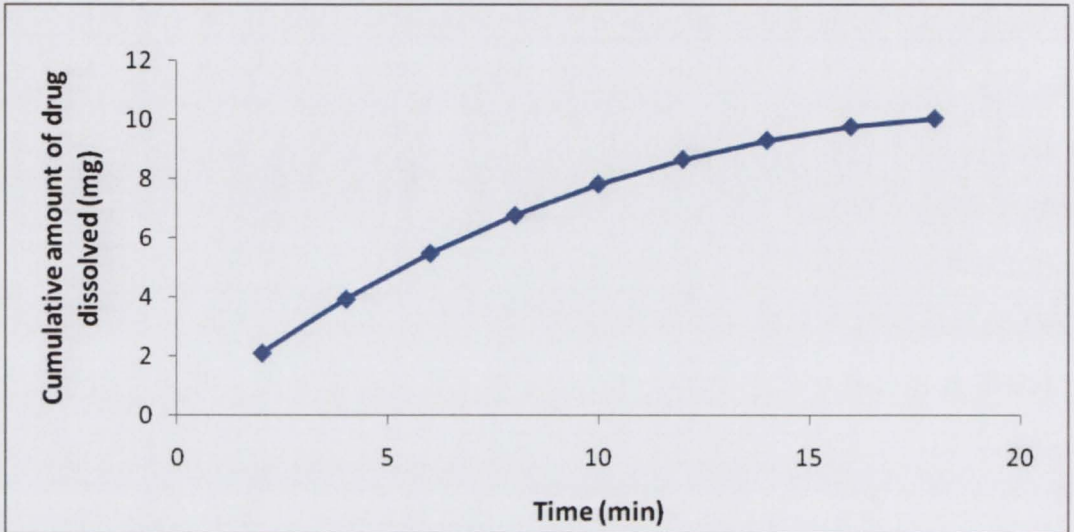

Fig 3.9 Predicted dissolution using particle motion equation

Fig 3.9 shows the predicted dissolution in the powder cell. The predicted dissolution takes 18 minutes to completely dissolve 10 mg of drug.
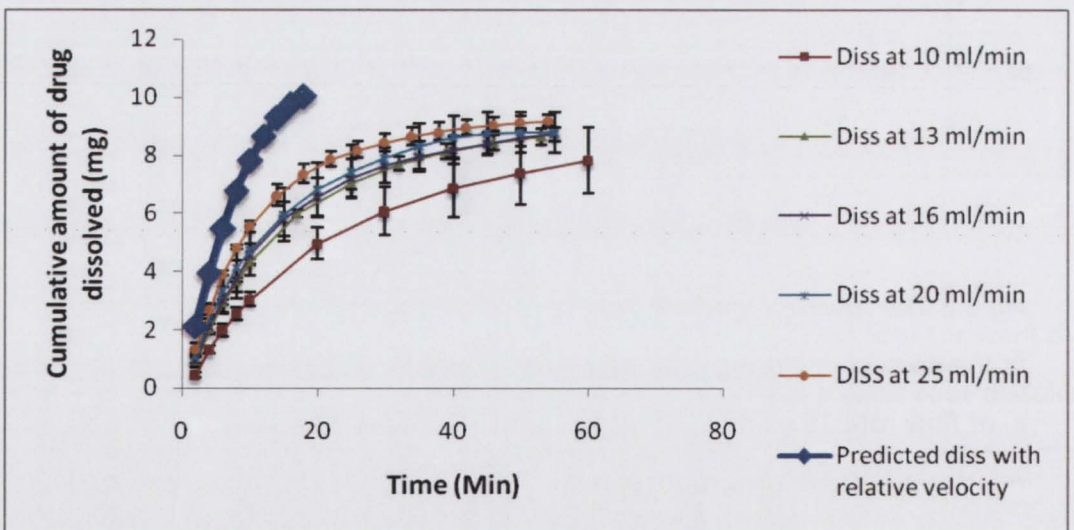

Fig 3.10 Predicted dissolution VS dissolution in method 1

When the dissolution profile of the prediction and the experimental dissolution is compared, the predicted dissolution is faster than the experimental dissolution. Fig 3.10 shows the comparison of the predicted dissolution with the experimental dissolution in the powder cell using method 1.The predicted dissolution is faster than the experimental dissolution, which may be due to clumping of particles in the powder cell.

3.3.3 Predicting dissolution according to BCS

As discussed in section 2.2.12 dissolution was predicted using the BCS equation (2.3) shown in fig 3.11. To dissolve 10 mg of drug in the predicted dissolution using BCS it takes nearly 60 minutes and in the experimental dissolution it takes nearly 60 minutes shown in the fig 3.10 but the time taken to dissolve 10 mg of drug in the predicted dissolution using relative velocity is 18 minutes.

The predicted dissolution using relative velocity is faster than the experimental dissolution potentially due to clumping of particles in the powder cell hence the experimental dissolution is slower and comparable to the predicted dissolution using BCS. However in the BCS prediction the relative velocity parameter is not used which might be the reason for the slower prediction in comparison to the predicted dissolution using relative velocity. Additionally, this may result in the BCS predicted dissolution rate being slower than the experimental dissolution as the parameter relative velocity is involved. The reason for experimental rate being comparable with the predicted dissolution using BCS may be is clumping of particle in the powder cell which reduces the total surface area exposed to the dissolution medium results in the decrease in the dissolution rate.

In predicting dissolution according to BCS the equation is taken from the dissolution number (section 2.2.19). Dissolution number is defined as the ration of the mean residence time to the dissolution time.
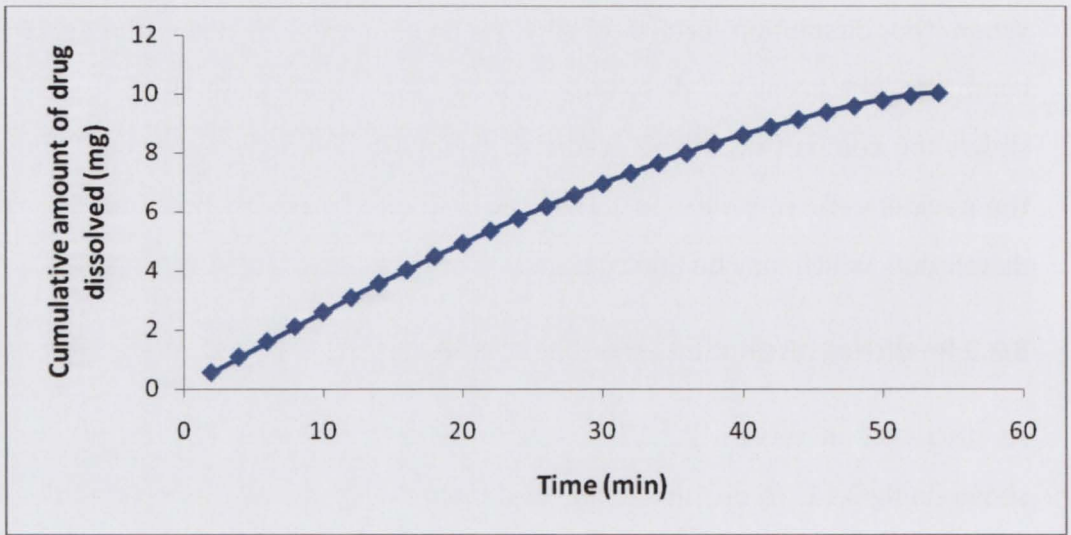
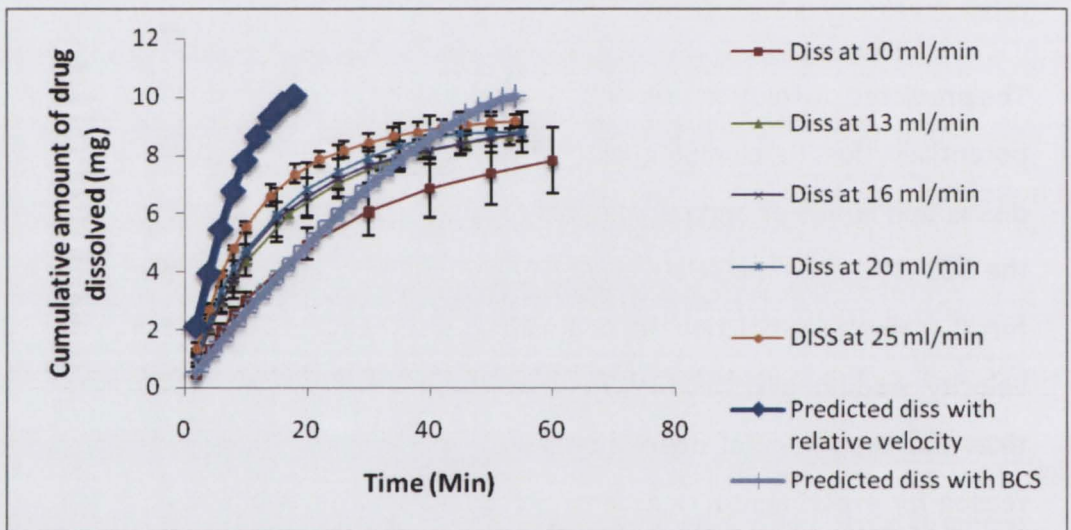*Fig 3.11 Predicted dissolution by using BCS equation.*

Fig 3.12 Comparison of the dissolutions in powder cell with predicted dissolutions

Fig 3.12 shows that the predicted dissolution from particle motion equation is faster than the experimental dissolution in the powder cell using method 1. The predicted dissolution by BCS is closer to the dissolution profile at 10 ml min^{-1} for the first 25 min min^{-1} and from then the BCS predicted dissolution is faster than the experimental dissolution at 10 ml min^{-1}. The experimental dissolution at flow rates 13, 16, 20 and 25 are closer to the predicted dissolution using the particle motion equation up to 50 % of drug dissolution

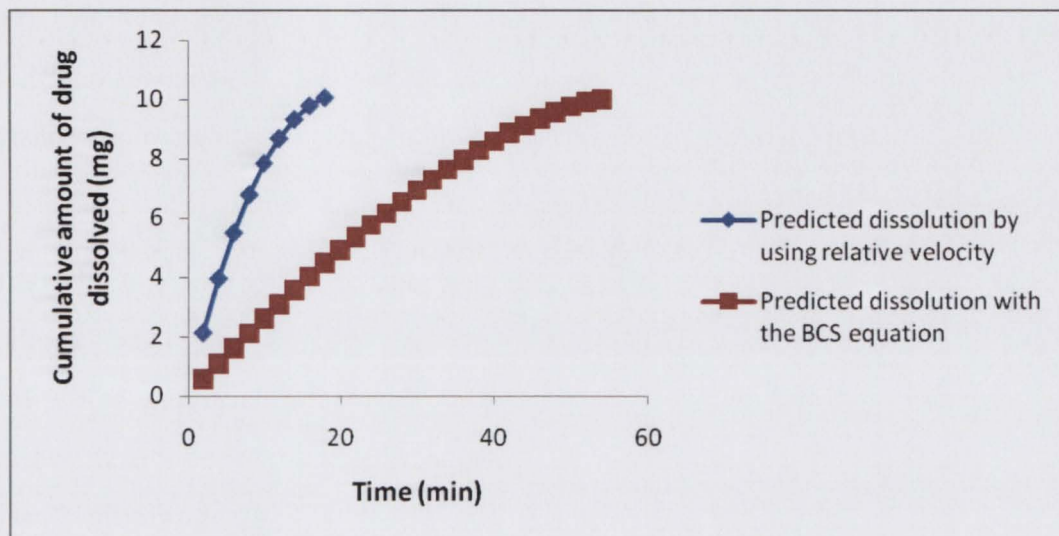and then the predicted dissolution using particle motion equation is faster than the experimental dissolution.

Fig 3.13 Comparison of predicted dissolution using particle motion equation and predicted dissolution constructed by using BCS equation.

When the predicted dissolution from particle motion equation is compared with the predicted dissolution from BCS as in fig 3.13, the predicted dissolution using particle motion equation is faster than the predicted dissolution using BCS. In the predicted dissolution from particle motion equation around 2 mg of drug dissolved within the first 2 minutes but in the predicted dissolution by BCS takes nearly 8 minutes to dissolve 2 mg of drug.

3.4 Dissolution in the powder cell using method 2

Dissolution experiments in the powder cell using method 2 were carried out to check whether the dissolution profile will be within the predicted range as the dissolution profile in the powder cell using method 1 is slower than the predicted dissolution using particle motion equation. Method 2 differs from method 1 in the placement of filter and it is placed halfway up the cell. In method 2 the drug particles have more space to move freely in the powder cell than in method 1. Method 1 also has free space for particles to

move freely but in method 2 the space is larger. The particle motion equation assumes no limit on the vertical space available for the particle to move.

From the fig 3.14 it can be seen that the dissolution at different flow rates in the powder cell using method 2 have similar profiles. All dissolutions have similar drug release pattern from the starting point to the end of the dissolution, due to having a constant relative velocity at different flow rates.

The relative velocity in the powder cell using method 2 is constant at different flow rates employed and the same to the relative velocity in the powder cell using method 1. This is because in method 1 and 2 the change is only in the placement of the insert in two methods. The relative velocity in the powder cell using method 2 is shown in fig.3.8. As there is no change in the relative velocity the dissolution rate at different flow rates didn't change.
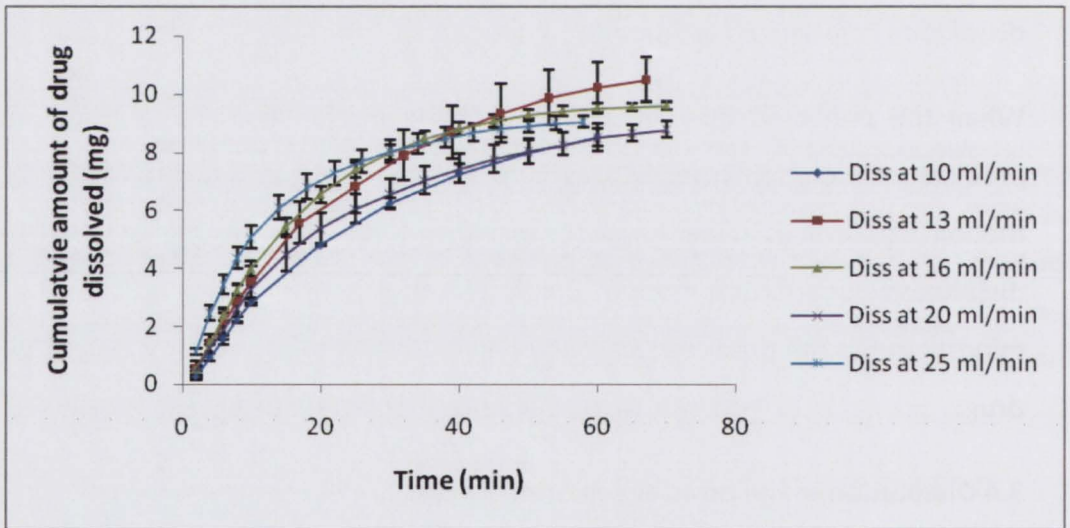

Fig 3.14 Cumulative amount of drug dissolution vs. time in powder cell using method 2 at different flow rates

3.4.1 Cube root dissolution rate constant

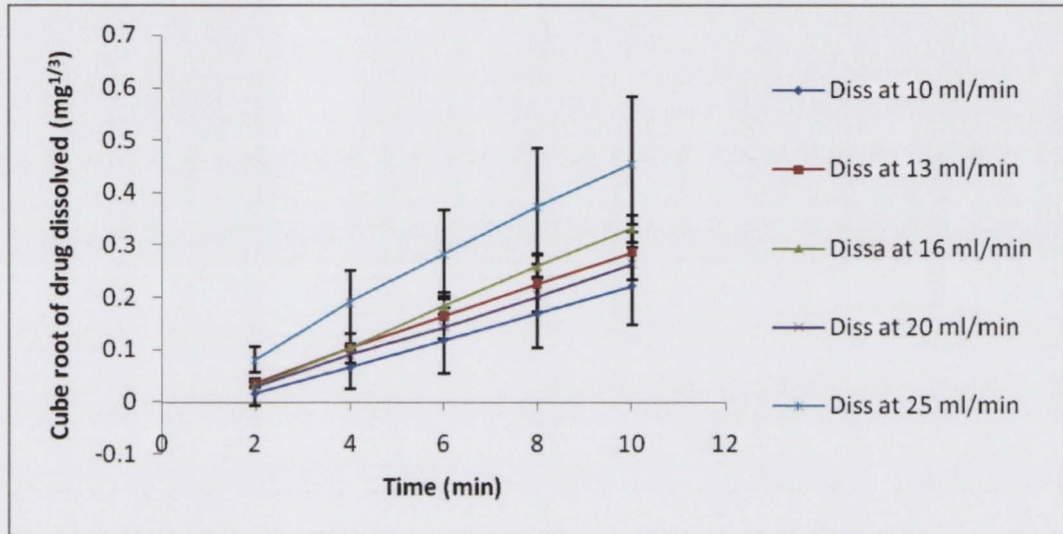As discussed in section 2.2.10 the cube root dissolution rate constant was determined (shown in fig 3.16).

Fig 3.15 Cube root of drug dissolved with respect to time

Fig 3.15 shows the cube root of drug dissolved at different flow rates employed and a similar cube root of drug dissolved is seen at different flow rates. Similar profiles at different flow rates are due to having a similar relative velocity at all flow rates employed. At flow rate 25 ml min^{-1} the cube root of drug dissolved is slightly faster potentially due to formation of eddies or non uniform laminar flow at higher flow rates.

The order of the cube root dissolution rate constant in method 2 didn't change with the flow rate except at flow rates 10 and 25 ml min^{-1} which followed a similar pattern as in method 1. The reason for lower dissolution rate constant at 10 ml min^{-1} is potentially due to the wall effect in which the flow of dissolution medium at the powder cell wall is lower than the flow rate employed (discussed in 1.3.1) and the reason for higher dissolution rate constant at 25 ml min^{-1} is due to turbulent flow (discussed in 1.3.1.2).

Dissolution in the powder cell using method 2 were carried out as dissolution in method 1 is slower than the predicted dissolution but even in method 2 the dissolution rate is similar to method 1 (cube root dissolution rate constant was compared)
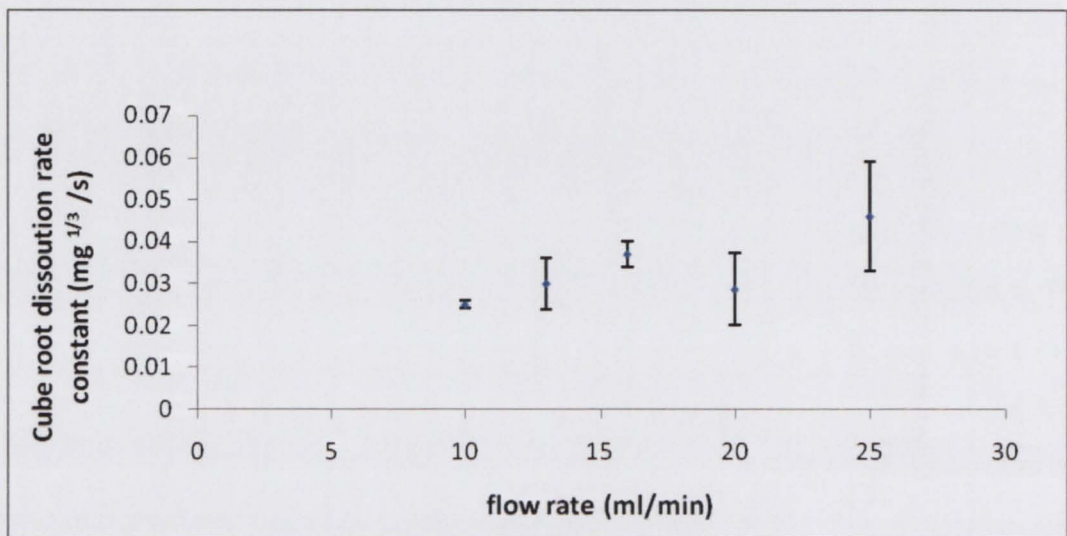

Fig 3.16 Flow rate vs.Cube root dissolution rate constant.

The changes in the arrangement of filter holder didn't make any difference in the dissolution rate which confirms that method 1 and 2 have similar cube root dissolution rate constant. The dissolution rate is independent on the initial position of the drug in the cell (as in method 1 the drug was allowed to move freely but had more space to move in method 2).

3.4.2 Predicted dissolution using particle motion equation

Dissolution was predicted same as in the method 2.2.11. The prediction in method 1 and method 2 is same as the difference between two methods is in the placement of filter but not in the relative velocity.
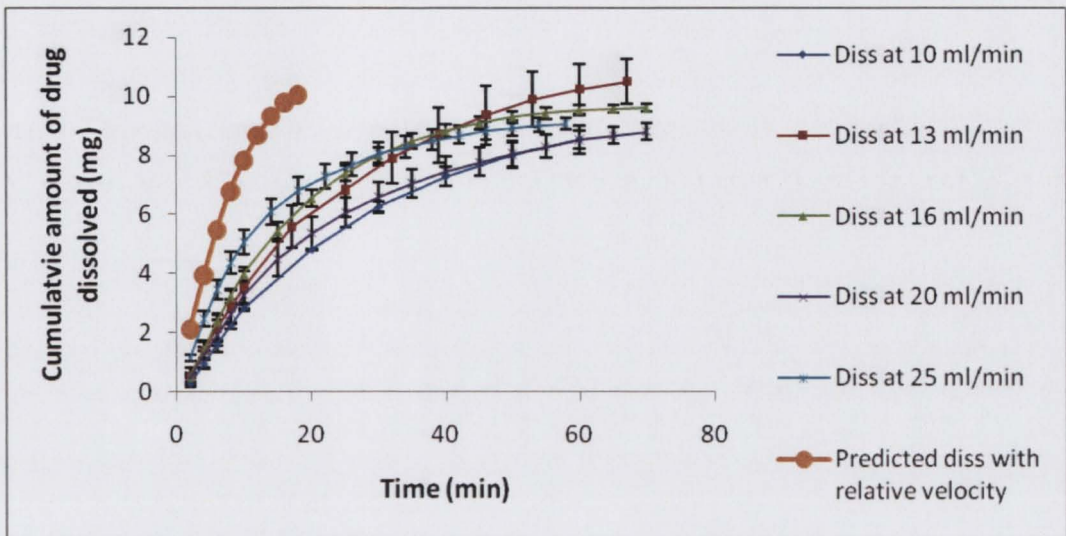
Fig 3.17 Comparison of dissolution in method 2 with predicted dissolution

When the predicted dissolution from particle motion equation and the experimental dissolution in the powder cell using method 2 were compared, the predicted dissolution from particle motion equation is faster than the experimental dissolution in the powder cell. Fig 3.17 shows the comparison of the predicted dissolution and the dissolution profiles in the powder cell using method 2.

Both in method 1 and 2 the predicted dissolution is faster than the experimental dissolution potentially due to clumping of particles in the powder cell as the equation assumes a dilute system with no interaction between particles (however interaction may occur due to high amount of drug inside the insert (10mg)).

When the experimental dissolution using method 2 is compared with the predicted dissolution from the BCS method it clearly shows that the experimental dissolution is comparable with the predicted dissolution using BCS at flow rate 10 ml min^{-1}.

Both the experimental dissolution at flow rate 10 ml min^{-1} using method 1 and 2 are comparable with the predicted dissolution from BCS but deviated from the predicted dissolution using particle motion equation.

At the initial stage of the dissolution profile at the flow rate 10 ml min^{-1} the dissolution is same as the predicted dissolution using BCS until 50% of drug dissolved and then the predicted dissolution using BCS is faster than the experimental dissolution.
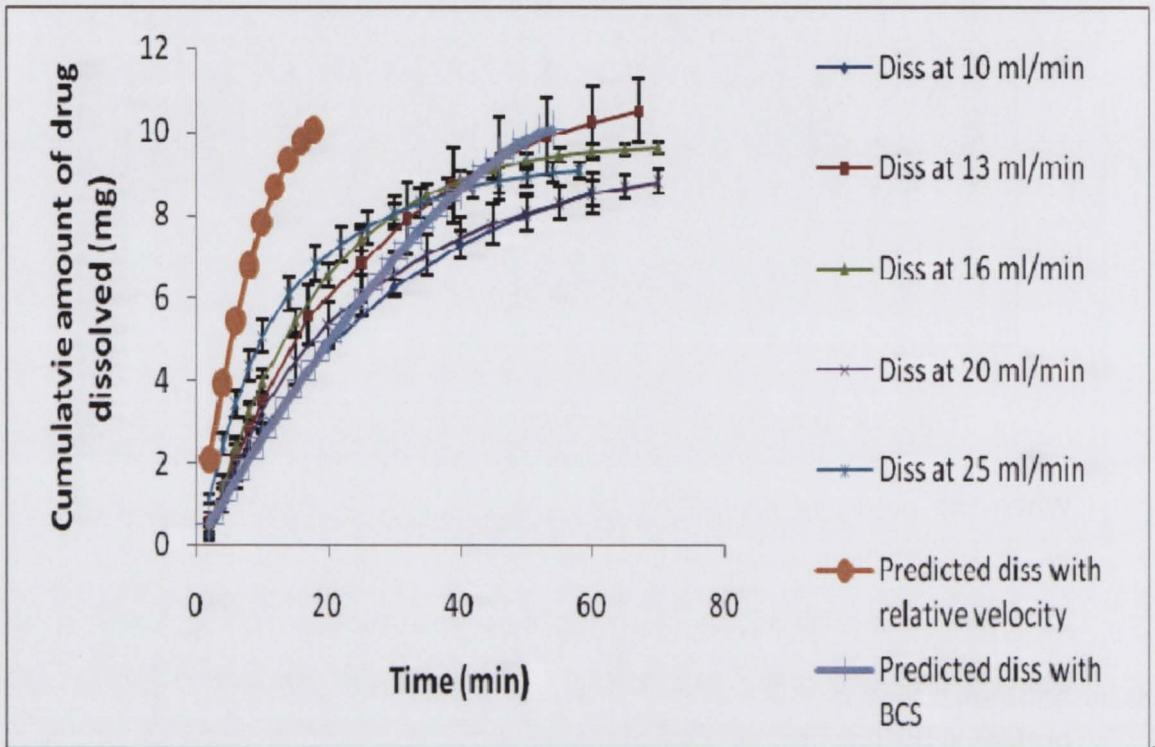

Fig 3.18 Predicted dissolution vs. Dissolution in powder cell using method 2

3.5 Dissolution in the powder cell using SLS with 5 mg of drug

The dissolutions discussed in the sections 3.3 and 3.4 were done with 10 mg of drug (Ibuprofen) in both methods (1 & 2). The experimental dissolution profile is slower than the predicted dissolution from the particle motion equation and the reason is possibly due to clumping of particles in the powder cell which reduces the total surface area exposed. So dissolutions were carried out using a surfactant sodium lauryl sulphate and the amount of drug used was reduced to 5 mg which could reduce the clumping of particles and the dissolution could be faster.

The sodium lauryl sulphate used was below the Critical Micelle Concentration limit as otherwise the relevant diffusion coefficient would be that of the micelle rather than or in

addition to that of the free drug. The percentage of SLS used was 0.018 %, the CMC of SLS is 0.23 gm litre^{-1} (Lide, 1995-1996), and therefore the concentration used in the current work corresponds to its use as wetting agent.

Dissolutions were done using method 1. Fig 3.19 shows the dissolution profile in method 1 using SLS with 5 mg of drug. Dissolutions at 10 and 13 ml min^{-1} have the same profile, at 16 ml/min the profile is nearer to 10 and 13 ml min^{-1} and then with the increase in the flow rate there is an increase in the dissolution rate which is not observed in the dissolution without SLS. The reason for increase is due to the higher flow rate employed due to which there is possibly an increase in non-uniform flow leading to the formation of eddies. Eddies increase the mass transfer resulted increase of dissolution rate. Use of SLS as well makes the dissolution faster as it avoid clumping of particles in the powder cell.
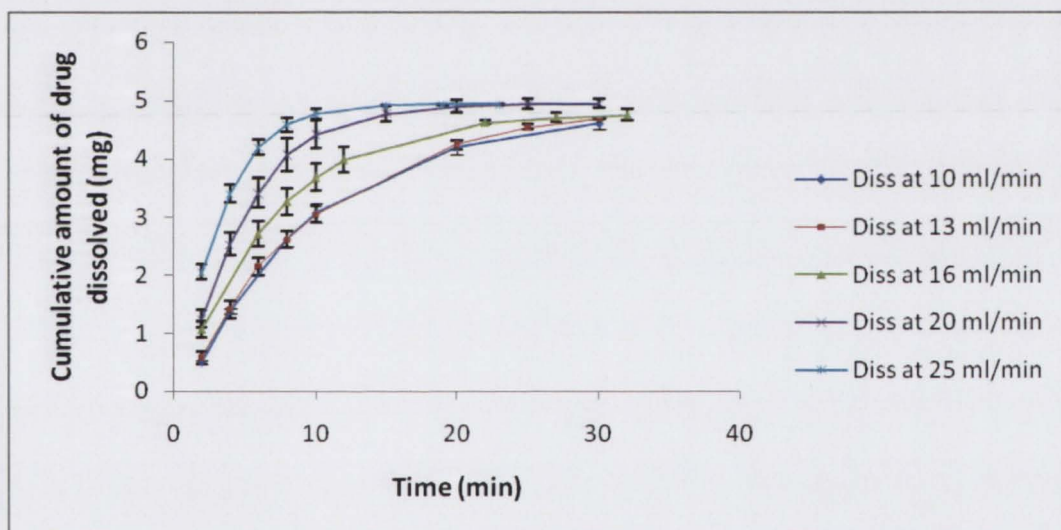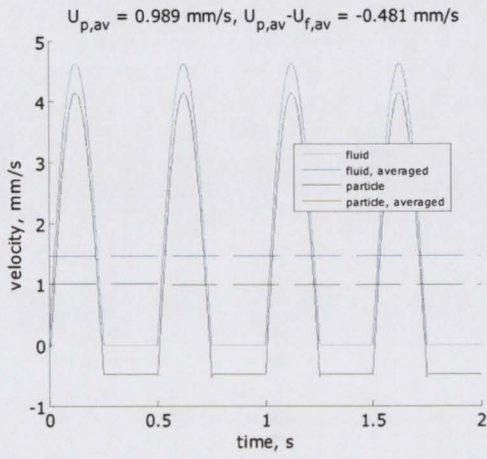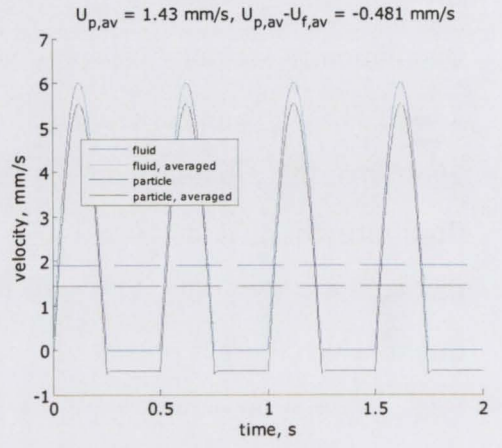

Fig 3.19 Dissolution profiles in the powder cell using method 1 with 0.018 % SLS
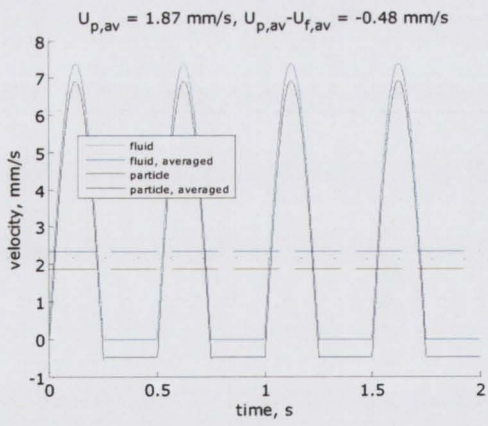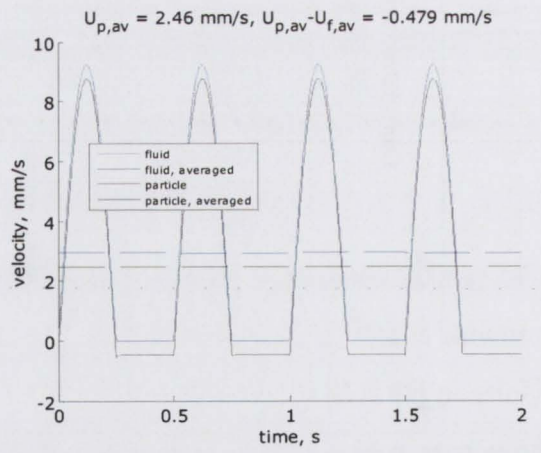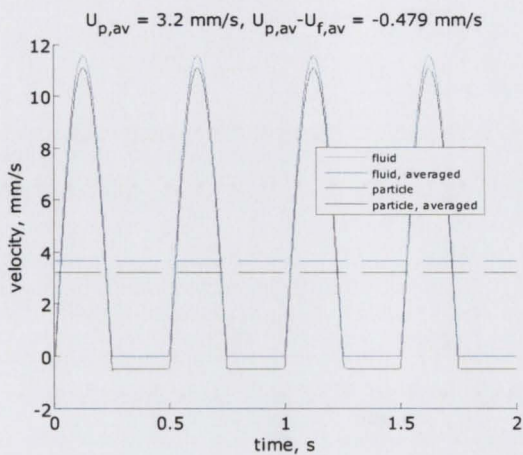
a

$U_{p,av} = 0.989$ mm/s, $U_{p,av}-U_{f,av} = -0.481$ mm/s

b

$U_{p,av} = 1.43$ mm/s, $U_{p,av}-U_{f,av} = -0.481$ mm/s

c

$U_{p,av} = 1.87$ mm/s, $U_{p,av}-U_{f,av} = -0.48$ mm/s

d

$U_{p,av} = 2.46$ mm/s, $U_{p,av}-U_{f,av} = -0.479$ mm/s

$U_{p,av}$ = 3.2 mm/s, $U_{p,av}-U_{f,av}$ = -0.479 mm/s

e

Fig 3.20 shows the average particle velocity and the relative velocity at different flow rates employed in the powder cell using SLS. (a-at flow rate 10 ml min^{-1}, b- at flow rate 13 ml min^{-1}, c- at flow rate 16 ml min^{-1}, d- at flow rate 20 ml min^{-1} and e- at flow rate 25 mlmin^{-1})

The predicted relative velocity is constant even when SLS is added to the dissolution medium so the dissolution profile at different lower flow rates didn't change. But at flow rate 20 and 25 ml/min the dissolution is faster (discussed in 1.3.1.2).

3.5.1 Cube root dissolution rate constant

Fig 3.21 shows the cube root of drug dissolved at different flow rates employed in the powder cell using SLS. The cube root of drug dissolved is similar at flow rates 10 and 13 ml/min, at flow rate 16 ml min $^{-1}$ the cube root of drug dissolved is faster between 2- 4 minutes from then the cube root of drug dissolved is parallel with the slope of 10 and 13 ml min^{-1}but at flow rate 20 and 25 ml/min the cube root of drug dissolved is faster due to the flow rate employed.
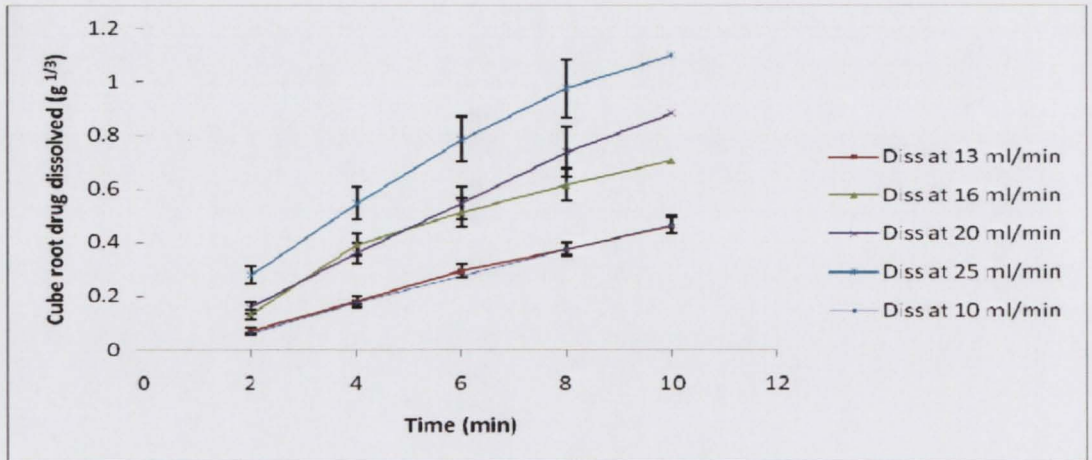
Fig 3.21 cube root of drug dissolved with respect to time

The cube root dissolution rate constant in the dissolution with 0.018 % SLS has nearly similar values at different flow rates employed except at flow rates 20 and 25 ml/min (shown in fig 3.22). At flow rates 20 and 25 ml/min the cube root dissolution rate constant is higher due to the flow rates employed, higher flow rates increase the turbulent flow results in the formation of eddies results in increase in mass transfer rate and finally the dissolution rate constant. The consistency in the cube root dissolution rate constant at flow rates of 10, 13 and 16 ml min^{-1} is due to the constant relative velocity in the flow through apparatus at different flow rates employed shown in fig 3.20 and the SLS added makes the drug particles free from clumping.
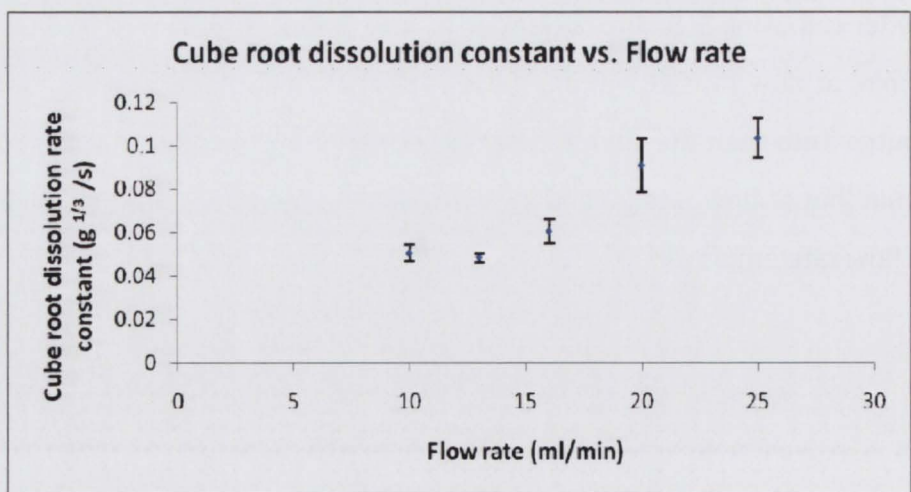

Fig 3.22 Cube root dissolution rate constant vs. flow rate

3.5.2 Predicted dissolution using particle motion equation

Dissolution was predicted as in the section 2.2.11. Saturated solubility of drug in 0.018 % SLS was used in predicting the dissolution using the particle motion equation. Along with the saturated solubility the other change in predicting dissolution was the amount of drug (5 mg) used. The predicted dissolution using particle motion equation is shown in fig 3.23.
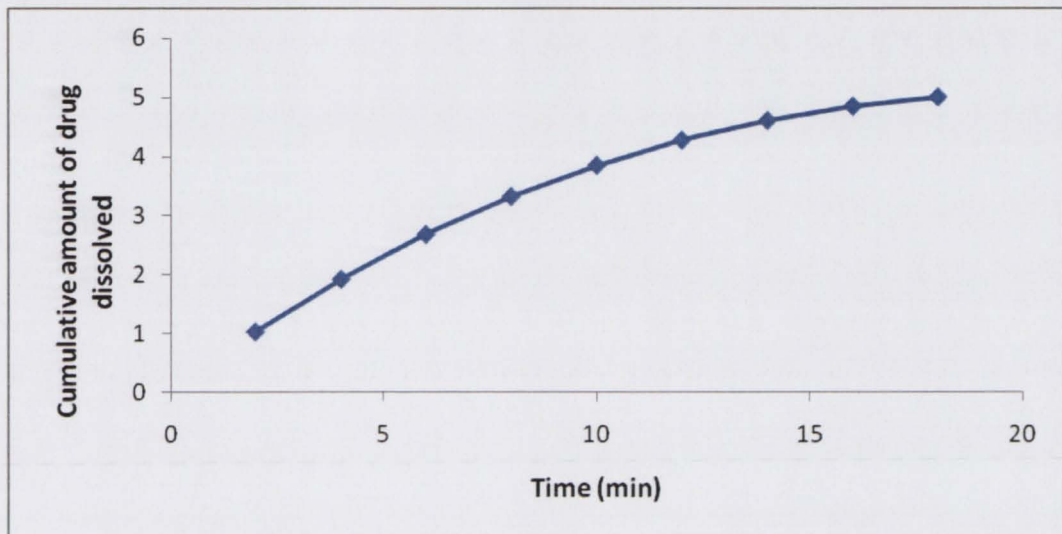

Fig 3.23 The predicted dissolution in phosphate buffer with 0.018 % SLS

The predicted dissolution using particle motion equation in the phosphate buffer with 0.018 % w/v SLS has similar dissolution profile as the predicted dissolution without SLS (method 1 and 2), due to having no difference in the saturated solubility of drug in phosphate buffer with SLS and without SLS, seen in table 3.1

The time taken to dissolve the whole amount of drug (5 mg) in predicted dissolution using SLS is 18 minutes and the time taken in predicted dissolution with 10 mg of drug without SLS is also 18 minutes, so the time needed to dissolve the whole drug did not depend on the amount of drug taken for dissolution as the prediction is based on individual particles dissolving.

Fig 3.24 shows the comparison of the predicted dissolution with the experimental dissolution (using SLS). The predicted dissolution is comparable with the experimental

58

dissolution which is not observed in the dissolution without SLS. Dissolution at the flow rate 10, 13, and 16 ml min^{-1} were slower than the predicted dissolution using SLS but dissolution at flow rate 20 and 25 ml min^{-1} is faster than the predicted dissolution using SLS.

At flow rate 16 ml min^{-1} the experimental dissolution is comparable with the predicted dissolution using SLS up to 80 % drug dissolution as shown in fig 3.24 but after that the predicted dissolution using SLS is faster.
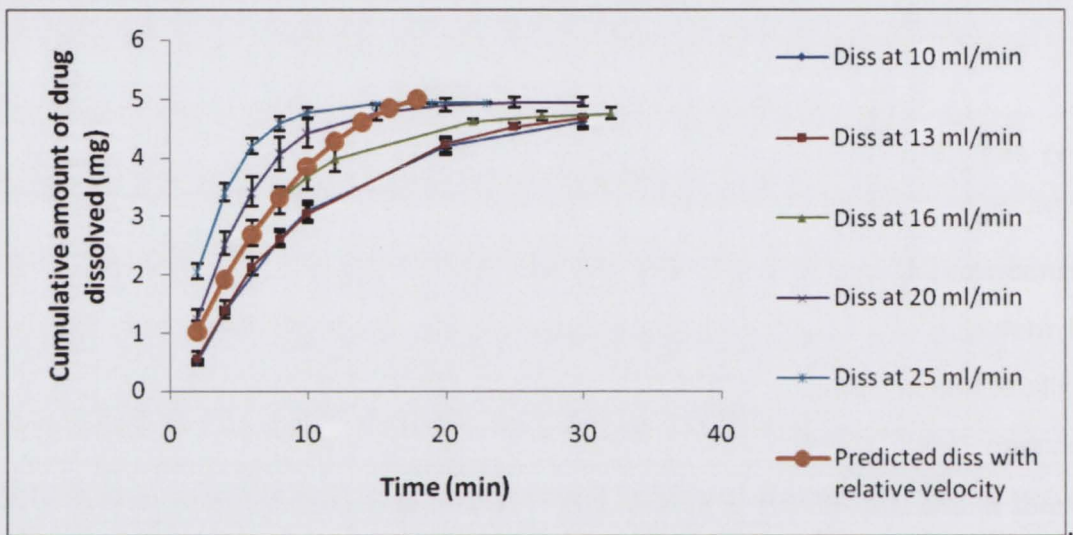
Fig 3.24 Comparison of dissolution profiles with the predicted dissolution in 0.018% SLS

3.5.3 Predicted dissolution according to the BCS

 Dissolution was predicted from BCS as in section 2.2.12. It resembles the predicted dissolution without SLS

Fig 3.25 The predicted dissolution using the BCS equation in buffer with 0.018 % SLS

When the experimental dissolution is compared with the predicted dissolution using relative velocity and BCS as in the Fig 3.26 it can be concluded that the predicted dissolution using the SLS is faster than the predicted dissolution using BCS equation.
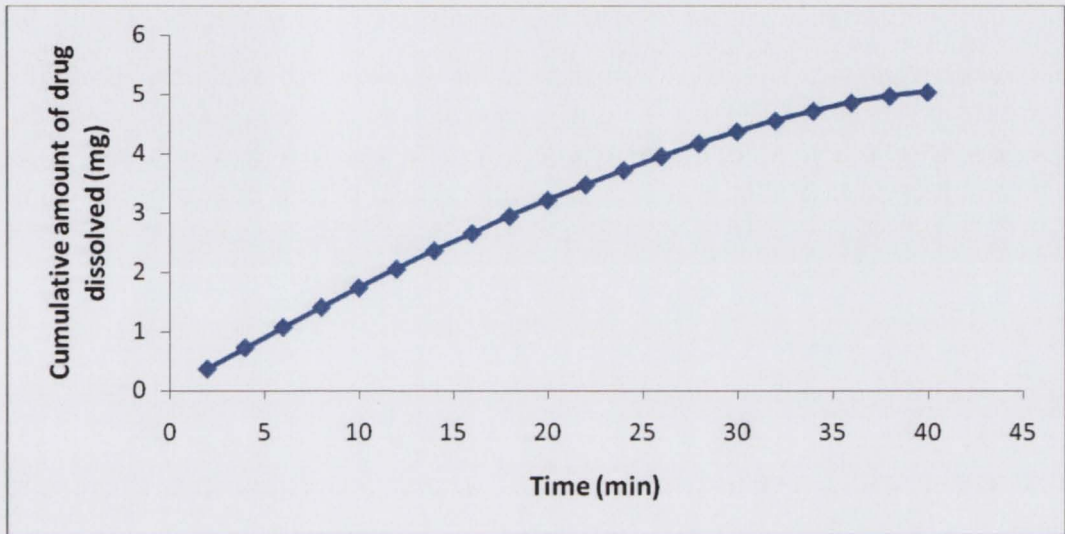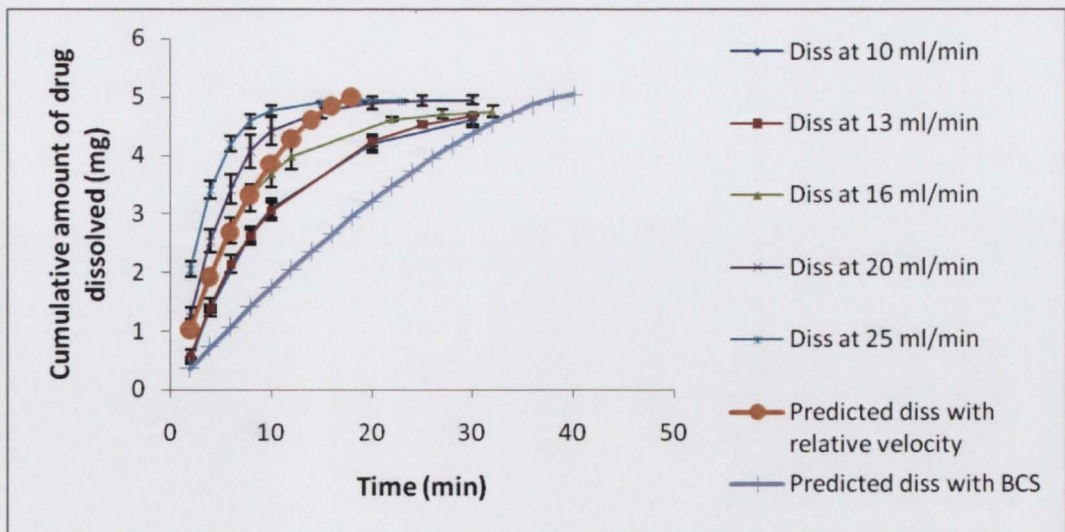

Fig 3.26 Comparison of dissolution profiles with the predicted dissolutions

The predicted dissolution using BCS is slower than the experimental and the predicted dissolution using particle motion equation.

3.6 Dissolution in the powder cell in 0.1 M HCl with SLS

Dissolutions were carried out in the powder cell using method 1 with 0.1 M HCL to simulate the fasting gastric conditions. SLS was used to avoid clumping of particles. Fig 3.27 shows the dissolution profile in 0.1 M HCL with 0.018 % SLS at different flow rates. The dissolution at different flow rates has similar profile due to having constant relative velocity at different flow rates.
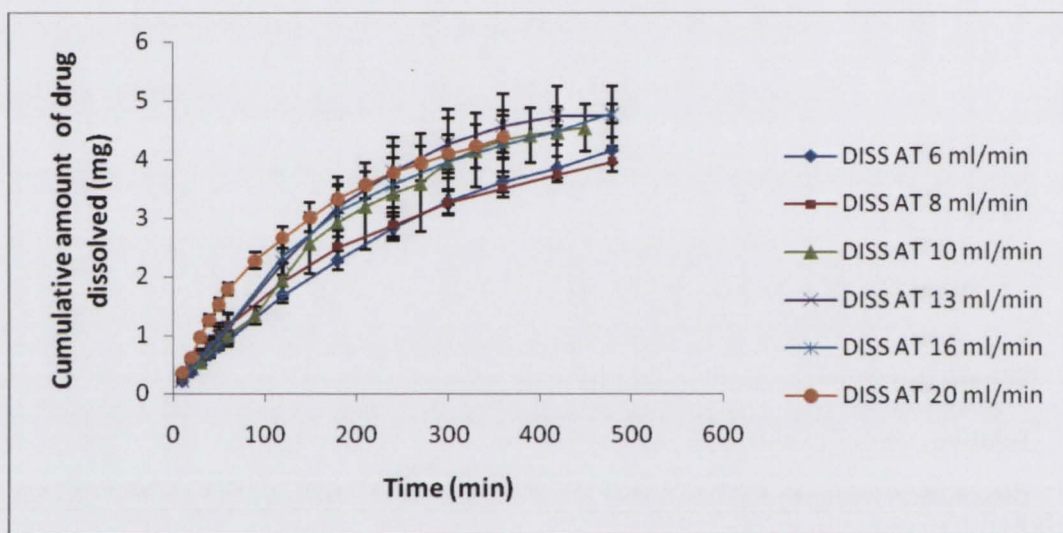
Fig 3.27 Dissolution profiles in the powder cell using 0.1 M HCl in 0.018 % SLS at different flow rates.

3.6.1 Cube root dissolution rate constant
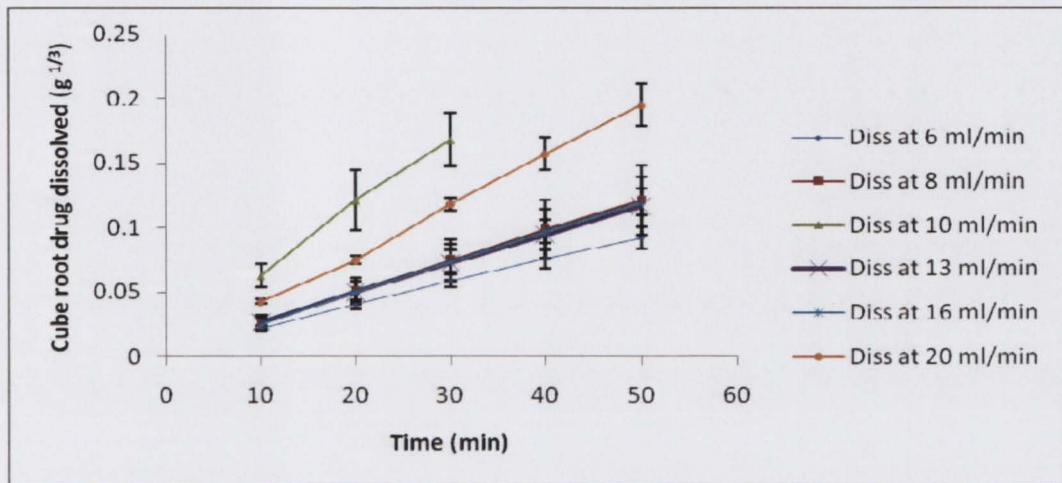
Fig 3.28 The cube root of drug dissolved with respect to time

Fig 3.28 shows that the cube root of drug dissolved at different flow rates employed have similar drug release pattern and didn't depend on the flow rate employed. Dissolution at flow rate 20 ml/min is slightly faster.

Fig 3.29 shows the cube root dissolution rate constant at different flow rates. From the fig 3.29 it can be confirmed that the cube root dissolution rate constant didn't change significantly with the increase in the flow rate as in the dissolutions in phosphate buffer with SLS and without SLS. The cube root dissolution rate constant at 20 ml min^{-1} suggests a trend towards an increase with increasing flow rate however it is not significantly different from that at 8 ml min^{-1}
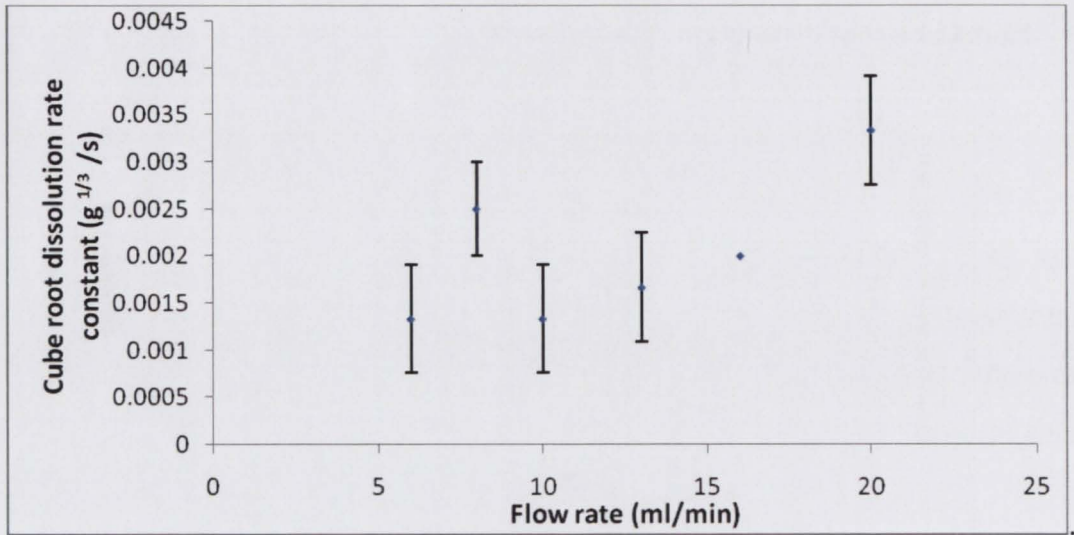
Fig 3.29 Cube root dissolution rate constant vs. flow rate

Dissolutions were carried out with 0.018 % w/v SLS which prevents clumping of drug particles therefore the dissolution rate constant didn't increase significantly with the flow rate due to having constant relative velocity at different flow rates employed (seen in fig 3.30).

a   b

$U_{p,av}$ = 1.84 mm/s, $U_{p,av}$-$U_{f,av}$ = -0.509 mm/s

$U_{p,av}$ = 2.43 mm/s, $U_{p,av}$-$U_{f,av}$ = -0.508 mm/s
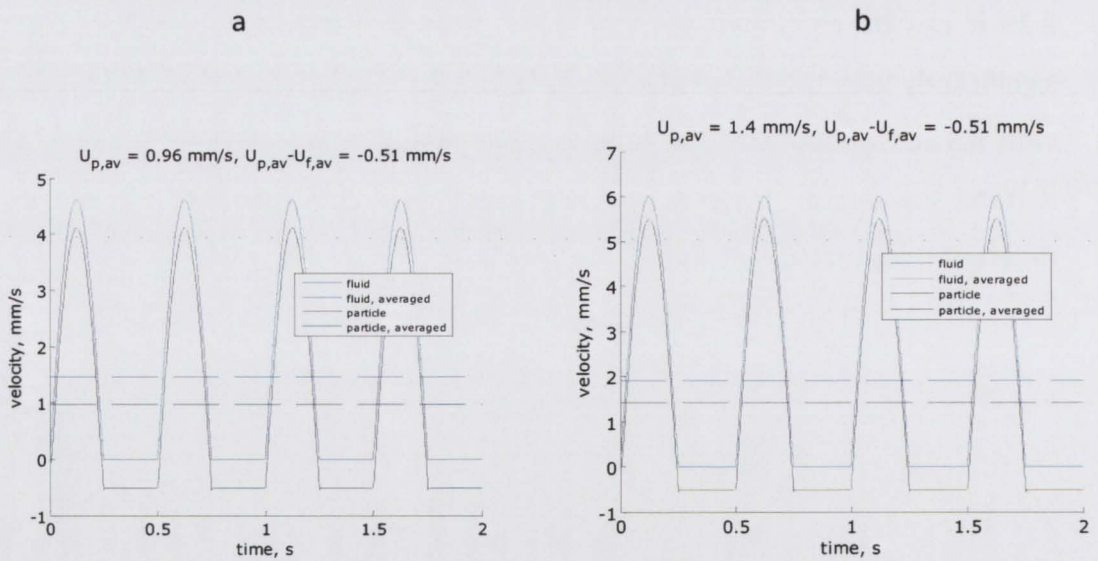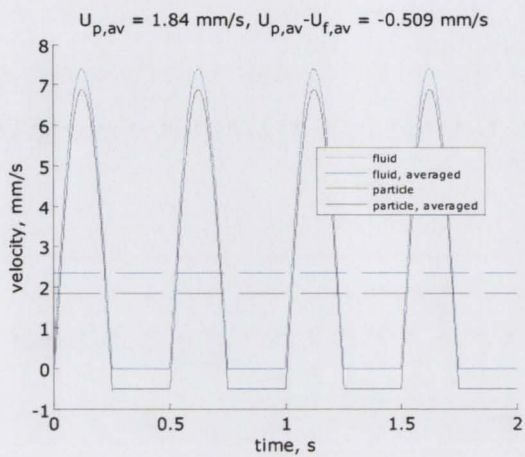
c
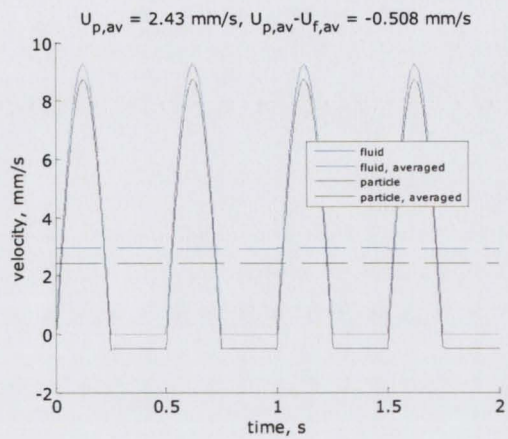
d

Fig 3.30 The average particle velocity and the average relative velocity at different flow rates employed in the powder cell with SLS for 0.1 M HCl dissolution (a- at flow rate 10ml min^{-1}, b- at flow rate 13 ml min^{-1}, c- at flow rate 16 ml min^{-1} and d- at flow rate 20 ml min^{-1}). The relative velocity in the graphs are represented as $U_{p,av}$ – $U_{f,av.}$ and a constant value.

3.6.2 Predicted dissolution using particle motion equation

Dissolution in 0.1 M HCl was predicted as in section 2.2.11. The following fig 3.31 shows the predicted dissolution in 0.1 M HCl.

Fig 3.31 predicted dissolution in 0.1 M HCl using particle motion equation

The predicted dissolution in 0.1 M HCl takes 13 hours to complete the dissolution of 5 mg of drug, which is comparable to the time taken for the experimental dissolution test as shown in fig 3.32
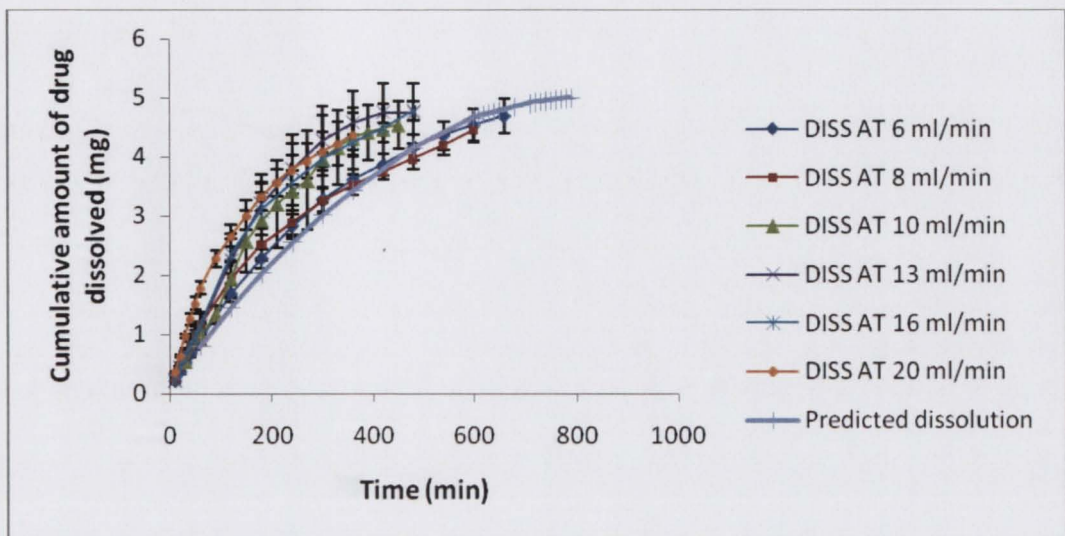
Fig 3.32 Comparison of predicted dissolution from particle motion equation with experimental dissolution

When the predicted dissolution using relative velocity is compared with the experimental dissolution it can be seen that the experimental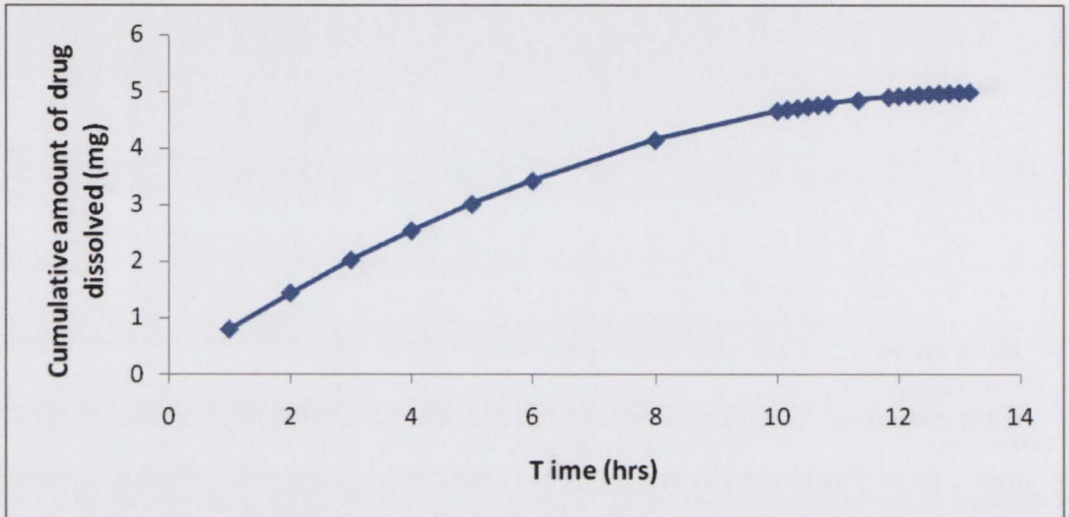 dissolution at flow rate 6 ml min^{-1} is comparable with the predicted dissolution using relative velocity. The predicted dissolution is slower (not significantly) than the experimental dissolution (at 6 ml min^{-1}) up to 80% drug dissolved and then the predicted dissolution is same as the experimental dissolution (at 6 ml min^{-1}).

3.6.3 Predicted dissolution according to the BCS

Dissolution in 0.1 M HCl with 0.018 % SLS was predicted using BCS principle. The time necessary to dissolve 5 mg of drug in predicted dissolution using BCS is 25 hours but in the predicted dissolution using particle motion equation is only 13 hours and in the experimental dissolution the time taken to dissolve 5 mg was 10-13 hours (3.33). The BCS used the dissolution number to define different classes of drugs and predicts the absorption of the drug depending on the dissolution number, dose number and absorption number. But in the actual dissolution the dissolution rate shows a higher dissolution rate which needs to be accounted for in the equation used to define the dissolution number.
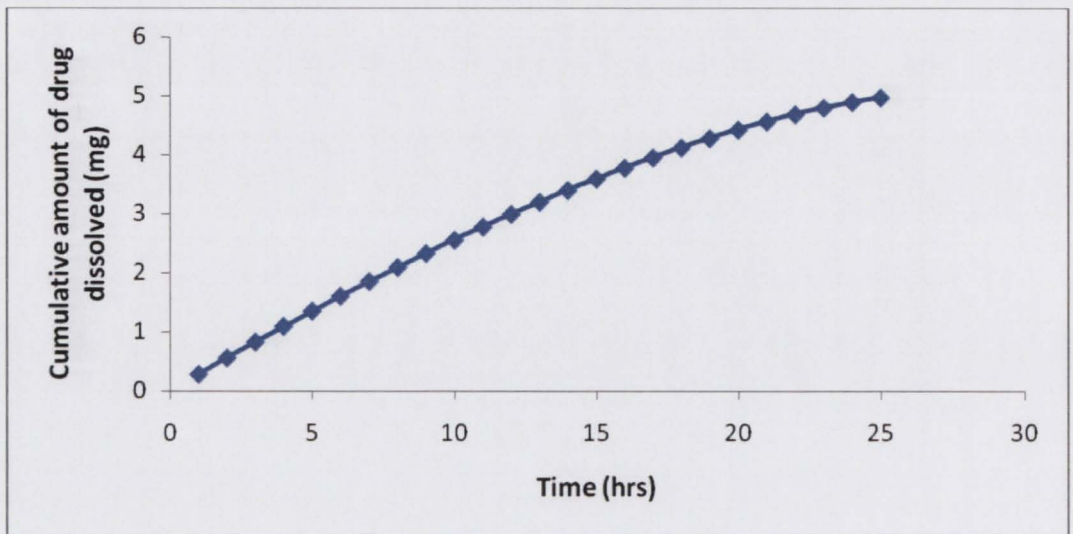
Fig 3.33 Predicted dissolution in 0.1 M HCl with SLS using BCS system

When experimental dissolution is compared with the predicted dissolution using particle motion equation and BCS system as shown in fig 3.34 the predicted dissolution using BCS is slower than the experimental dissolution and the predicted dissolution from particle motion equation.
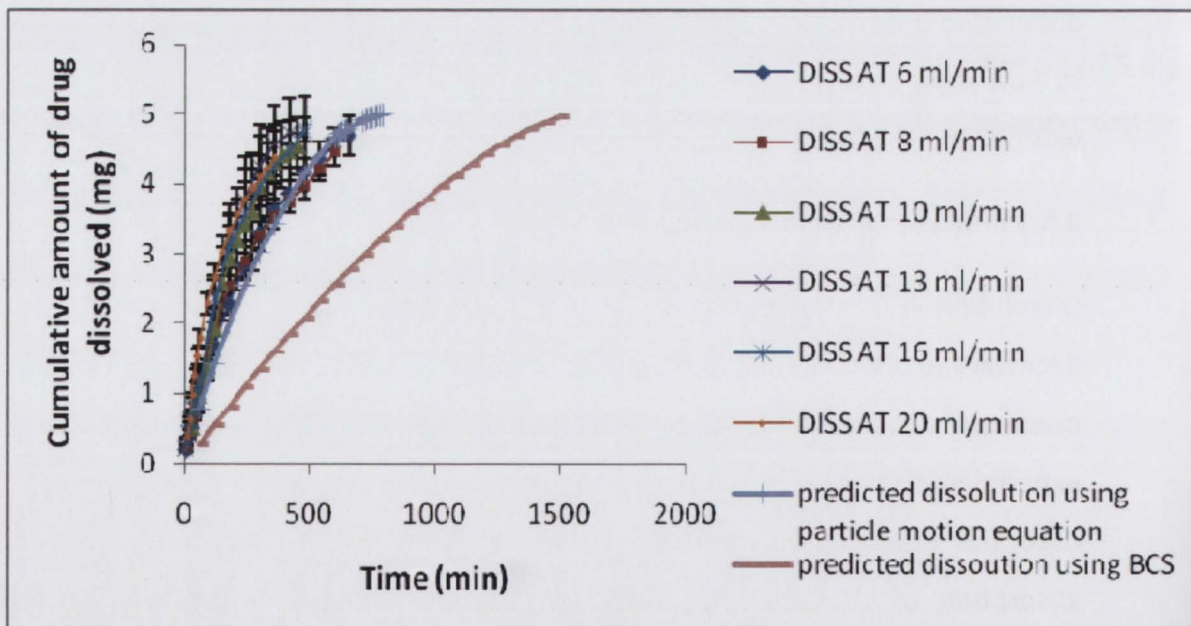
Fig 3.34 Comparison of predicted dissolution from particle motion equation and BCS with experimental dissolutions.

3.7 Dissolution in the powder cell using method 1 in viscous medium (0.5 % HPMC)

To simulate the fed postprandial stomach conditions dissolution in 0.5 % HPMC was carried out (Parojcic et al, 2007).
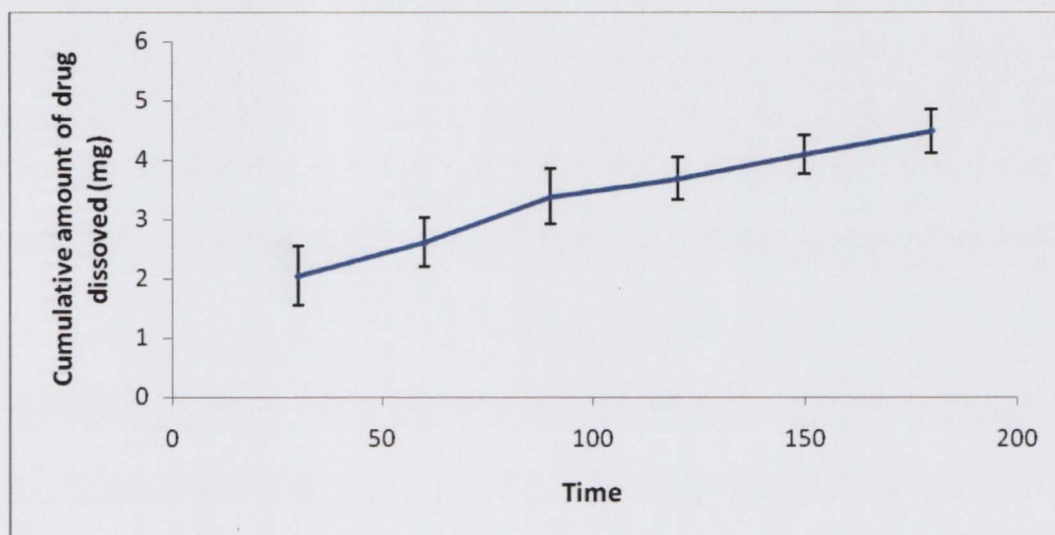
Fig 3.35 dissolution profile in viscous medium (phosphate buffer pH 5.8 with 0.5 % HPMC in 0.018 % SLS)

Fig 3.35 shows the dissolution profile in viscous medium at flow rate 8 ml min^{-1}. Dissolution was carried out using closed system. Samples were collected at the beginning of the dissolution but the samples were not properly mixed due to highly viscous medium (the samples were taken close to the point at which the medium re entered the reservoir), therefore the measured amount of dissolved was too large at early time points and was omitted. To dissolve 5 mg of drug it takes 3 hours in viscous medium (phosphate buffer pH 5.8 in 0.5 % HPMC with 0.018 % SLS) shown in fig 3.35.

3.7.1 Cube root dissolution rate constant

The cube root dissolution rate constant in viscous medium (0.5 % HPMC) is higher than in dissolution in 0.1 M HCl and lower than the dissolution in phosphate buffer pH 6.6 with 0.018 % SLS. The decrease in cube root dissolution rate constant is due to the lower solubility at pH 5.8 compared to pH 6.6. Additionally the viscous medium which reduces

the flow of the dissolution medium and also changes in the relative velocity in the powder cell may have affected the cube root dissolution rate constant. The predicted dissolution using particle motion equation is shown in fig 3.36

Dissolution was predicted in viscous medium using particle motion equation as discussed in section 2.2.18
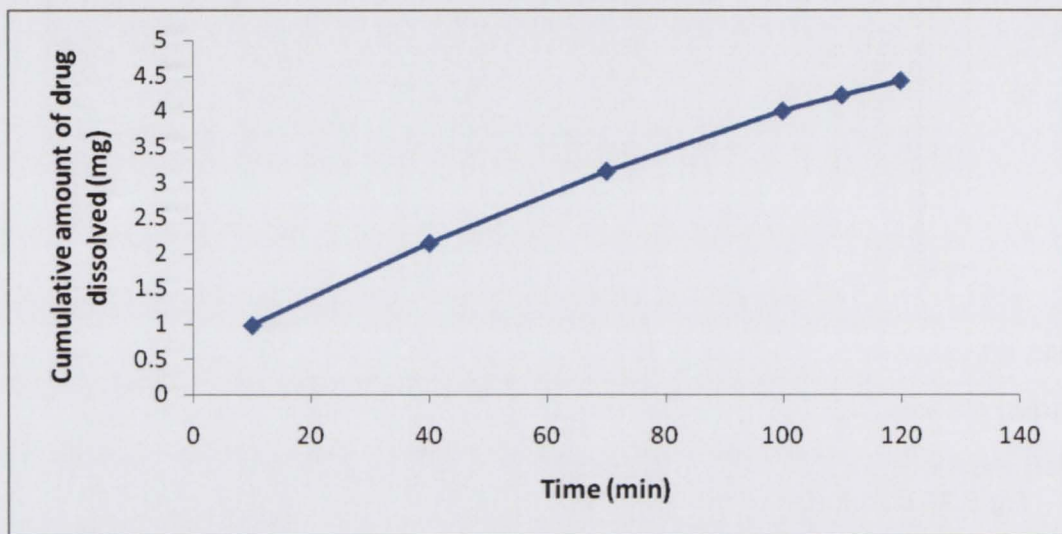
Fig 3.36 Predicted dissolution in viscous medium (phosphate buffer pH 5.8 in 0.5 % HPMC with 0.018 % SLS)

The predicted dissolution takes nearly 2 hours to dissolve 4.5 mg of drug, which is a little faster than the duration of the experimental dissolution. When the predicted dissolution and the experimental dissolution are compared as in fig 3.37 the experimental dissolution has comparable dissolution profile up to 60 % with the predicted dissolution.
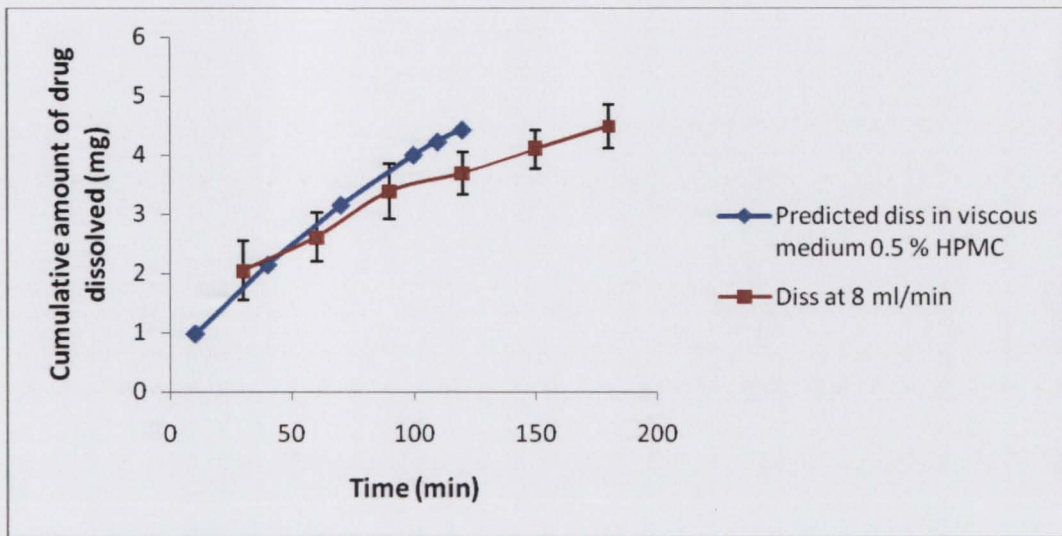
Fig 3.37 Comparison of predicted dissolution with experimental dissolution

3.7.2 Predicted dissolution according to the BCS
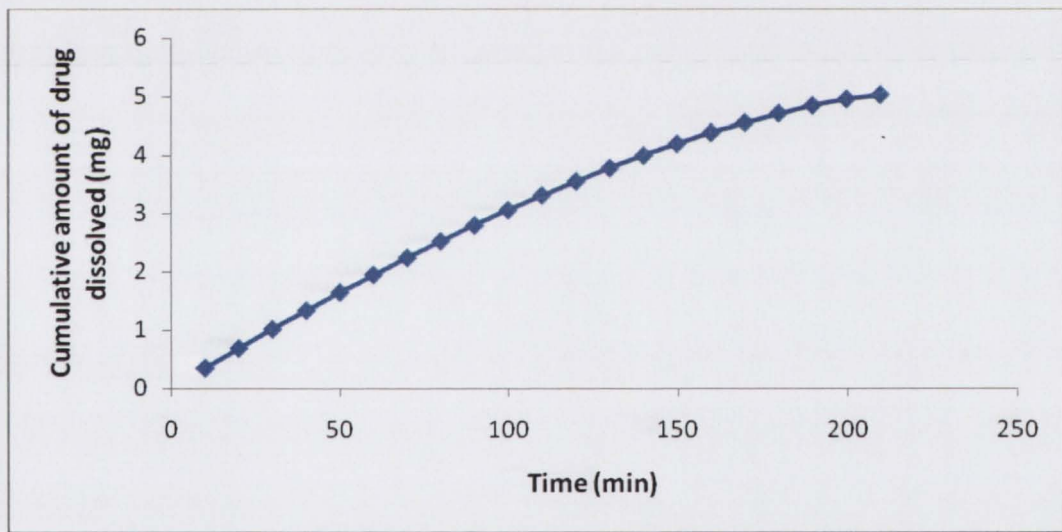
Fig 3.38 Predicted dissolution using BCS in viscous medium (0.5 % HPMC)

As described in section 2.2.12 dissolution was predicted in viscous medium (0.5 % HPMC). When predicted dissolution using particle motion equation and BCS are compared it can be concluded that predicted dissolution using particle motion equation is faster than the predicted dissolution using BCS as shown in fig 3.39.

70
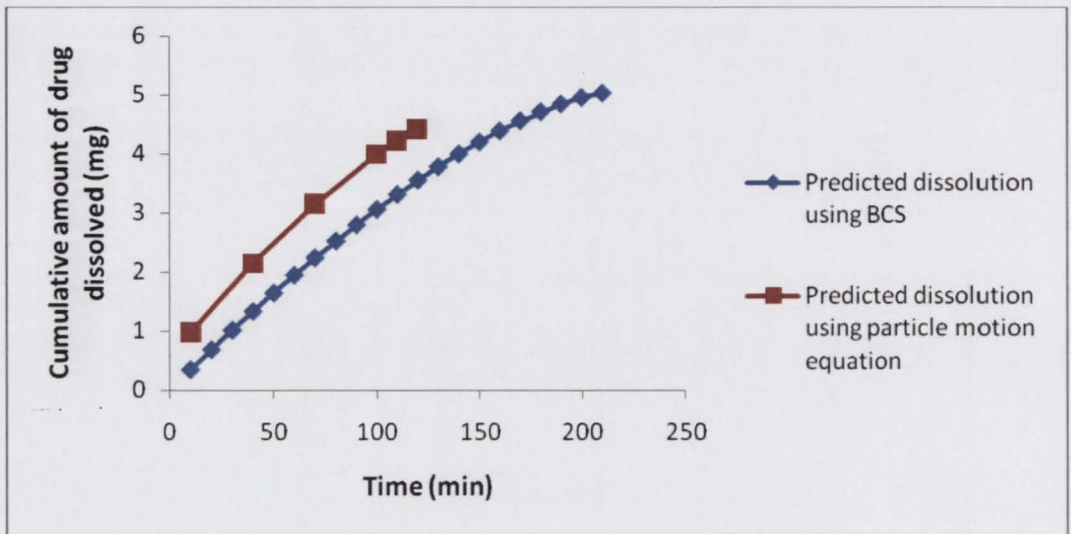
Fig 3.39 Comparison of predicted dissolution using particle motion equation and BCS

When the experimental dissolution compared with the predicted dissolution from the particle motion equation and BCS it was confirmed that the experimental dissolution was slow than the predicted dissolution using particle motion equation and faster than the predicted dissolution using BCS shown in fig 3.40
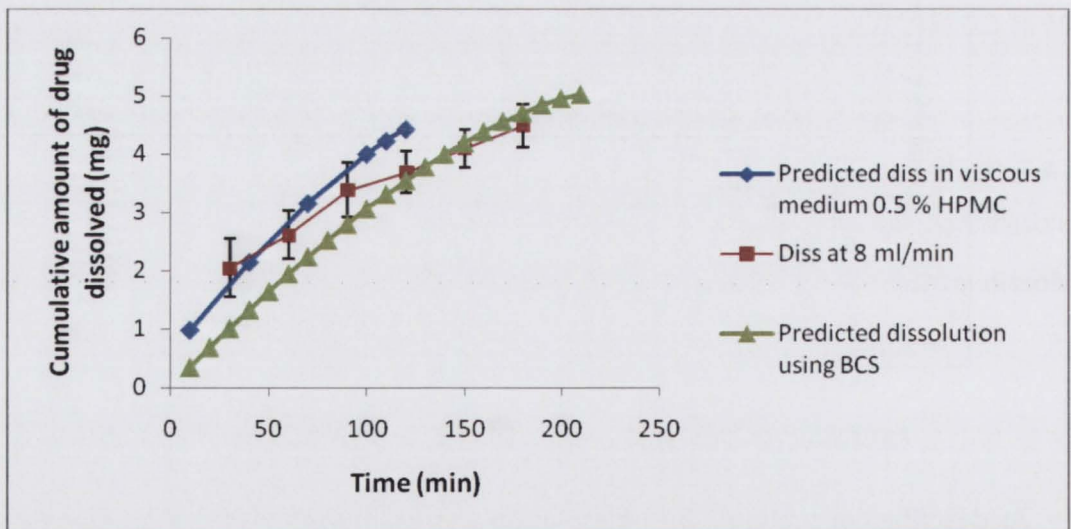
Fig 3.40 comparison of experimental dissolution (viscous medium-0.5 % HPMC) with predicted dissolution using BCS and particle motion equation.

The experimental dissolution showed similar dissolution profile to the predicted dissolution using particle motion equation but at the end of the dissolution it showed same profile to the predicted dissolution using BCS. As discussed earlier predicted dissolution using BCS has no involvement of relative velocity which might be the reason for the slower dissolution than the predicted dissolution using particle motion equation.

3.8 Dissolution in the powder cell using method 1 in viscous medium (1 % HPMC)

Dissolutions were carried out in powder cell using method 1 in viscous medium (1 % HPMC in 0.018 % SLS) showed in fig 3.41.

Dissolution in 1 % HPMC was carried out to simulate the fed postprandial stomach conditions (Klein etal, 2004). Fig 3.41 shows the dissolution profile at a flow rate of 8 ml min^{-1} in the powder cell. Dissolution was carried out using closed system. Samples were collected at the beginning of the dissolution but samples were not properly mixed due to highly viscous medium.
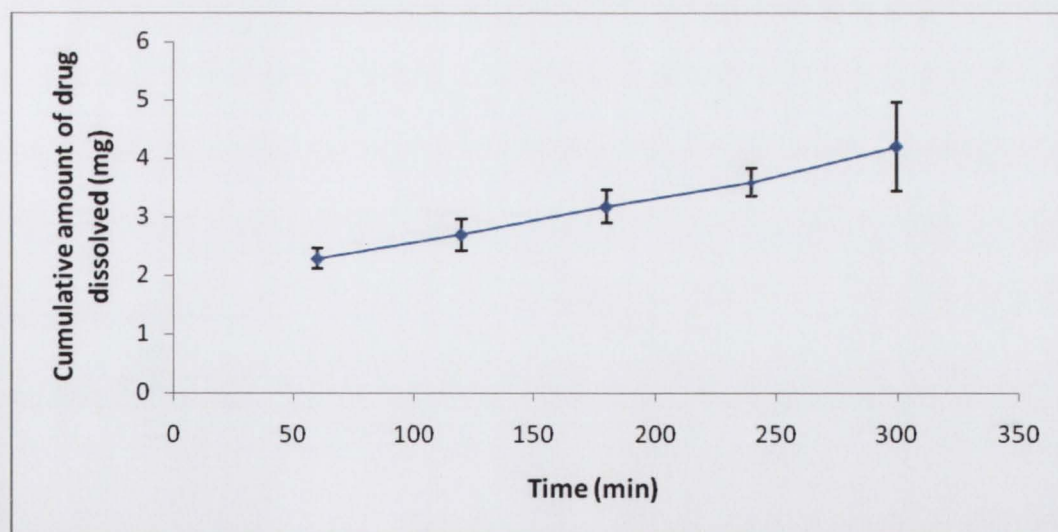
Fig 3.41 Dissolution profile in viscous medium (1% HPMC with 0.018 % SLS) at flow rate 8 ml min^{-1}.

Samples were collected one hour after starting the dissolution and analysed, so in the fig 3.41 the dissolution profile starts from 60 minutes and in the first 60 minutes up to 50 % drug dissolved and to dissolve the rest of the drug it takes four hours shown in fig. 3.41. To predict the dissolution in viscous medium (1% HPMC with SLS in phosphate buffer pH 5.8) MATLAB code was used but due to high viscous medium the MATLAB didn't run.
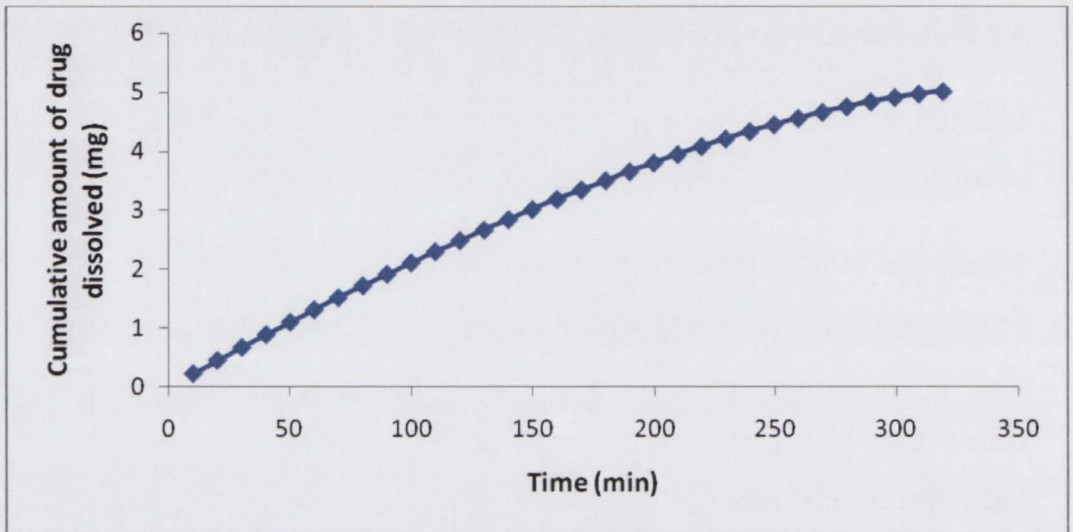
Fig 3.42 predicted dissolution in 1 % HPMC with 0.018 % SLS using BCS
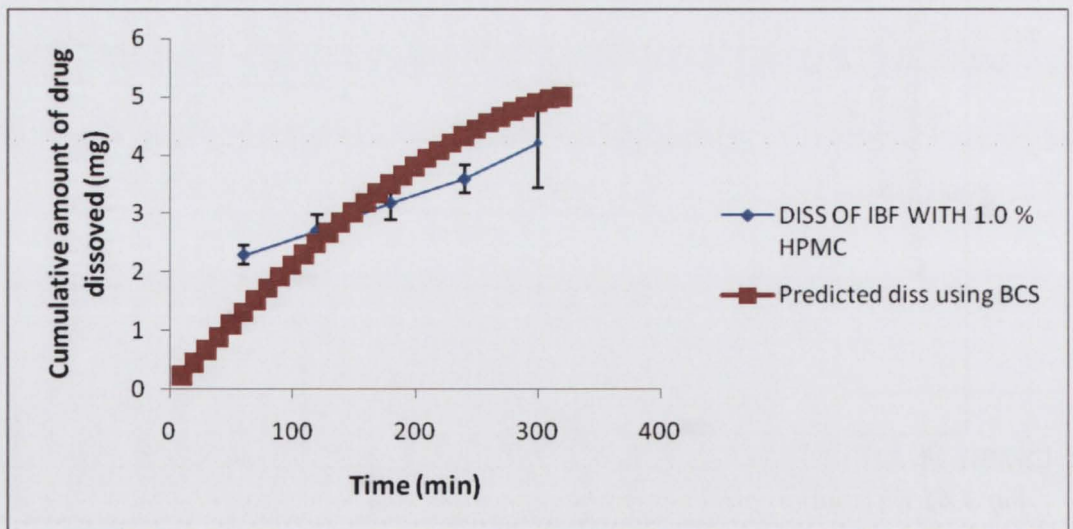
Fig 3.43 comparison of predicted dissolution from BCS with the experimental

Dissolution was predicted in viscous medium with 1 % HPMC in 0.018 % SLS as discussed in section 2.2.12.To complete 5 mg of drug it takes nearly 6 hours (fig 3.42).

When the experimental dissolution compared with the predicted dissolution using BCS (fig 3.43) it can be seen that the experimental dissolution is faster until 60 % drug dissolved and then it is slower than the predicted dissolution using BCS.

DISCUSSION

4 Discussion

Zhang et al, (1994), Cammarn and Sakr (2000) and Wu et al (2006) studied the effect of hydrodynamics on tablet orientation in the flow thorough apparatus at various conditions. Bhattachar et al (Bhattachar et al, 2002) studied the dissolution of powdered drug in the flow through apparatus, concluded that the loading of the drug plays an important role to get best dissolution profile. Hence to study the effect of hydrodynamics on the powdered drug in the powder cell and in the standard cell, the flow through apparatus was used and to simulate gastrointestinal conditions different dissolution media were used. A MATLAB code was used to determine the relative velocity in the flow through apparatus. Dissolution was predicted theoretically using the relative velocity values and the dissolution was predicted according to BCS (equation 2.3). The predicted dissolution rates using the relative velocity equation (equation 1.9) and the BCS were compared with the experimental dissolution rates.

Dissolutions were carried out in the standard cell of size 22.6 mm diameter. The drug was loaded in the form of slurry. The main disadvantage of slurry is that the drug is mixed with the buffer before administered into the standard cell which can affect the dissolution rate, hence dissolutions were also carried out in the powder cell. The powder cell is designed in such a way that the drug can be placed using an insert which prevents the floating of the drug (which can occur in USP 1 and 2) additionally there is no need to prepare slurry in contrast to the standard cell. In the powder cell two methods can be used and methods differ only in the placement of the insert shown in fig (2.1 and 2.2). The disadvantage of the powder cell is that the powder cell is not suitable for dissolution with viscous medium as the powder cell was designed with many filters to filter the undissolved drug particles. The viscous medium cannot flow through the filters especially at higher flow rates so dissolutions were carried out without any filters (in 0.5 % HPMC top filter was left) in the powder cell and the collected samples was filtered. Even though the samples were filtered another problem faced was the mixing of the samples, as the closed system was used for dissolution with viscous medium. Early samples show a very

high amount of drug dissolved and samples were taken close to where medium returns from the cell to the reservoir. So the samples were analysed after apparent proper mixing was achieved (increase in the absorbance with time) and used to calculate the cube root dissolution rate constant.

Dissolutions were done using viscous medium to stimulate the fed conditions in the postprandial stomach. The work of Sandra Klein (Klein et al, 2004) and Jelena Parojcic (Parojcic et al, 2007) simulate the fed state. Jelena Parojcic had a correlation of 0.5 % HPMC with the fed state using 0.5 % HPMC and in vivo data from fed state and Sandra Klein (Klein et al, 2004) measured the viscosity of an homogenised meal (Found relevant to 1 % HPMC). HPMC, K4M grade was used from COLORCON. From the fig 4.1 the apparent viscosity values were taken. From in- house CFD simulations of water at 37 °C the flow through cell at flow rate 16 ml/min has a shear rate of 30 -40 s^{-1} and a semi log plot was used to select the viscosity values from the fig 4.1 (point at which the extended line matches with the semi-log axis). Fig 4.1 shows that the apparent viscosity depends on the shear rate. With 0.5 % HPMC the apparent viscosity did not change with the change in shear rate at the relevant values of 30-40 s^{-1}, so the viscosity value was taken as 30 m Pa.s (semi-log plot was used to take the value on y- axis) and similarly the apparent viscosity was taken taken as 380 m Pa.s for 1% HPMC. The apparent viscosity for 1 % HPMC changed minimally with the relevant change in the shear rate from ~10 s^{-1} to ~40 s^{-1} shown in fig 4.1.
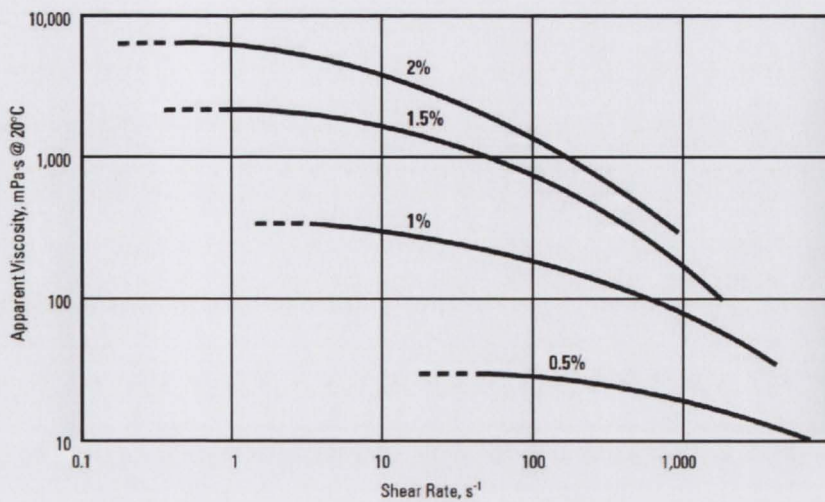
Fig 4.1 The effect of shear rate on apparent viscosity at different concentrations (taken from Dow online information resources)

As discussed in the section 2.2.18 dissolution rates were predicted using the particle motion equation to calculate the relative velocity. Experimental dissolution was compared with the predicted dissolution. In the powder cell using method 1 and 2 the experimental dissolution is faster than the predicted dissolution using the relative velocity parameter from the particle motion equation. The experimental dissolution is possibly slower due to clumping reducing the total surface area exposed to the dissolution medium which reduces the dissolution rate therefore SLS was used below the CMC limit to avoid clumping in the powder cell. The concentration of SLS used was below CMC limit as otherwise micellar diffusion of drug will occur in addition to diffusion of free drug. Along with addition of SLS the amount of drug placed in the powder cell was reduced to 5 mg (from 10 mg). Dissolution in the powder cell using SLS and 5 mg of drug was faster than the dissolution in dissolution medium with no SLS and 10 mg. Dissolution profiles using SLS and 5 mg were comparable with the predicted dissolution using the relative velocity from the particle motion equation. SLS used in the dissolution medium makes particles free from clumping resulting in an increase of total surface area exposed leading to an increase in the dissolution rate.

An attempt was made to predict the dissolution in viscous medium (1 % HPMC) using the particle motion equation however due to the high viscosity value of the dissolution medium the MATLAB program did not run smoothly. Nevertheless, a predicted dissolution rate using the BCS equation was constructed in viscous medium as it has no parameter of relating viscosity. Dissolution was carried out only at a flow rate of 8 ml/min. At higher flow rates the viscous medium did not flow freely due to obstruction by the filters and the filter head so dissolution flow rates were limited to 8 ml/min.

Predicted dissolution using 4 different sized particles

The particle size distribution shows that different sized particles of the ibuprofen used in the dissolution studies could be divided in to four bins, shown in appendix 5. The average of the particle size with each bin was 40, 127, 195 and 295 µm. When predicting dissolution using the particle motion equation only the average particle size 200 µm was used. Therefore dissolution using the particle motion equation was predicted considering four different sized particles to investigate the influence of using a particle size distribution rather than one average particle size on the dissolution rate. The predicted dissolution using four different sized particles is shown in fig 4.2
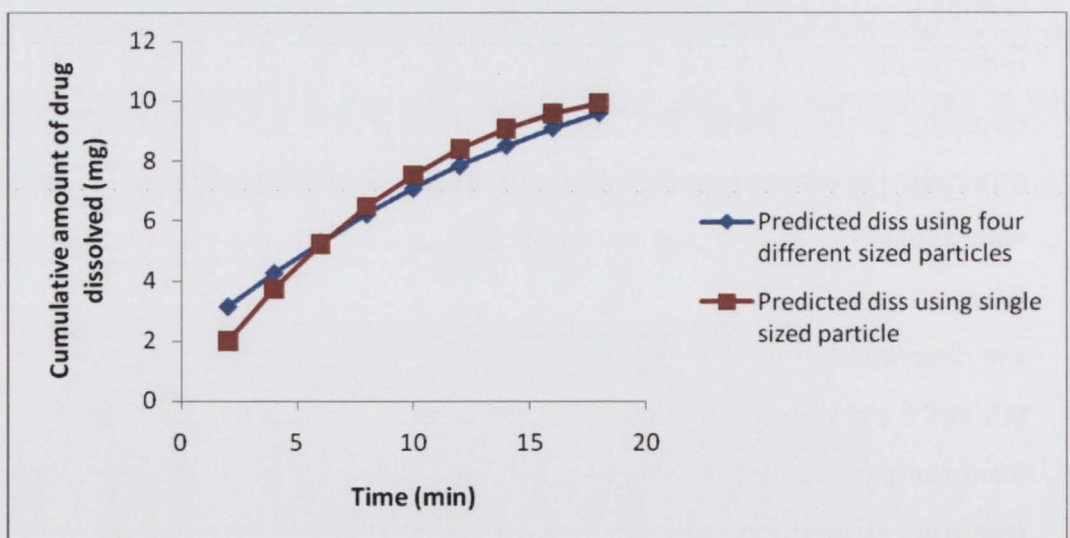
Fig 4.2 The predicted dissolution using four different typed sized particles and comparison with the predicted dissolution using single sized particle.

When the predicted dissolution using a single sized particle (200 µm) compared with the predicted dissolution with four different sized particles it can be concluded that the dissolution in four sized particles is same as the single sized particle dissolution (fig 4.2). The dissolution rate was same from 8 min to the end of the dissolution (showed in fig 4.2), however at earlier time points a difference can be observed in the amount of drug dissolved. 2.5 mg of drug was dissolved in the predicted dissolution from four different sized particles, but in single sized particle dissolution (predited) only 2 mg of drug is dissolved at 3 min of time (shown in fig 4.2).

Fig 4.3 shows the comparison of the dissolution using four different sized particles with the experimental dissolution in the powder cell using method 1 without SLS. The predicted dissolution using four different sized particles is faster than the experimental dissolution. The dissolution rate at 25 ml/min is closer to predicted dissolution up to the point at which 50 % of drug is dissolved. After this point the predicted dissolution is faster than the experimental dissolution.
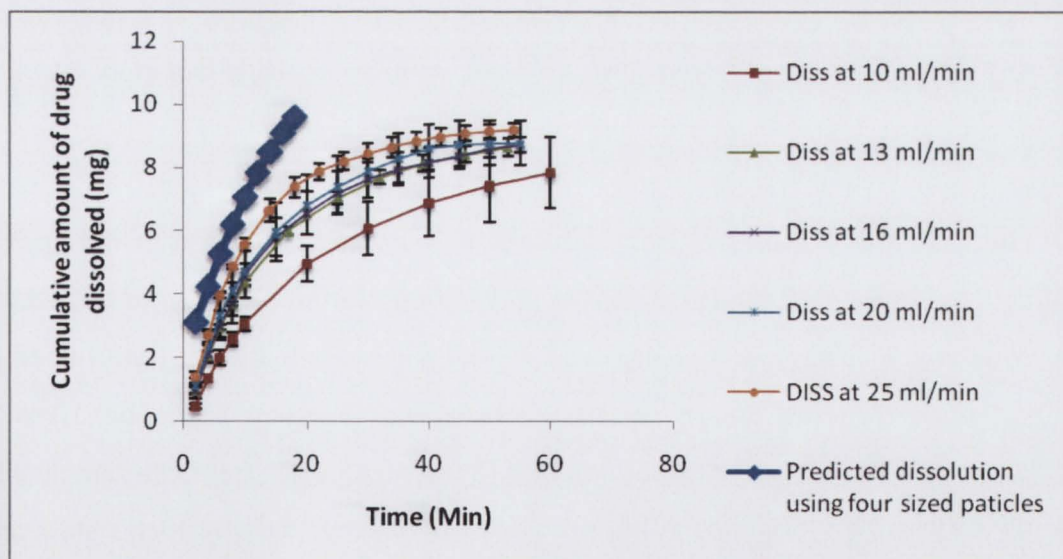
Fig 4.3 comparison of predicted dissolution from four different sized particles with the experimental dissolution in the powder cell using method 1 wit out SLS

79

In predicted dissolution using average of single particle sized particle the amount of drug released was 2 mg at 2 minutes but in the predicted dissolution using four different sized particles the amount of drug dissolved is 3 mg.
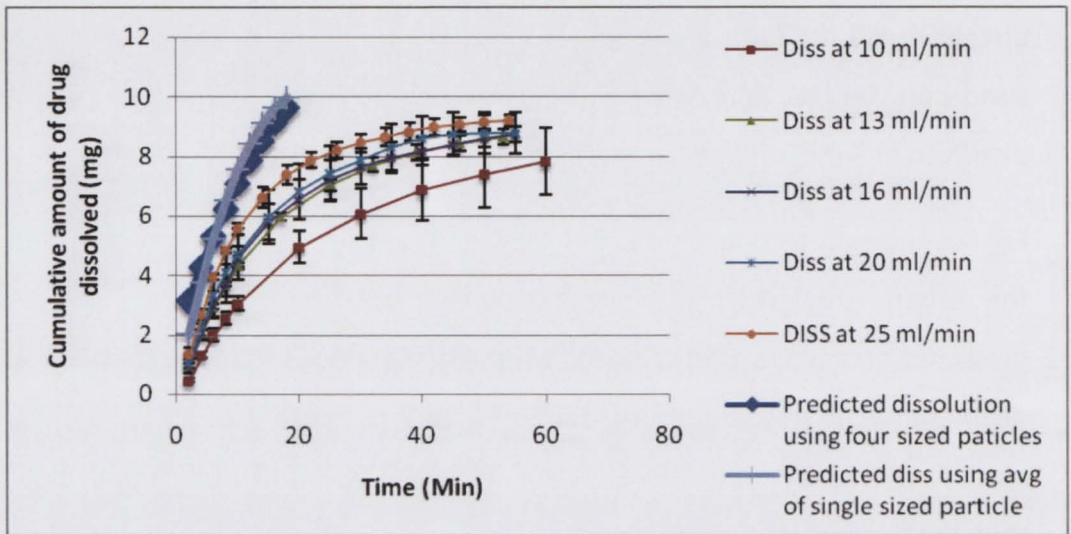
Fig 4.4 shows the comparison of the predicted dissolution from one average particle size and from four different sized particles with the experimental dissolution.

The relevance of particle density vs. true density

The true density of the drug (Ibuprofen) particles was determined using a helium pycnometer and the particle density of the ibuprofen particles were determined by MCS services, UK (discussed in section 2.2.7). The particle density was determined to be 1.018 g/cc and the true density of the particles was determined to be 1.1047 g/cc. The difference in the density values was due to the small pore size in the sample which cannot be determined using helium pycnometer. The density of the particles plays an important role in the MATLAB code used to determine the relative velocity in the prediction of dissolution.

a

$U_{p,av}$ = 1.11 mm/s, $U_{p,av}$-$U_{f,av}$ = -0.364 mm/s

b

$U_{p,av}$ = 1.55 mm/s, $U_{p,av}$-$U_{f,av}$ = -0.362 mm/s

c

$U_{p,av}$ = 1.99 mm/s, $U_{p,av}$-$U_{f,av}$ = -0.363 mm/s

d

$U_{p,av}$ = -1.24 mm/s, $U_{p,av}$-$U_{f,av}$ = -2.71 mm/s

$U_{p,av}$ = -0.801 mm/s, $U_{p,av}$-$U_{f,av}$ = -2.71 mm/s

$U_{p,av}$ = -0.357 mm/s, $U_{p,av}$-$U_{f,av}$ = -2.71 mm/s
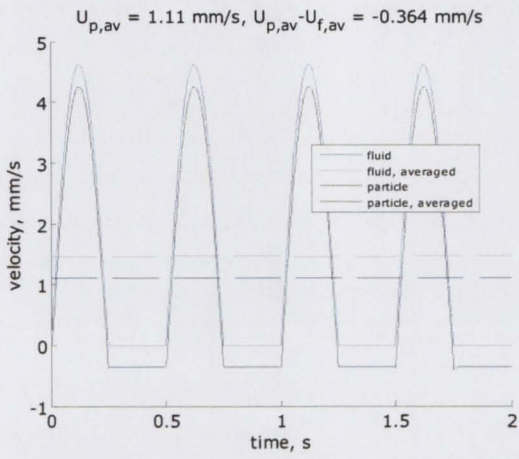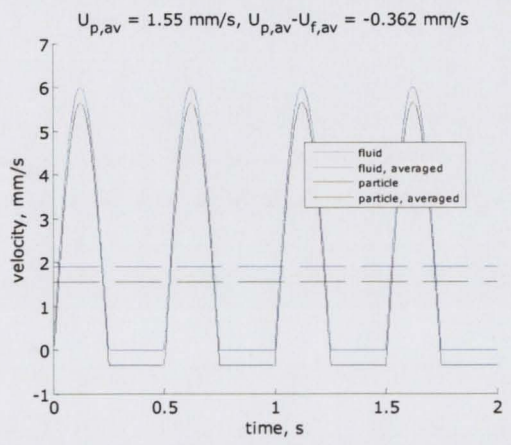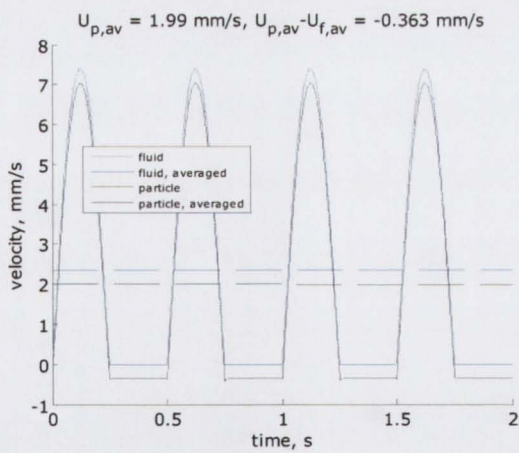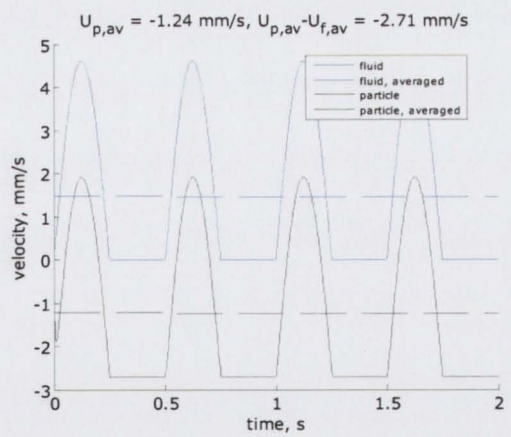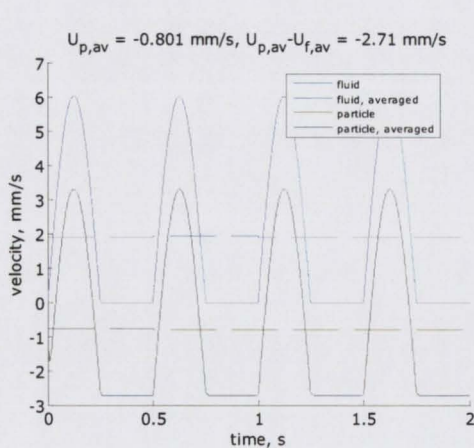
e
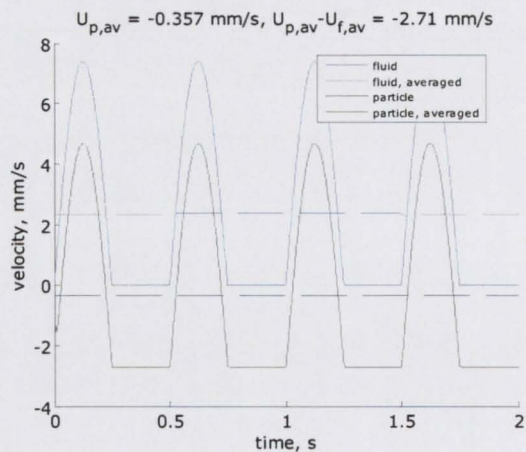
f

Fig 4.5 Shows the difference between the relative velocity values using particle density (MCS services, UK) and the true density determined using helium pycnometer in the MATLAB code (a – at flow rate 10 ml/min, b – at flow rate 13 ml/min, c – at flow rate 16 ml/min with particle density; d – at flow rate 10 ml/min, e – at flow rate 13 ml/min, f – at flow rate 16 ml/min with true density). The relative velocity in the graphs is represented as $U_{p,av}$ – $U_{f,av}$ and a constant value.

The relative velocity using particle density (MCS services) shows a value of 0.363 mm/s and the relative velocity using true density shows a value of 2.71 mm/s (fig 4.5).

Fig 4.6 shows the predicted dissolution using particle motion equation with true density (1.1047 g/cc)

The predicted dissolution using true density is faster than the dissolution with particle density (MCS services, UK) due to the higher relative velocity value calculated. The predicted dissolution using true density takes 6 minutes to dissolve 5 mg of drug (fig 4.6) but in the predicted dissolution using particle density it takes 18 minutes to dissolve 5 mg of drug (fig 3.23).

Significance of predicted dissolution

1. It is possible to predict the dissolution time required for the experimental dissolution. From this information it is easy to estimate the amount of buffer required for the dissolution, useful in dissolution with poorly soluble drugs and finally to select operating conditions such as open or closed system.

2. By comparing the predicted dissolution with the experimental value it is possible to estimate the effect of parameters in the experiment which are not included in the dissolution prediction equation. For example when the predicted dissolution using relative velocity from the particle motion equation and the BCS equation were compared, it can be concluded that predicted dissolution from the particle motion equation was faster than the predicted dissolution from the BCS equation. This might be due to the physical parameter relative velocity being included in the particle motion equation.

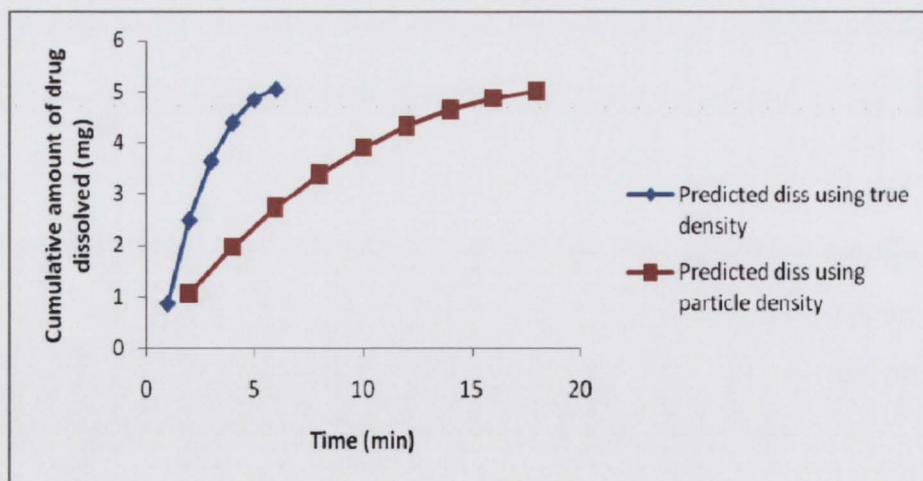3. Using the predicted dissolution profile it is possible to determine the amount of drug released at particular time which could be useful as an input in pharmacokinetic studies (PK software). It is possible to attempt to predict the dissolution in the fasted and fed state conditions in the gastrointestinal tract. This could be used with in vivo results to develop an in vitro-in vivo correlation.

Fig 4.7 shows the predicted dissolution in the simulated fasting state. The dissolution was predicted for the drug (ibuprofen) considering a standard gastric emptying time (40 min). Chen worked on the gastric emptying time in fasted and fed state (Chen et al, 2008) and the gastric emptying time in humans on an average is 40 (40±2) minutes in fasted state. Therefore dissolution was predicted considering 40 minutes as standard gastric emptying

83

time and after 40 minutes the dissolution was predicted considering pH 6.6. A bio-relevant prediction is helpful to estimate the drug dissolution in fed and fasted state for a novel drug or dosage form, potentially reducing the number of experimental dissolution studies which have difficulties as in preparing viscous medium and running the flow through apparatus with viscous medium.
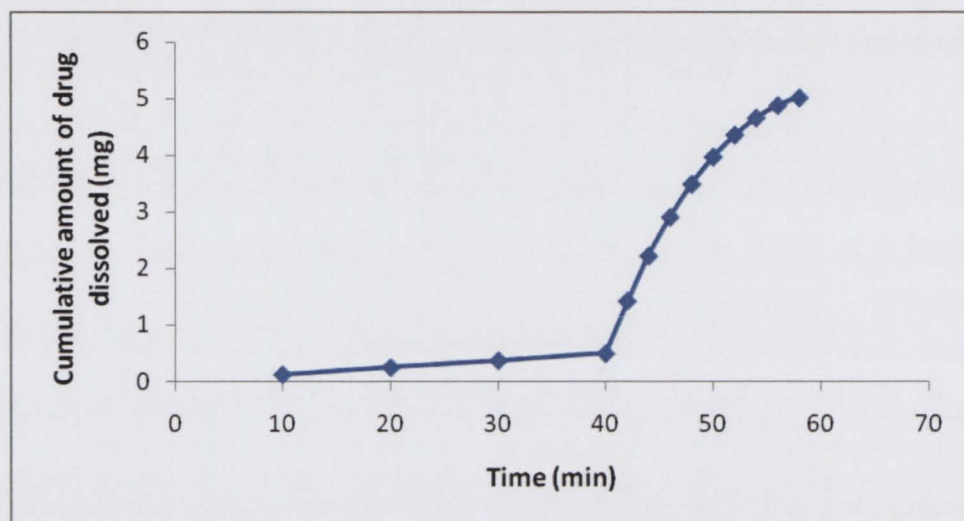
Fig 4.7 Predicted dissolution in simulated fasting state

The only requirement to predict dissolution in bio-relevant medium is the saturated solubility of the drug, the density of the fluid, and the density of the particle. The prediction of dissolution in fed state is already discussed in section 3.7.2. Fig 4.8 shows the comparison of predicted dissolution in simulated fasted state and fed state.
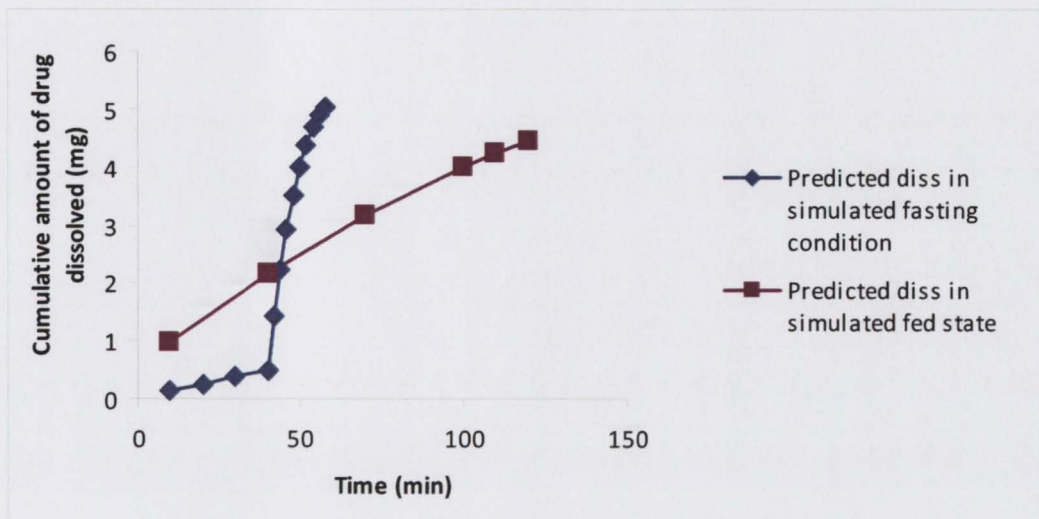
Fig 4.8 Comparison of predicted dissolution in simulated fasting and fed state

4. Dissolution was predicted according the BCS equation. To predict the dissolution the parameter used was dissolution number which is a ratio of the mean residence to dissolution time (time required for a particle to dissolve). To predict the dissolution rate the parameter dissolution time was used from the dissolution number and predicted at a series of time points. The experimental dissolution in the flow through apparatus suggests that the dissolution is faster than the predicted dissolution from BCS. The faster dissolution in the flow through apparatus is due to the parameter relative velocity. So the dissolution number is not fitted with the parameter relative velocity in the BCS classification. The results in the flow through apparatus suggest that the consideration of relative velocity or a more accurate dissolution rate prediction such as that presented here using the relative velocity value from the particle motion equation, may result in a more precise BCS classification. If the parameter relative velocity is considered in the dissolution time and if these results in a faster dissolution time, then the dissolution number will increase as dissolution number is the ratio of mean residence to dissolution time.

CONCLUSION

6 CONCLUSION

Dissolutions were carried out in various dissolution media (phosphate buffer pH 6.6 with sodium lauryl sulphate (SLS) with 5 mg of drug and without SLS with 5 or 10 mg of drug, 0.1 M HCl with SLS; in phosphate buffer pH 5.8 with 0.5% HPMC and 1% HPMC with SLS) to simulate the fasting and fed state in the Gastro intestine. Dissolution was predicted using particle motion equation 1.11 according to BCS equation 2.3.

When the experimental dissolution without SLS is compared with the predicted dissolution using the particle motion equation and the BCS equation the it is not comparable with the dissolution from prediction using the particle motion equation. This may be due to clumping of particles reducing the surface area exposed and resulting in lower than predicted dissolution. The experimental dissolution is comparable with the predicted dissolution using BCS as the BCS equation does not account for relative velocity and results in the prediction of a slower dissolution rate. The experimental dissolution is comparable with the predicted dissolution using the particle motion equation after adding SLS and reducing amount of drug to 5 mg from 10 mg.

The particle motion equation is not suitable for modelling of dissolution unless SLS is added below the CMC limits. Along with the addition of SLS the other requirement to ensure a dilute particulate system is a limit on the amount of drug used in the dissolution (reduction from 10 mg to 5 mg in the current work). 5 mg of drug is recommended for better results. The predicted dissolution using the BCS equation was comparable with the experimental dissolution with out SLS shown in fig 3.12 and 3.18 which tells that the BCS equation was better than the relative viscosity equation but the BCS equation is not suitable for modelling a dissolution as the equation does not have viscosity and relative velocity parameters which plays an important role in the dissolution.

Dissolutions were carried out in the powder cell using method 1 in phosphate buffer pH 6.6 with SLS, 0.1 M HCl and in viscous media in the flow through apparatus. Dissolutions were carried out in the powder cell using method 1 and 2 in phosphate buffer pH 6.6 without SLS in the flow-through apparatus. In any dissolution a correlation was not

achieved between the cube root dissolution rate constant and the flow rate. Dissolutions were carried out in the tablet cell as well using the flow-through apparatus in phosphate buffer pH 6.6 (without SLS) and a correlation between the dissolution rate constant and the flow rate was not achieved.

The relative velocity is constant in the tablet cell and in the powder cell (method 1 and 2) and was determined to be 0.538 mm s^{-1} (in phosphate buffer pH 6.6 without SLS) relative to the average particle size at the beginning of the dissolution test. From the results it can be concluded that the cube root dissolution rate constant is constant at different flow rates employed except at very low flow rates and at higher flow rate (discussed in section 1.3.1 and 1.3.1.2). The consistency of the cube root dissolution rate constant is due to having constant relative velocity at any flow rate employed, applicable to drugs in the powder form.

It is concluded that usage of SLS below the CMC limits makes dissolution easier as SLS facilitates wetting which makes drug particles free from clumping which can occur in the powder cell of the flow- through apparatus. Dissolutions were carried out using viscous medium (0.5 % and 1 % HPMC) in the flow through apparatus to simulate the gastrointestinal conditions. The final conclusion regarding the dissolution in viscous medium using flow through apparatus is that the dissolution should be carried out with out any filters in the powder cell for 1 % HPMC medium and with bottom filter in the powder cell for 0.5 % HPMC medium.

When the dissolutions are compared for biorelevance, dissolutions were carried out at different pH values, in media of different viscosities and it is concluded that the GIT fluid velocities resulting from motility of the stomach and intestine will not affect the dissolution rate of drug particles (powder form) due to having a constant relative velocity between the drug particles and GIT fluids. However other gastrointestinal forces such as grinding motions may affect the dissolution process.

The dissolution from the average of single sized particle was compared with the dissolution of four different sized particle and no difference was seen expect at the early time points shown in fig 4.2. The dissolution from the average of four different sized particles was more agreeable with the experimental at the early time points and after it was followed with the dissolution of four different sized particles shown in fig 4.4.

REFERENCES

7 REFERENCES

Anderberg. E.K., Nystorm. C., (1990). Physicochemical aspects of drug release X. Investigation of the applicability of the cube root law for characterization of the dissolution rate of fine particulate materials. Int. J.Pharm.62. 143-15.

Amidon. G.L., Lennernas. H., Shah. V.P., Crison. J.R., (1995). A theoretical basis for a biopharmaceutic drug classification-the correlation on in vitro drug product dissolution and in vivo bioavailability Pharm.Res. 12. 413-420

Basset. A. B., (1888). Treatise on the motion of a sphere in a viscous liquid, Phil.Trans.R.Soc.Lon. 179.43-63

Brunner, L., Tolloczko, S., (1900). Z. Phys.Chem.35, 283-290

Brunner. E ., (1904).Z. Phys. chem., 47.56-102

Berthoud. A., (1912). J. chem. Phys., 10.624-635

Butler.A.Q., Ransey. J.C., (1952). Drug standards. 20, 217.

Bhattachar.S.N., Wesley.J.A., Fioritto.A., Martin.P.J.,Babu.S.R., (2002). Dissolution testing of a poorly soluble compound using the flow-through cell dissolution apparatus.236. 135-143

Bently.J P., (2005).Principles of measurement systems, Pearson, 4 [th] edition

Catsten. J.T., (1974), Theories of dissolution- single particulate systems.In: Dissolution Technology, Academy of pharmaceutical sciences, Washington, 1-28

Cammarn.S.R., Sakr.A., (2000). Predicting dissolution via hydrodynamics: salicylic acid tablets in flow through cell dissolution.201.199-209.

Chen. E. P., Mahar Doan. M.K., Portelli. S., Coatney . R., Vaden. V., Shi. W., (2008), Gastric pH and Gastric time in fasted and fed conscious cynomolgus monkeys using the bravo pH system.Pharm.Res.25.

Danckwerts. P. V., (1951). Significance if liquid-film coefficients in gas absorption. Ind.Eng.Chem.43, 1460-1467

Dressman. J. B., Amidon. G. L., Reppas.C., Shah. V.P., (1998). Dissolution testing as a prognostic tool for oral drug absorption: immediate release dosage forms. Pharm.Res.15. 11-22.

Dressman. J. B, Reppas. C., (2000). Invitro- invivo correlations for lipophilic, poorly water soluble drugs. Eur.J.Pharm.Sci.11.73-80.

Dressman.J., Kramer.J., Johannes K., (2005). Pharmaceutical dissolution testing, Taylor and Francis

Dokoumetzidis. A., Macheras. P., (2006). A century of dissolution research: From Noyes and Whitney to the Biopharmaceitics classification system.321.1-11.

D'Arcy D.M.,Liu.B.,O'Dwyer.R.,Bradely.G.,Corrigan.O.I., (2008). Dissolution in the flow through apparatus – use of computational fluid dynamics (CFD) to investigate hydrodynamic effects, AAPS.J, 10(S_2),1092.

Edwards. L.J., (1951), The dissolution and diffusion of aspirin in aqueous media. Trans. Faraday Soc.47, 1191-1210

Emara.L.H., Taha.N.F., Mursi.N.M. (2009). Investigation of the effect of the different flow-through cell designs on the release of diclofenac sodium SR tablests.Dissolution technologies.

Filleborn. V.M., (1948). A new approach to tablet disintegration testing. Am.J.Pharm.120, 233.

Franklin. R. E., (1949). A study of the fine structure of carbonaceous solids by measurements of true and apparent densities.1.Coals. Trans. Faraday soc. 45,274-286.

Gohel. MC., Panchal. MK., (2002). Refinement of lower acceptance value of the similarity factor F2 in comparision of dissolution profiles. Disso Techno .9(1).

Hixon. A.W., Crowell. J.H., (1931). Dependence of reaction velocity upon surface and agitation.I. Theorictical consideration. Ind. Eng. Chem. 23. 923-931.

Healy, A.M., (1995). Investigations of the dissolution mechanisms of acidic drug-excipient compacts. Thesis Ph.D.Pharmaceutics,TCD.

Jillavenkates . A., Dapkunas. S. J., Lin-sen. L., (2001). Particle size characterization, NIST special publication 960-1.

Klein.S., Butler.J.,Hempenstall.J.M., Reppas.C., Dressman.J.B., (2004).Media to stimulate postprandial stomach I. Matching the physicochemical characterstics of standard breakfasts. JPP.56, 605-610

Kakhi.M, (2009).classifications of flow regimes in the flow through cell. Eur. pharm. sci. 37, 531-544

Levich.V.G., (1962). Physicochemical hydrodynamcis, Prentice-Hall, Inc

Lide. D. R., (1995-1996). Hand book of chemistry and physics., CRC, seventy sixth edition

Looney.T.J., (1997).USP apparatus 4-applying the technology. Dissolution technologies.

Melling. A., (1997), Tracer particles and seeding for particle image velocimetry, Meas.Sci.Technol, 8(12). 1406-1416

Noyes.A.A., Whitney.W.R., (1897). The rate of solution of solid substances in their own solutions. J.Am.Chem.Soc.19, 930-934.

Nelson. E., (1957). Solution rate of theophylline salts and effects from oral administration. J.Am.Pharm.Assoc.Sci. Ed 46, 607-614.

Nelson. K. G., Shah. A. C., (1975). Evaluation of a convective diffusion drug dissolution rate model. J. Pharm.Sci., 64. 610-614

Nelson. K. G., Shah. A. C., (1987). Transport in dissolution kinetics I: Convective diffusion to assess the role of fluid viscosity under forced flow. J. Pharm. Sci., 76.799-802

Oh. D. M., Curl. R. L., Amidon. G.L., (1993). Estimation the fraction dose absorbed from suspensions of poorly soluble compounds in humans: a mathematical model.Pham.Res.10. 264-270.

Pernarowksi. M., Woo. W., Searl. R. o., (1968). Continuous flow apparatus for the determination of the dissolution characteristics of tablets and capsules. J. Pharm.sci.1419, 57.

Plummer.L.N., Wigley. T.M.L., (1976). The dissolution of calcite in CO_2-saturated solutions at 25°C and 1 atmosphere total pressure. Geochim. Cosmochim. Acta. 40. 191-202

Parojcic.J., Vasiljevic.D., Ibric.S., (2007). Tablet disintegration and drug dissolution in viscous media: Paracetamol IR tablets. J.Pharm.Sci. 355.93-99

Ranz. W.E., Marshall. W.R., Jr., (1952). Evaporation from drops. I. Chem. Eng. Progress 48, 141-146.

Ranz. W.E., Marshall. W.R., Jr., (1952). Evaporation from drops. II. Chem. Eng. Progress 48, 173-180.

Sherwood. TK., Woertz. BB., (1939).The role of eddy diffusion in mass transfer between phases. Trans. Am. Inst. Chem. Eng.35.517-540

Strickland. W. A., Busse. L.W. Jr., Higuchi. T., (1956). The Physics of tablet compression XI.Determination of porosity to tablet granulations. J. Am. Pharm. Assoc.sci. Ed 45, 482.

Sheng.J.J., Sirois.P.J., Dressman.J.B., Amidon.G.!., et. al., (2008). Particle diffusinal layer thickness in a USP dissolution apparatus 2: A combined function of particle size and paddle speed.J.P.S.97. 4815-4829.

United Stated Pharmacopeia 28/National formulary 23, (2005).Pharmaceitical convention Inc., Rockwell , MD, USA.

Wurster. D. E ., Taylor. P. W., (1965). Dissolution rates. J. Pharm. sci.54.169-175

Wilderman. M., (1909). Z. Phys.Chem.66, 445-495.

Wu.Y., Ghaly.E.S., (2006). Effect of hydrodynamic environment on tablet dissolution testing flow-through dissolution apparatus. P R Health. Sci.J.25.75-83.

Zhang.G.H.,Vadino.W.A., Yang.T.T.,Cho.W.P., Chaudry.I.A., (1994). Evaluation of the flow-through cell dissolution apparatus: Effects of flow rate, glass beads and tablet position on drug release from different type of tablets.20.2063-2078.

APPENDICES

APPENDIX I -Parameters used in MATLAB code for determining relative velocity

Parameters	Phosphate buffer with No SLS pH 6.6	Phosphate buffer with SLS	In 0.1 M HCl with SLS	0.5 % HPMC with SLS	1 % HPMC with SLS
Particle diameter (m)	200 e-6	200 e-6	200 e-6	200 e-6	200 e-6
Particle density (kg/m^3)	1.018 e3	1.018 e3	1.018 e3	1.018 e3	1.018 e3
Fluid density (kg/m^3)	1000	1002	1001	1004	1003
Fluid dynamic viscosity (pa.s)	7 e^{-4}	7 e^{-4}	7 e^{-4}	3 e^{-2}	38 e^{-2}

Table A 1.1 The different parameters used in MATLAB code for determining relative velocity

Peak velocity used MATLAB code	In powder cell	Peak velocity Used MATLAB code	In tablet cell
Peak velocity At 10 ml/min m s^{-1}	0.004619	Peak velocity At 4 ml/min m s^{-1}	0.000544
Peak velocity At 13 ml/min m s^{-1}	0.006006	Peak velocity At 7 ml/min m s^{-1}	0.000961
Peak velocity At 16 ml/min m s^{-1}	0.007392	Peak velocity At 10 ml/min m s^{-1}	0.001374
Peak velocity At 20 ml/min m s^{-1}	0.009241	Peak velocity At 16 ml/min m s^{-1}	0.002198
Peak velocity At 25 ml/min m s^{-1}	0.011551	Peak velocity At 20 ml/min m s^{-1}	0.002746

Table A 1.2 The peak velocities used in the powder cell and in the tablet cell

The four different sized particles used, radius (cm)	0.0040	0.0127	0.0195	0.0295

Table A 1.3 The four different sized particles determined using particle size distribution
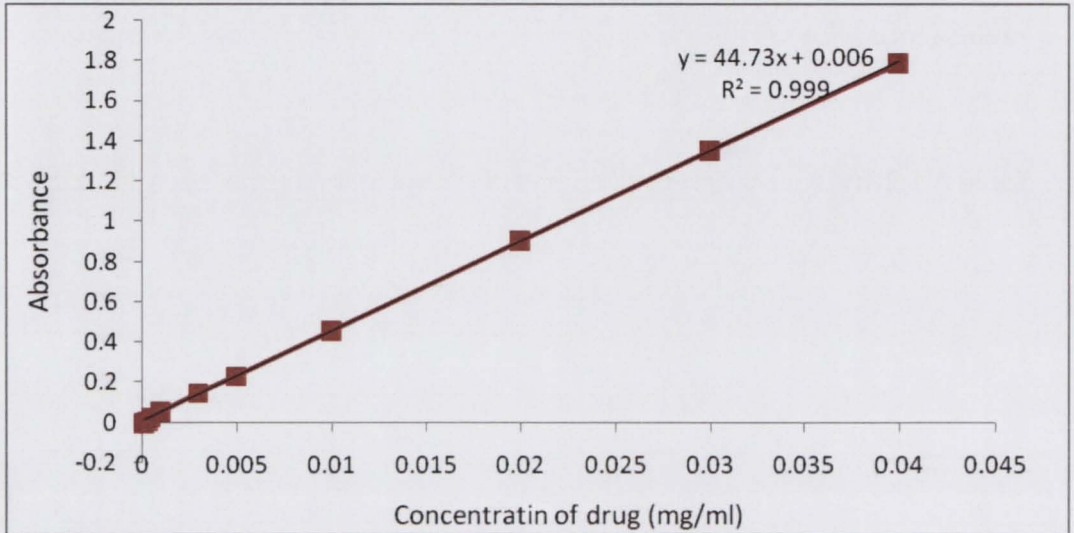
Fig A 2.1 calibration curve of Ibuprofen in Phosphate buffer pH 6.6
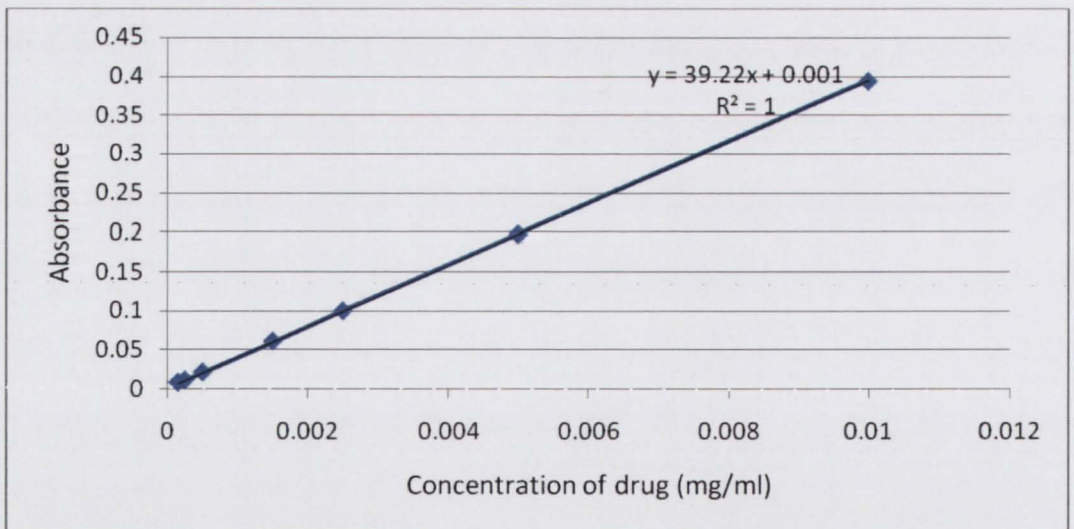
Fig A 2.2 calibration curve of Ibuprofen in 0.1 M HCl

W1, g (Weight of empty bottle)	W2, g (weight of bottle with water)	W3,g (weight of bottle with buffer)	W2-w2, g (weight of water)	Volume of bottle (cm³)	Average of the volume of bottle	W3-w1, g (weight of buffer sol)	Density of buffer sol	Average of density of buffer sol	Std dev
16.52	41.39	41.4	24.87	24.94	24.88	24.88	1.000	1.002	0.002
16.56	41.37	41.48	24.81	24.88		24.92	1.002		
16.59	41.35	41.6	24.76	24.83		25.01	1.005		

Table A 3.1 Density measurement of phosphate buffer with SLS (0.018%) pH 6.6

W1, g (Weight of empty bottle)	W2, g (weight of bottle with water)	W3,g(weight of bottle with buffer sol	W2-w2, g (weight of water)	Volume of bottle (cm³)	Average of the volume of bottle	W3-w1, g (weight of buffer sol)	Density of buffer solution (g/cm³)	Average of density of buffer sol(g/cm³)	Std dev
16.45	41.38	41.59	24.93	25.002	25.00	25.14	1.005	1.004	0.0008
16.49	41.42	41.59	24.93	25.002		25.1	1.003		
16.48	41.43	41.59	24.95	25.02		25.11	1.004		

Table A 3.2 Density measurement of 0.5 % HPMC with SLS in phosphate buffer pH 5.8

W1, g (Weight of empty bottle)	W2, g (weight of bottle with	W3, g (weight of bottle with buffer sol	W2-w2, g (weight of water)	Volume of bottle (cm³)	Average of the volume of bottle	W3-w1, g weight of buffer sol	Density of buffer solution (g/cm³)	Average of density of buffer sol(g/cm³)	Std dev
16.45	41.47	41.62	25.02	25.09	24.93	25.17	1.009	1.003	0.005
16.73	41.46	41.63	24.73	25.80		24.90	0.9987		
16.67	41.50	41.64	24.83	25.90		24.97	1.001		

Fig A 3.3 Density measurement of Ibuprofen in 1 % HPMC with SLS in phosphate buffer pH 5.8

W1, g (Weight of empty)	W2, g (weight of bottle with)	W3,g (weight of bottle with buffer sol)	W2-w2, g (weight of water)	Volume of bottle (cm^3)	Average of the volume of bottle	W3-w1, g (weight of buffer	Density of buffer solution (g/cm^3)	Average of density of buffer	Std dev
16.5	41.37	41.49	24.87	24.94	24.88	24.99	1.004	1.001	0.002
16.58	41.36	41.48	24.78	24.85		24.9	1.0005		
16.59	41.38	41.48	24.79	24.86		24.89	1.0001		

Table A 3.4 Density measurement of Ibuprofen in 0.1 M HCl

W1, g (Weight of empty	W2, g (weight of bottle	W3,g (weight of bottle	W2-w2,g (weight of water)	Volume of bottle (cm³)	Average of the volume of bottle	W3-w1, g (weight of buffer	Density of buffer solution	Average of density of buffer	Std dev
16.55	41.46	41.54	24.91	24.98	24.97	24.99	1.001	1.000	0.001
16.73	41.56	41.67	24.83	24.90		24.94	0.9991		
16.82	41.48	41.83	24.97	25.04		25.01	1.002		

Table A 3.5 Density measurement in phosphate buffer without SLS pH 6.6

Weight of sample (g)	Volume (cm^3) in Pycnometer	Density (g/ cm^3)	Average of density (g/ cm^3)
0.371	0.3361	1.1039	1.1047
0.371	0.3360	1.1041	
0.371	0.3357	1.1052	
0.371	0.3356	1.1054	
0.371	0.3357	1.1051	

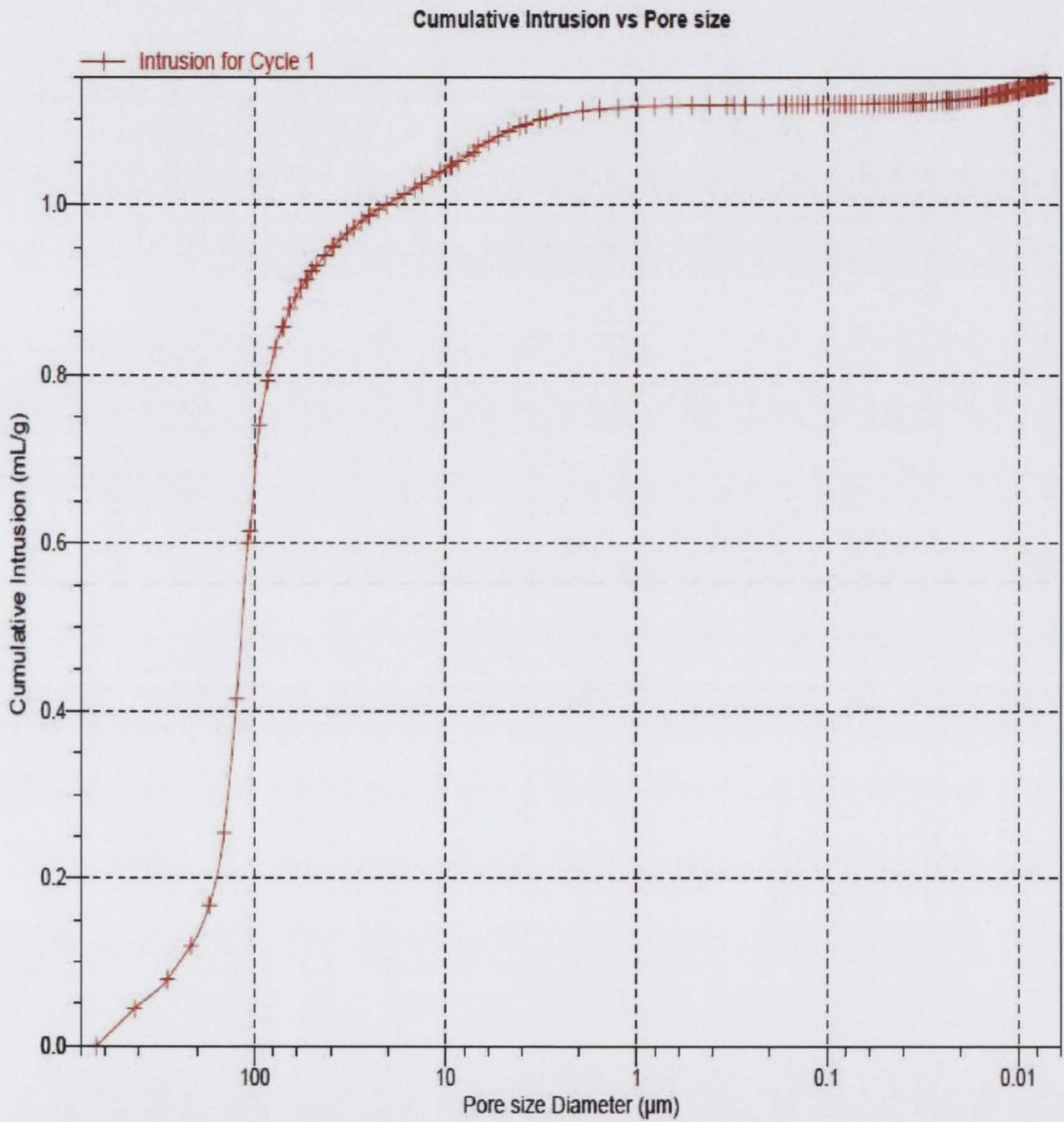Table A.3 6 True density of Ibuprofen particles in helium pycnometer.

Fig 4.1 Particle density results from MCA services UK, cumulative intrusion vs. pore size diameter
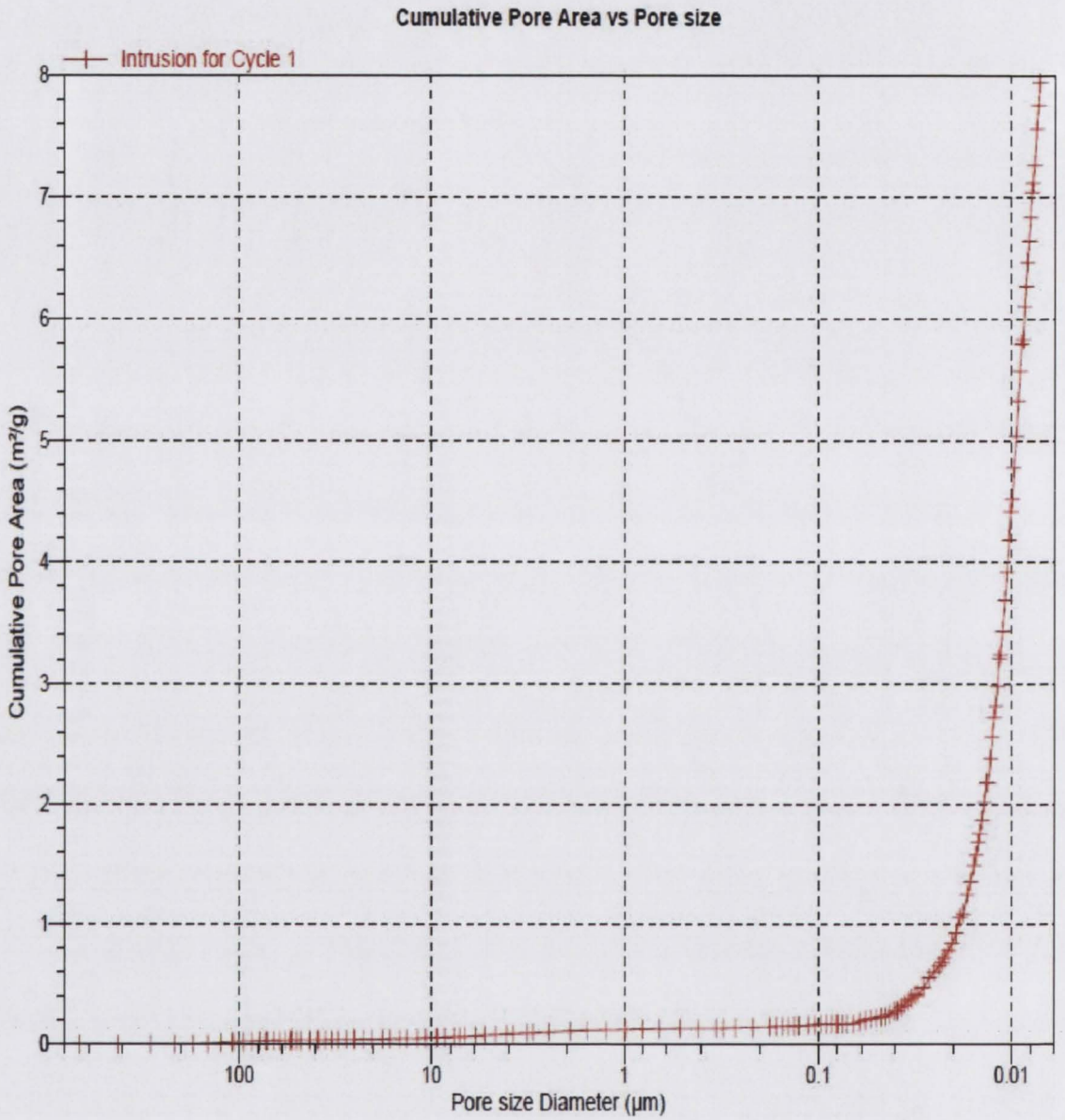
Fig 4.2 Particle density results from MCA services UK, cumulative pore area vs. pore size